

Probability-Based Evaluation of Degraded Reinforced Concrete Components in Nuclear Power Plants

Brookhaven National Laboratory

**U.S. Nuclear Regulatory Commission
Office of Nuclear Regulatory Research
Washington, DC 20555-0001**



AVAILABILITY OF REFERENCE MATERIALS IN NRC PUBLICATIONS

NRC Reference Material

As of November 1999, you may electronically access NUREG-series publications and other NRC records at NRC's Public Electronic Reading Room at www.nrc.gov/NRC/ADAMS/index.html.

Publicly released records include, to name a few, NUREG-series publications; *Federal Register* notices; applicant, licensee, and vendor documents and correspondence; NRC correspondence and internal memoranda; bulletins and information notices; inspection and investigative reports; licensee event reports; and Commission papers and their attachments.

NRC publications in the NUREG series, NRC regulations, and *Title 10, Energy*, in the Code of *Federal Regulations* may also be purchased from one of these two sources.

1. The Superintendent of Documents
U.S. Government Printing Office
Mail Stop SSOP
Washington, DC 20402-0001
Internet: bookstore.gpo.gov
Telephone: 202-512-1800
Fax: 202-512-2250
2. The National Technical Information Service
Springfield, VA 22161-0002
www.ntis.gov
1-800-553-6847 or, locally, 703-605-6000

A single copy of each NRC draft report for comment is available free, to the extent of supply, upon written request as follows:

Address: Office of the Chief Information Officer,
Reproduction and Distribution
Services Section
U.S. Nuclear Regulatory Commission
Washington, DC 20555-0001

E-mail: DISTRIBUTION@nrc.gov
Facsimile: 301-415-2289

Some publications in the NUREG series that are posted at NRC's Web site address www.nrc.gov/NRC/NUREGS/indexnum.html are updated periodically and may differ from the last printed version. Although references to material found on a Web site bear the date the material was accessed, the material available on the date cited may subsequently be removed from the site.

Non-NRC Reference Material

Documents available from public and special technical libraries include all open literature items, such as books, journal articles, and transactions, *Federal Register* notices, Federal and State legislation, and congressional reports. Such documents as theses, dissertations, foreign reports and translations, and non-NRC conference proceedings may be purchased from their sponsoring organization.

Copies of industry codes and standards used in a substantive manner in the NRC regulatory process are maintained at—

The NRC Technical Library
Two White Flint North
11545 Rockville Pike
Rockville, MD 20852-2738

These standards are available in the library for reference use by the public. Codes and standards are usually copyrighted and may be purchased from the originating organization or, if they are American National Standards, from—

American National Standards Institute
11 West 42nd Street
New York, NY 10036-8002
www.ansi.org
212-642-4900

Legally binding regulatory requirements are stated only in laws; NRC regulations; licenses, including technical specifications; or orders, not in NUREG-series publications. The views expressed in contractor-prepared publications in this series are not necessarily those of the NRC.

The NUREG series comprises (1) technical and administrative reports and books prepared by the staff (NUREG-XXXX) or agency contractors (NUREG/CR-XXXX), (2) proceedings of conferences (NUREG/CP-XXXX), (3) reports resulting from international agreements (NUREG/IA-XXXX), (4) brochures (NUREG/BR-XXXX), and (5) compilations of legal decisions and orders of the Commission and Atomic and Safety Licensing Boards and of Directors' decisions under Section 2.206 of NRC's regulations (NUREG-0750).

DISCLAIMER: This report was prepared as an account of work sponsored by an agency of the U.S. Government. Neither the U.S. Government nor any agency thereof, nor any employee, makes any warranty, expressed or implied, or assumes any legal liability or responsibility for any third party's use, or the results of such use, of any information, apparatus, product, or process disclosed in this publication, or represents that its use by such third party would not infringe privately owned rights.

Probability-Based Evaluation of Degraded Reinforced Concrete Components in Nuclear Power Plants

Manuscript Completed: March 2001
Date Published: April 2001

Prepared by
J. I Braverman, C. A. Miller
B. R. Ellingwood^a
D. J. Naus^b
C. H. Hofmayer, S. Shteyngart, P. Bezler

Brookhaven National Laboratory
Upton, NY 11973-5000

^aSchool of Civil and Environmental Engineering
Georgia Institute of Technology
Atlanta, GA 30332

^bOak Ridge National Laboratory
Oak Ridge, TN 37831

T. Y. Chang, NRC Project Manager

Prepared for
Division of Engineering Technology
Office of Nuclear Regulatory Research
U.S. Nuclear Regulatory Commission
Washington, DC 20555-0001
NRC Job Code W6684



**NUREG/CR-6715 has been reproduced
from the best available copy.**

ABSTRACT

This report describes the research performed to address concerns related to aging degradation of reinforced concrete structures at nuclear power plants (NPPs). The aging effects due to reinforced concrete degradation mechanisms are studied in order to develop analytical methods and degradation acceptance limits for concrete flexural and shear wall members. The focus of this phase of the research program is to perform a probability-based evaluation of degraded reinforced concrete members. The research effort develops fragility modeling procedures for undegraded and degraded reinforced concrete structural components subjected to earthquake ground motions. These quantitative methods provide a basis for evaluating reinforced concrete structures in nuclear plants for continued service and for developing guidelines for in-service inspection and repair. The probability-based degradation acceptance limits that are developed can be used as a tool for making risk-informed decisions regarding degradation of reinforced concrete members.

This study is being conducted under Phase II of a multi-year research program sponsored by the Nuclear Regulatory Commission (NRC) to assess age-related degradation of structures and passive components for U.S. nuclear power plants. A full description of the Phase I effort, which has identified reinforced concrete members and other components for further research in Phase II, is presented in NUREG/CR-6679.

CONTENTS

	<u>Page</u>
Abstract	iii
Executive Summary	xi
Acknowledgements	xv
1 Introduction	1
1.1 Background	1
1.2 Objective and Scope	2
2 Age-Related Degradation Mechanisms and Manifestations	5
2.1 Concrete Material Systems	5
2.2 Mild Steel Reinforcing Systems	12
2.3 Anchorage Embedments	17
2.4 Important Aging Effects for Use in this Study	18
3 Structural Impact of Reinforced Concrete Degradation and Review of Experimental Evidence	31
3.1 Cracking and Corrosion	31
3.2 Performance of Degraded Structures	35
4 Degradation Detection and Condition Assessment	71
4.1 Detection Methods for Concrete	71
4.2 Detection Methods for Reinforcing Steel.....	79
4.3 Condition Assessment	81
5 Fragility Methodology	121
5.1 Role of Fragility in Probabilistic Safety Assessment	121
5.2 Fragility Modeling Concepts	122
5.3 Limit States for Structural Performance Evaluation and Their Analysis	123
5.4 Databases to Support Fragility Assessment	124
6 Evaluation of Reinforced Concrete Flexural Members	131
6.1 Sample Problem and Analytical Model	131
6.2 Finite Element Model	134
6.3 Fragility Curves for Undegraded and Degraded Beams	136
6.4 Generalization of Results	138
7 Evaluation of Reinforced Concrete Shear Walls	171
7.1 Validation of ANSYS for Shear Walls	171
7.2 Deterministic Analysis of a Representative Shear Wall	173
7.3 Fragility Analysis of Shear Wall	176
7.4 Generalization of Results	177

TABLE OF CONTENTS (Continued)

	<u>Page</u>
8	Perspectives on the Role of Structural Degradation on Plant Seismic Risk and Resulting Acceptance Limits211
8.1	Plant Risk211
8.2	Degradation Acceptance Limits216
8.3	Extrapolation of Results to Wind Loads219
8.4	Effects of Degradation on Building Response and Response Spectra220
9	Summary, Conclusions, and Recommendations223
9.1	Summary223
9.2	Conclusions224
9.3	Recommendations for Possible Future Research230
10	References233

Figures

2.1	Types of Chemical Reactions Responsible for Concrete Degradation 19
2.2	Bond Strength Between Concrete and Steel 20
2.3	Factors Leading to Depassivation of Steel in Concrete 21
2.4	Carbonation Penetration 21
2.5	Variation of Critical Chloride Content with Environment 22
2.6	Effects and Visible Signs of Corrosion on RC Structures 22
2.7	Properties of Corroded Steel Reinforcement 23
2.8	Loss of Steel Section Due to Corrosion 24
3.1	Summary of Concrete Crack Types 43
3.2	Examples of Crack Types that can Form in Concrete Structures 44
3.3	Surface Crack Width, Carbonation Depth, and Corrosion 45
3.4	Effect of Crack Width on Corrosion Length 45
3.5	Crack Width and Corrosion of 8-mm ϕ Bar in Marine Environment 46
3.6	Corrosion Depth vs Crack Width After 10-Year Exposure 47
3.7	Distribution of Corrosion Depths in Figure 3.6 47
3.8	Variation of Crack Width with Depth 48
3.9	Crack Width vs Corrosion 49
3.10	Beam Test Specimen 49
3.11	Beam Test Specimens 50
3.12	Crack Width vs Corrosion 51
3.13	Load vs Deflection Curves (w/o Splices) for Static Loading 51
3.14	Load vs Deflection Curves (w Splices) for Static Loading 51
3.15	Effect of Corrosion on Steel Properties 52
3.16	Beam Test Specimens 52
3.17	Performance of Beams w and w/o Hooked Anchors 52
3.18	Details of Test Specimens 53
3.19	Loading Patterns 53
3.20	Effect of Corrosion on Ultimate Load of Beams 54

3.21	Slab Test Specimens	55
3.22	Effect of Corrosion on Strength	55
3.23	Effect of Corrosion on Load vs Deflection	55
3.24	Cracking in Beams and Columns Due to Corrosion	56
3.25	Qualitative Representation of Damage in RC Structures Due to Corrosion	56
3.26	Pattern of Precracks and Rebar Corrosion Before Loading	57
3.27	Corrosion Formation vs Exposure Cycles	58
3.28	Normalized Flexural Strength vs Exposure Cycles	58
3.29	Normalized Flexural Strength vs Amount Corrosion	58
3.30	RC Structural Wall Specimen and Test Set Up	59
3.31	Cracks in RC Structural Wall Specimen Due to Corrosion	59
3.32	Summary of Shear Test Results	60
3.33	Detail of RC Column Specimen	61
3.34	Crack Patterns at Different Drift Angles for Column Specimens	61
3.35	Specimen Configuration and Initial Crack Pattern	62
4.1	Ultrasonic Pulse Velocity Test	97
4.2	Schematic of Ultrasonic Pulse-Echo Test Setup	98
4.3	Principle of Impact-Echo System	98
4.4	Spectral Analysis of Surface Waves (SASW) Test Setup	99
4.5	Schematic of Radiography Method	99
4.6	Schematic of Copper-Copper Sulfate Half-Cell Potential System	100
4.7	Three-Electrode Linear-Polarization Method to Measure Corrosion Current	100
4.8	Schematic of Four-Electrode Method for Measurement of Concrete Resistance	101
4.9	Schematic of Setup for Galvanostatic Pulse Measurement	101
4.10	Schematics of Some Typical Crack Patterns that Represent the Common Causes of Concrete Degradation	102
4.11	Summary of Crack-Induced Phenomena Associated with the Design, Construction, and Service Phases of a Reinforced Concrete Structure	103
4.12	Damage State Chart Relating Environment Exposure, Crack Width, and Necessity for Additional Evaluation or Repair	104
4.13	Damage State Chart Relating Environmental Exposure, Half-Cell Potential Reading, and Necessity for Additional Evaluation or Repair	105
4.14	One Approach to the Evolution of Structural Safety with Time as Dictated by Steel Corrosion	106
4.15	Representation of the Progressive Change with Time of the Deterioration Levels and Loss of Structural Performance of a Reinforced Concrete Member Subjected to Chloride Attack	106
6.1	Shear and Moment Diagram for Propped Cantilever	140
6.2	Sample Beam Problem	141
6.3	Limit Analysis of Propped Cantilever	142
6.4	ANSYS Beam Model	143
6.5	Crack Patterns Predicted with ANSYS	144
6.6	Comparison of ANSYS and Analytic Beam Deflection Prediction	145
6.7	Lognormal Distribution for Undegraded Beam	146
6.8	Fragility Curve for Undegraded Beam	147
6.9	Fragility Curve for Bottom Spall	148
6.10	Fragility Curve for Top Spall	149
6.11	Fragility Curve for Top and Bottom Spall	150
6.12	Fragility Curve for 10% Steel Loss Top and Bottom	151

6.13	Fragility Curve for 20% Steel Loss Top and Bottom	152
6.14	Fragility Curve for 20% Bottom Steel Loss and Bottom Spall	153
6.15	Fragility Curve for 20% Top Steel Loss and Top Spall	154
6.16	Lognormal Distribution for 20% Steel Loss	155
6.17	Comparison of Fragility Curves	156
6.18	Effect of Spall in Flexural Member with 3/4" Cover	157
6.19	Effect of Spall in Flexural Member with 1-1/2" Cover	158
6.20	Effect of Spall in Flexural Member with 3" Cover	159
6.21	Effect of Degraded Concrete Strength on Beam Moment Capacity	160
6.22	Effect of Degraded Steel Area on Beam Moment Capacity	161
7.1	Configuration of Experimental Shear Walls	180
7.2	ANSYS Model of Experimental Wall	181
7.3	Comparison of Measured and Predicted Load-Deflection Behavior	182
7.4	Comparison of Measured and Predicted Crack Patterns	183
7.5	Example Problem Shear Wall Design	184
7.6	Moment Capacity of Wall	185
7.7	Sample Shear Wall	186
7.8	Shear Wall Design Case - Undegraded Load-Deflection Curve	187
7.9	Sample Shear Wall - Design Case Crack Patterns	188
7.10	Sample Shear Wall - Design Case Deformation	189
7.11	Shear Wall - Design Case - Undegraded, Variation on F_t - Tensile Strength, + & - 20%	190
7.12	Shear Wall - Design Case - Undegraded, Variation on B_f - Coeff. of Friction, + & - 25%	191
7.13	Lognormal Distribution for Undegraded Shear Wall	192
7.14	Shear Wall - Sample Results - Undegraded, Variation on Sample Data	193
7.15	Fragility Curve for Example Shear Wall	194
7.16	Fragility Curve for $H/L = 0.5$; $\rho = 0.003$	195
7.17	Fragility Curve for $H/L = 1$; $\rho = 0.003$	196
7.18	Fragility Curve for $H/L = 2$; $\rho = 0.003$	197
7.19	Fragility Curve for $H/L = 0.5$; $\rho = 0.012$	198
7.20	Fragility Curve for $H/L = 1$; $\rho = 0.012$	199
7.21	Fragility Curve for $H/L = 2$; $\rho = 0.012$	200

Tables

2.1	Degradation Factors that can Impact the Performance of Safety-Related Concrete Structures	25
2.2	Reactivity of Various Materials with Concrete and Steel	28
2.3	Expected Carbonation Depths	29
2.4	Expected Times to Corrosion (Years)	29
3.1	Interacting Factors for Mechanisms Producing Premature Concrete Degradation	63
3.2	Classification of Intrinsic Cracks	64
3.3	Identification of Concrete Defects	65
3.4	Relation Between Crack Width and Corrosion	69
3.5	Expected Time Periods to Develop Visible Crack Width	69

4.1	Nondestructive Test Methods for Determining Material Properties of Hardened Concrete in Existing Construction	107
4.2	Nondestructive Test Methods to Determine Structural Properties and Assess Conditions of Concrete	108
4.3	Exposure Classes for Concrete Structures	109
4.4	Limiting Values for Exposure Class XA in Table 4.3	109
4.5	Influence of Moisture State on Durability Processes	110
4.6	Forms of Distress and Deterioration to be Noted in a Visual Condition Assessment	111
4.7	Outline of Recommended Information for a Survey and Sampling of Field Concrete	112
4.8	Selected NDT Methods for Condition Assessment of Concrete Structures	113
4.9	Classifications and Rating of Cracks and Surface Damage Developed by RILEM	114
4.10	Cracks Widths to Prevent Corrosion of Steel Reinforcement	116
4.11	Classification of Carbonation-Induced Damage	117
4.12	Inspection Intervals for Routine and Extended Inspections Based on Environmental Conditions	118
4.13	Recommended Inspection Intervals for NPP Concrete Structures	119
5.1	Structural Resistance Statistics for Reinforced Concrete Components Subject to Static Forces	128
5.2	Steel and Concrete Strength Statistics for Components Subjected to Dynamic Forces	129
6.1	Statistical Analysis of Undegraded Propped Cantilever Beam	162
6.2	Summary of Results for Degraded Beams	163
6.3	Statistical Analysis of Degraded Propped Cantilever (Bottom Spall)	164
6.4	Statistical Analysis of Propped Cantilever (Top Spall)	165
6.5	Statistical Analysis of Propped Cantilever (Top and Bottom Spall)	166
6.6	Statistical Analysis of Propped Cantilever (10% Steel Loss)	167
6.7	Statistical Analysis of Propped Cantilever (20% Steel Loss)	168
6.8	Statistical Analysis of Propped Cantilever (20% Bottom Steel Loss and Bottom Spall)	169
6.9	Statistical Analysis of Propped Cantilever (20% Top Steel Loss and Top Spall)	170
7.1	Statistical Analysis of Undegraded Wall	201
7.2	Summary of ANSYS Shear Wall Fragility Analyses (Using 19 Latin Hypercube Samples)	202
7.3	Summary of ANSYS Shear Wall Fragility Analyses (Using Mean Values for Random Variables)	202
7.4	Statistical Analysis of Shear Wall Using the Barda et al. Methodology, Aspect Ratio = 0.5, Steel Ratio = 0.003	203
7.5	Statistical Analysis of Shear Wall Using the Barda et al. Methodology, Aspect Ratio = 1, Steel Ratio = 0.003	204
7.6	Statistical Analysis of Shear Wall Using the Barda et al. Methodology, Aspect Ratio = 2, Steel Ratio = 0.003	205
7.7	Statistical Analysis of Shear Wall Using the Barda et al. Methodology, Aspect Ratio = 0.5, Steel Ratio = 0.012	206

7.8	Statistical Analysis of Shear Wall Using the Barda et al. Methodology, Aspect Ratio = 1, Steel Ratio = 0.012	207
7.9	Statistical Analysis of Shear Wall Using the Barda et al. Methodology, Aspect Ratio = 2, Steel Ratio = 0.012	208
7.10	Summary of Shear Wall Fragility Based on Barda Methodology	209
7.11	Summary of ANSYS Shear Wall Capacities, Effect of Degradation for Varying Aspect Ratios	210
8.1	Flexural Members, Probability-Based Crack Acceptance Limits, Considering Loss of Steel Area and Concrete Spalling.....	221
8.2	Flexural Members, Probability-Based Crack Acceptance Limits, Without Concrete Spalling	222
8.3	Shear Walls, Probability-Based Crack Acceptance Limits, Considering Loss of Steel Area and Concrete Spalling.....	222

EXECUTIVE SUMMARY

All commercial nuclear power plants (NPPs) contain concrete structures whose performance and function are necessary to protect the safety of plant operating personnel and the general public. Although these structures are passive under normal operating conditions, they play a key role in mitigating the impact of extreme environmental events such as earthquakes, high winds, and tornadoes. The past performance of reinforced concrete structures in NPPs has been good, with the majority of problems identified during construction and corrected at that time. However, as these structures age, incidences of degradation due to various aging mechanisms are likely to increase the potential threat to their functionality and durability. Some evidence of this has been reported in NUREG-1522 and NUREG/CR-6679.

Concrete structural components, such as shear walls, slabs, beams and columns, that are found in the reactor building, control or auxiliary building, and other balance-of-plant facilities, are designed and constructed in accordance with criteria in ACI Standards 318, 349, 359, and the NRC Standard Review Plan 3.8.4. Such components generally have substantial safety margins when properly designed and constructed; however, these codes have not explicitly addressed aging and the available margins for aged or degraded concrete structures are not known. Aging can lead to changes in engineering properties and may affect the dynamic properties, structural resistance/capacity, failure mode, and location of failure initiation.

In Phase I of this research effort, reported in NUREG/CR-6679, a study was performed to identify and evaluate age-related degradation occurrences of structures and passive components at NPPs. The Phase I effort consisted of (1) the collection and analysis of degradation occurrences, (2) a review of available technical information such as NRC and industry programs, NUREG reports, and other technical publications, and (3) a scoping study to identify those structures and passive components which should be studied in the Phase II program. The scoping study identified reinforced concrete members as one of several components that should be evaluated in detail to determine the effects of age-related degradation. This selection of components was made based on four criteria: number of degradation occurrences, adequacy of existing programs, importance to current licensing activities, and risk significance.

This NUREG report presents the results of the assessment of reinforced concrete members, which were identified in the Phase I effort as having the potential to impact plant safety. The objective of the current research program is to develop analytical methods and acceptance limits for degraded reinforced concrete members. Results from risk evaluation programs conducted by the United States Nuclear Regulatory Commission (USNRC), such as the Individual Plant Examination of External Events (IPEEE) program, show that external events can be significant contributors to core damage frequency (CDF). In some cases, structures and passive components have been found to be significant risk contributors when subjected to external events such as earthquakes. Therefore, the research program focuses on developing fragility models for evaluation of degraded reinforced concrete members subjected to earthquake forces. These analytical methods are used to develop probability-based degradation acceptance limits based on the impact of the degradation on overall plant risk. The objectives of the program are achieved by performing four major activities: evaluation of degradation mechanisms and condition assessment methods, structural evaluation of degraded concrete components, fragility and risk evaluation of degraded components, and development of probability-based degradation acceptance limits.

Section 2 of the report describes the aging mechanisms and corresponding aging effects encountered for reinforced concrete structural components. Reinforced concrete structures and components in NPPs are subject to a phenomenon known as aging, leading to changes in engineering properties that may impact their ability to withstand various challenges in service from operating conditions, the natural environment, and accidents. Aggressive environmental factors and influences can cause degradation in material strength and stiffness. Descriptions of degradation are presented for concrete material, reinforcing steel,

and anchorage embedments. Types of aging mechanisms discussed include chemical attack from leaching, sulfates, acids and bases, and alkali-aggregate reactions; and physical attack from freezing and thawing, abrasion/erosion/cavitation, thermal exposure/thermal cycling, irradiation, fatigue/vibration, and settlement. Section 2 ends with a summary of the aging effects that are particularly important for plant safety and should be considered in this research effort. The predominant aging mechanisms/effects that were selected are corrosion of embedded reinforcement, cracking, and spalling of concrete cover.

Section 3 addresses the physical impact of reinforced concrete degradation and discusses the results of test data presented in the literature on performance of degraded reinforced concrete members. A review of the performance of NPP reinforced concrete structures indicates that concrete cracking and corrosion of embedded steel reinforcement are the most prevalent manifestation of concrete degradation. Relationships between crack characteristics and corrosion occurrence are discussed first. This relates crack characteristics such as width, orientation or type, propagation status, frequency and shape to the promotion of corrosion. Also discussed is the relationship between corrosion significance and concrete cracking. This relates the level of corrosion (i.e., loss of steel cross-sectional area) to the visual characteristics of the concrete at the surface (e.g., width of concrete cracks). Both of these relationships are discussed using tests performed on degraded reinforced concrete members consisting of beams, slabs, shear walls, and columns.

Techniques for detection of degradation in reinforced concrete structures and appropriate condition assessment methods are presented in Section 4. These are needed to determine the existing performance of reinforced concrete structures and to identify the extent and causes of any observed degradation. Nondestructive and destructive detection methods for concrete degradation are described, followed by methods for detecting damage in reinforcing steel. Information provided is focused on the methods most commonly used and on those that represent good practice for the detection of degradation of reinforced concrete structures. In addition to detection techniques, important elements of condition assessment programs are presented. These include considerations for development of an in-service inspection program, inspection scheduling, and qualification of inspection personnel.

Section 5 of the report introduces the fragility methodology which is needed to develop the probability-based degradation acceptance limits. The role of fragility in a probabilistic safety assessment (PSA) is explained. Fragility modeling concepts are presented to assess in probabilistic terms, the capability of a structural component or system to withstand a specified event (sometimes referred to as a review-level event). The fragility modeling process leads to a median-centered estimate of system performance, coupled with an estimate of the uncertainty in performance. Fragility curves can be developed using this methodology for both undegraded and degraded components to determine the effect of degradation in probabilistic terms. Limit states, which are needed to perform the fragility analysis, are defined for flexural and shear members. In the case of the beam the limit state is based on the ultimate capacity of the member in flexure, while for the shear wall the limit state is based on deformation limits which would cause appurtenant safety-related mechanical or electrical equipment to malfunction. A fragility analysis requires databases to define probabilistic models and statistics for all parameters that play a significant role known to affect the performance of the structure in service. Parameters for which statistical data were developed for concrete include compressive strength, tensile strength, initial tangent modulus, and maximum compressive strain. For steel, parameters include yield strength and modulus of elasticity. Additional parameters considered are placement of reinforcement, bar cover, and structural modeling uncertainty. The uncertainties are propagated through the analysis of the structural components using a Latin Hypercube sampling plan.

Analysis of indeterminate reinforced concrete flexural members is presented in Section 6 of the report. The sample problem is a propped cantilever beam with a twenty-foot span designed using the procedures in ACI 318-99. The load-deflection behavior of the beam is evaluated using the procedures defined in

ACI 318 and then compared to a computerized finite element solution. The closed-form analytical method in accordance with the ACI-318 code was used to calculate the deflection for increasing uniform load. The limit state (ultimate capacity) for the beam corresponds to a uniform load at which a collapse mechanism forms in the beam. These results are verified with the finite element solutions using the commercially available computer program ANSYS. Based on the very close agreement between the ACI-318 analytical method and the finite element method, the ACI-318 method is utilized to generate the beam fragility curves for both undegraded and degraded beams. Two cases of postulated degradation are considered; loss of steel cross-sectional area and loss of concrete cover (concrete spalling). For degradation of reinforcement steel, a 10% loss and 20% loss of steel area is considered. Variations for loss of concrete cover include top spall, bottom spall, or both top and bottom spall. The loss of steel area and concrete spalling were considered individually and in combination with one another. The results of this analysis for a propped beam are then generalized to other flexural members (beams and slabs). The effects of degradation as measured by the reduction in fragility are summarized for all of the various cases discussed above.

Section 7 of the report presents the analysis performed for reinforced concrete shear walls. The first step was to benchmark the analytical approach for predicting the structural response of shear walls. This was achieved by selecting a wall for which test data are already available and then performing a finite element analysis of the same wall in order to compare their load-deflection curves and cracking patterns. This effort demonstrated that the finite element method using the ANSYS code could reasonably predict the limit state as defined in this research effort. Then, a representative shear wall, typical of those found in NPPs was developed and designed. The shear wall is assumed to be part of an enclosure of a square room having similar shear walls on all sides and a ceiling with similar dimensions. Therefore, all models utilized in this analytical effort considered this configuration (not just the single shear wall). The evaluation of the shear wall model is performed using analytical solutions and a finite element solution. The analytical solutions consisted of the ACI 318 design code methodology and an analysis developed for low-rise walls by Barda et al., both of which are semi-empirical in nature. As expected for low-rise shear walls, the ACI methodology led to very conservative (i.e., low) ultimate capacities. The approach of Barda et al. resulted in capacities that were consistent with the results obtained from the finite element solution using the ANSYS code. However, the limit state for the shear wall in the present study is defined as the deformation corresponding to four times the deformation at onset of yielding of the overall model. Since neither the ACI nor the Barda et al. methodologies could be used to predict the load-deflection curve, the fragility was based on the ANSYS finite element analysis. Fragility analyses were performed for undegraded and degraded conditions. Degradation cases considered are loss of steel area and loss of steel area in combination with concrete spalling. Additional analyses were then performed to generalize the results to walls of different aspect ratios and larger reinforcement ratios. The results of how degradation affects the reduction in fragility are summarized for all of these cases.

The effects of aging degradation on overall plant risk are addressed in Section 8. The reductions in component fragilities calculated in Section 6 for flexural members and Section 7 for shear walls are utilized to evaluate the effect on plant risk. An existing PRA study for Zion Unit 1 is used to make a qualitative assessment of the effect of the reduced fragility on core damage frequency (CDF). The postulated deterioration due to corrosion of reinforcement and concrete spalling in the reinforced concrete beam and shear wall modeled in Sections 6 and 7 led to changes in median capacity that were substantially less than in the severe cases considered in the assessment for Zion Unit 1. Using knowledge about hazard curves throughout the US, inferences from the Zion evaluation are drawn for other plants in the Eastern and Western US. To evaluate the significance of the changes in CDF, the guidelines presented in the NRC Regulatory Guide 1.174 were utilized. The changes in CDF fell within Region II of the acceptance guidelines of the regulatory guide indicating that the changes are "small" and cumulative impacts are to be "tracked."

Section 8 also develops probability-based acceptance limits for reinforced concrete flexural members and shear walls. The acceptance limits are based on levels of degradation that would have to occur to increase plant risk significantly. These limits correspond to severe levels where significant degradation has likely occurred. In this context, degradation resulting in more than a 20% reduction in a component's capacity has been defined as excessive. Acceptance limits are developed for visual inspection of concrete degradation. Quantitative limits are established for crack widths and concrete spalling based on the evaluation and analysis performed.

Section 9 summarizes the results of the research program and presents the conclusions reached regarding the evaluation of degraded reinforced concrete members at NPPs. The results of the analyses provide the technical basis for developing probability-based degradation acceptance limits which was the objective of this phase of the program. This may be achieved by developing methodologies for performing structural analyses of degraded reinforced concrete members, conducting fragility and risk evaluations, relating the level of degradations to observable manifestations, and recommending acceptance limits based on these relationships. The acceptance limits developed in this research can be used during plant inspections to evaluate whether age-related degradation of the concrete and reinforcement potentially has a significant effect on plant risk. Since the results of this research were developed using a probabilistic risk assessment methodology, the acceptance limits may be used to determine whether more detailed inspections and evaluations are warranted but should not be used as a "design basis" for acceptance of a degraded condition or for NRC licensing activities such as license renewal (10 CFR Part 54) which rely on the "current licensing basis" of NPPs. The probability-based acceptance limits do provide a useful tool for making risk-informed decisions regarding the suitability of a degraded concrete structure to continue service with or without repair.

ACKNOWLEDGEMENTS

The research program described in this report was sponsored by the Office of Nuclear Regulatory Research of the U.S. Nuclear Regulatory Commission. The authors would like to express their gratitude to Dr. T.Y. Chang, NRC Project Manager, for the technical and administrative support he has provided in performing this study.

Thanks are given to the various authors and organizations that provided authorizations to reprint certain tables and figures which were essential to convey the knowledge currently available relating to degradation of reinforced concrete structures.

The authors also express special thanks to Ms. S. Signorelli for her secretarial help throughout this program and in the preparation of this report.

1 INTRODUCTION

1.1 Background

As of 1997 there were 104 operating nuclear power plants (NPPs) that had been licensed for commercial operation in the United States. These plants have the capability to generate approximately 610 gigawatts of electric power, which represents about 22 percent of the nation's total electric generation.

Approximately two-thirds of these plants received their construction permit over 25 years ago, and the majority have been in operation for over 20 years. Assurance of the continued safe operation of these plants as they age is an important maintenance and regulatory issue.

All commercial NPPs contain concrete structures whose performance and function are necessary to protect the safety of plant operating personnel and the general public. Although these structures are essentially passive under normal operating conditions, they play a key role in mitigating the impact of extreme environmental events such as earthquakes, high winds, and tornadoes. Moreover, the importance of these structures in accident mitigation is amplified by the so-called "common cause" effect, in which failure of a structure may lead to failure or loss of function of appurtenant mechanical or electrical components and systems. Results from risk evaluation programs conducted by the United States Nuclear Regulatory Commission (USNRC), such as the Individual Plant Examination of External Events (IPEEE) program, indicate that external events can be significant contributors to core damage frequency (CDF). In some cases structures and passive components have been found to be significant risk contributors when subjected to these external events. Thus, the impact of poor structural performance on plant risk can be more serious than a brief examination of plant safety systems might indicate (Ellingwood and Song, 1996; Ellingwood, 1998).

Reinforced concrete structures and components in NPPs are subject to a phenomenon known as aging, leading to changes in engineering properties that may impact their ability to withstand various challenges in service from operating conditions, the natural environment, and accidents. Aggressive environmental factors and influences can cause degradation in material strength and stiffness. Concrete strength can be reduced by chemical attack by sulfates and other acids, alkali-aggregate reactions, leaching and efflorescence. Reinforcement strength is affected mainly by corrosion (Naus, et al., 1996), which leads to a reduction in bar area and may impact the bond developed between the concrete and reinforcement. The expansive products of corrosion may also lead to cracking and spalling of the concrete cover to the reinforcement. While the overall performance of the safety-related concrete structures at NPPs has been good, the number of occurrences of age-related degradation has been increasing as the plants age (Ashar and Bagchi, 1995; Naus, Oland, and Ellingwood, 1996; Braverman et al., 2000). Incidences of degradation have been identified in intake structures/pumphouses, tendon galleries, masonry walls, anchorages, containments, and other concrete structures, often in areas exposed to water, aggressive chemicals, or the effects of freeze-thaw cycling.

Concrete structural components, such as shear walls, slabs, beams and columns, that are found in the reactor building, control or auxiliary building, and other balance-of-plant facilities, are designed and constructed in accordance with criteria in ACI Standards 318, 349, and the NRC Standard Review Plan 3.8.4. Such components generally have substantial safety margins when properly designed and constructed; however, the available margins for aged or degraded concrete structures are not known. Aging can lead to changes in engineering properties and may affect the dynamic properties, structural resistance/capacity, failure mode, and location of failure initiation.

Time-dependent changes to structural components and systems are random in nature, as are potential future challenges to the system from operating conditions or natural phenomena hazards. Safety

evaluations of existing structures should be conducted rationally and systematically within a probabilistic framework. In the Structural Aging Program (Naus, et al., 1996), a reliability-based framework for condition assessment and probability-based life prediction of concrete structures in NPPs was developed. This framework enabled time-dependent stochastic changes in resistance as well as randomness in structural loads to be taken into account, and provided a basis for assessing the capability of existing concrete structures to withstand design-basis (or larger) events during a period of future service. Questions that were addressed by this research include:

- What aging factors are significant for concrete structures in terms of future reliability?
- What is the significance of aging in a system of structural components in terms of aging of the individual components?
- What is the remaining service life of a concrete component if reliability is to be maintained without inspection/repair?
- Which nondestructive inspection techniques are most useful for informative reliability-based condition assessment?

For practical reasons, structural condition assessment must focus on a few critical structural components and systems within the NPP. An importance ranking strategy has been developed to identify that subset of structural components that are most significant for plant safety (Hookham, 1991). This list can be further reduced by considering the impact of degradation of the structural components identified on plant risk explicitly in probabilistic terms.

Structural components and systems that are dominant contributors to plant risk should receive the focus of attention in in-service condition assessment. These dominant contributors can be identified through the formalism of a probabilistic safety assessment, or PSA. A key ingredient of any PSA is an assessment of structural fragility. The fragility of a structural component or system defines the conditional probability of its attaining a performance limit state, which may range from loss of function to incipient collapse, given the occurrence of a particular operational or environmental demand. A structural fragility provides a probabilistic measure of safety margin with respect to design-basis or other events specified by the designer, owner, or regulatory authority. Such a margin can be used to evaluate degradation conditions identified during an inspection, and can provide a means to assess if the observed degradation might be expected to have a significant impact on plant risk.

1.2 Objective and Scope

The overall objective of this phase of the research effort is to develop analytical methods and probability-based degradation acceptance limits for degraded NPP reinforced concrete structures. The research effort develops fragility modeling procedures for undegraded and degraded reinforced concrete structural members subjected to earthquake ground motions. These quantitative methods provide a basis for evaluating reinforced concrete structures in nuclear plants for continued service and for providing guidelines for in-service inspection and repair. Four major activities used to accomplish the objective are:

(1) condition assessment:

Describe condition assessment techniques that can be used, by an experienced engineer using visual or other nondestructive evaluation methods, to quantify levels of degradation. Degradation

mechanisms/aging effects of interest are those associated with concrete and steel strength, concrete cracking and spalling, and corrosion of reinforcement.

(2) structural evaluation of degraded concrete components:

Evaluate the effects of degradation on the structural performance of reinforced concrete components. This entails assessing how reduction in concrete compressive strength, concrete area, steel cross-sectional area, and bond strength affect the strength, stiffness, and ductility of reinforced concrete shear walls and flexural members.

(3) fragility and risk evaluation of degraded concrete components:

Develop fragilities from analytical methods using closed-form solutions or finite element analysis, for use in assessing the impact of degradation on the overall seismic risk to NPPs. The analysis will include uncertainties due to inherent randomness and modeling that have been identified.

(4) probability-based degradation acceptance limits:

Utilize fragilities for undegraded and degraded reinforced concrete components to provide insight on the quantitative impact of structural deterioration on residual margins of safety and to develop probability-based degradation acceptance limits. These degradation acceptance limits can be used as guidance for the evaluation of degradation effects on reinforced concrete flexural members and shear walls.

The results of these activities will assist in the development of a technical basis for the validation and improvement of analytical methods and acceptance criteria that can be used in making risk-informed decisions and to address technical issues related to degradation of concrete structures.

2 AGE-RELATED DEGRADATION MECHANISMS AND MANIFESTATIONS

As concrete ages, changes in its properties occur as a result of continuing microstructural changes (e.g., slow hydration, crystallization of amorphous constituents, and reactions between cement paste and aggregates), as well as environmental influences. These changes do not have to be detrimental to the point that reinforced concrete will not be able to meet its functional and performance requirements. Concrete, however, can suffer undesirable degrees of change with time because of improper design or construction specifications, a violation of specifications, or environmental effects.

The longevity, or long-term performance, of reinforced concrete structures is primarily a function of the durability or propensity of these structures to withstand the potential effects of degradation. Table 2.1 presents a summary of the degradation factors that can potentially impact the performance of the basic constituents that comprise reinforced concrete structures (i.e., concrete and mild steel reinforcement.)^{*} (IAEA, 1998). Also contained in the table is a listing of primary manifestations of each degradation factor, potential degradation sites, and general remarks.

2.1 Concrete Material Systems

The durability of concrete materials can be limited as a result of adverse performance of its cement-paste matrix or aggregate constituents under either chemical or physical attack. In practice, these processes may occur concurrently to reinforce each other. In nearly all chemical and physical processes influencing the durability of concrete structures, dominant factors involved include transport mechanisms within the pores and cracks,^{**} and the presence of water.

2.1.1 Chemical attack

Chemical attack involves the alteration of concrete through chemical reaction with either the cement paste or coarse aggregate, or embedded steel reinforcement.^{***} Generally, the attack occurs on the exposed surface region of the concrete (cover concrete), but with the presence of cracks or prolonged exposure, chemical attack can affect entire structural cross sections. Chemical causes of deterioration can be grouped into three categories: (1) hydrolysis of cement paste components by soft water; (2) cation exchange reactions between aggressive fluids and the cement paste; and (3) reactions leading to formation of expansion products (Mehta, 1986). The rate of chemical attack on concrete is a function of the pH of the aggressive fluid and the concrete permeability, alkalinity, and reactivity. Figure 2.1 presents a summary of the types of chemical reactions responsible for concrete deterioration and the detrimental effects that can occur (Mehta and Gerwick, 1982). Chemical attack of concrete may occur in several different forms as highlighted in the following sections.

* Post-tensioning systems are not considered in this report as they are primarily utilized in NPP containment structures which are not being addressed by this study. Liner systems also are not addressed. Anchorage to concrete will be briefly discussed.

** Cracking occurs in virtually all concrete structures and, because of concrete's inherently low tensile strength, can never be totally eliminated. Cracks are significant from the standpoint that they can indicate major structural problems such as differential settlement (active cracks); provide an avenue for ingress of hostile environments (active or dormant cracks); and may inhibit a component from meeting its performance requirements (active or dormant cracks) (e.g., diminished shielding capacity).

*** Corrosion of embedded steel reinforcement due to carbonation of the concrete or the action of chloride ions is covered under the section addressing mild steel reinforcement.

Leaching and Efflorescence

Pure water that contains little or no calcium ions, or acidic groundwater present in the form of dissolved carbon dioxide gas, carbonic acid, or bicarbonate ion, tends to hydrolyze or dissolve the alkali oxides and calcium-containing products. The rate of leaching is dependent on the amount of dissolved salts contained in the percolating fluid, rate of permeation of the fluid through the cement paste matrix, and temperature. Extensive leaching causes an increase in porosity and permeability, thus lowering the strength of the concrete and making it more vulnerable to hostile environments (e.g., water saturation and frost damage, or chloride penetration and corrosion of embedded steel). Leaching can also reduce the alkalinity of the concrete locally (i.e., lower the pH). The rate of leaching can be controlled by minimizing the percolation of water through the concrete. Concretes produced using low water-cement ratios, adequate cement content, and proper compaction and curing are most resistant to leaching.

Efflorescence can be of two types: primary and secondary (Bensted, 1994). Primary efflorescence refers to uniform deposits of calcium carbonate caused by transport of calcium hydroxide (highly soluble in water) in solution through concrete capillaries to the surface where it evaporates and deposits solid, white calcium hydroxide. The calcium hydroxide then reacts with atmospheric carbon dioxide to form calcium carbonate. Secondary efflorescence refers to water penetrating the surface of the concrete structure where it can dissolve calcium salts. Secondary efflorescence is caused by a reaction in solution and arises locally and unevenly, and is usually caused by rain or condensation. Since it is a surface effect, efflorescence is primarily an aesthetic problem rather than a durability problem, but may indicate that alterations to the cement paste are taking place in the concrete. In rare cases, excessive efflorescence deposits can occur within the surface pores of the concrete causing expansion that may disrupt the surface (PCA, 1997).

Sulfate attack

Magnesium and alkali sulfates present in soils, groundwater, and seawater react with the calcium hydroxide and alumina-bearing phases of portland cement to form gypsum and ettringite. These reactions, if enough water is present, have a much higher volume than the reactants to result in expansion and irregular cracking of the concrete that can lead to progressive loss of strength and mass. The rate and degree of attack depend on the amount of available (soluble) sulfate, the presence of water, the composition of the cement, and certain characteristics of the concrete such as permeability. Guidelines for assessing the potential degree of severity of expected attack have been established (CSA, 1990; ACI 201.2R, 1987). The categories listed by CSA include: negligible attack [up to 150 ppm sulfate (SO_4) in groundwater or up to 0.10% SO_4 in soil], mild but positive attack (with corresponding values of 150 to 1,000 ppm and 0.10 to 0.2%), considerable attack (with corresponding values of 1,000 to 2,000 ppm and 0.20 to 0.50%), and severe attack (with corresponding values of over 2,000 ppm and 0.50%). ACI 201.2R adds an additional category of very severe attack with corresponding values of over 10,000 ppm and 0.50%. Concrete elements that may be exposed to attack by sulfates in soils and groundwaters include footings, foundation walls, retaining walls, piers, culverts, piles, pipes, and surface slabs. The severest attack occurs on elements where one side is exposed to sulfate solutions and evaporation can take place at the other (Swenson, 1999). Structures subjected to seawater are more resistant to sulfate attack because of the presence of chlorides that form chloro-aluminates to moderate the reaction. Concretes that use cements low in tricalcium aluminate and those that are dense and of low permeability are most resistant to sulfate attack. Improved sulfate resistance can also be attained through use of admixtures such as pozzolans and blast-furnace slag.

Delayed Ettringite Formation

Structures undergoing delayed ettringite formation (DEF) can exhibit expansion and cracking. The distress often is attributed to excessive steam curing that prevents the formation or causes decomposition of ettringite that is normally formed during the early hydration of portland cement. Use of cements having high sulfate contents in which the sulfate has very low solubility also can lead to DEF. In one case where this has been reported (Mielenz et al., 1995), it was thought that the occurrence of DEF was due to the sulfate formed in the clinker of the cement being present as anhydrite and as a component of the silicate phases which are slowly soluble. Ettringite is the product of the reaction between sulfate ions, calcium aluminates, and water. If structures susceptible to DEF are later exposed to water, ettringite can reform in the paste as a massive development of needle-like crystals, causing expansive forces that result in cracking. The extent of development of DEF is dependent on the amount of sulfate available for late ettringite development in the particular concrete and on the presence of water during the service life. Elevated temperatures also increase the potential for damage due to DEF. Prevention or minimization of DEF can be accomplished by lowering the curing temperature, limiting clinker sulfate levels, avoiding excessive curing for potentially critical sulfate to aluminate ratios, preventing exposure to substantial water in service, and using proper air entrainment. Neither the mechanisms involved in DEF nor their potential consequences relative to concrete durability are completely understood. DEF leads to a degradation in concrete mechanical properties such as compressive strength, and can promote increased permeability. A detailed review of over 300 publications dealing with DEF is available (Day, 1992).

Acids and Bases

Acids present in groundwater (e.g., sulfuric or carbonic) and certain plant internal fluids (e.g., boric and sulfuric acids) can combine with the calcium compounds in the hydrated cement paste (i.e., calcium hydroxide, calcium silicate hydrate, and calcium aluminate hydrate) to form soluble materials (calcium salts of attacking acid) that are readily leached from the concrete to increase its porosity and permeability. Organic acids have similar effects. As a result of these reactions, the structure of the hardened concrete is destroyed. The main factor determining the extent of attack is not so much the aggressiveness of the attacking acid, but more the solubility of the resulting calcium salt. The less soluble the salt, the stronger will be its passivating effect. The rate of deterioration is also accelerated if the aggressive chemical solution is flowing. Since under acid attack there is a conversion of the hardened cement, the concrete permeability is not as important as for other types of chemical attack (e.g., leaching and sulfate attack). Due to the large buffering capacity of concrete and the relatively small amount of acid contained in rain, acid rain will convert only an insignificant amount of the concrete (CEB, 1992). Acid rain is even a smaller threat to NPP structures than general civil engineering concrete structures because of their massive cross sections.

As hydrated cement paste is an alkaline material, high quality concretes made with chemically stable aggregates normally are resistant to bases. However, sodium and potassium hydroxides in high concentrations (> 20%) can cause concrete to disintegrate. Under mild chemical attack, a dense concrete with low water-cement ratio may provide suitable resistance. As corrosive chemicals can attack concrete only in the presence of water, designs to minimize attack by acids and bases generally involve the use of protective barrier systems. Table 2.2 presents a listing of the reactivity with concrete of various chemicals that may be found in NPPs or the surrounding environment. Additional information on the effect of chemicals on concrete is available in ACI 515.1R, 1985.

Alkali-Aggregate Reactions

Expansion and cracking, leading to loss of strength, stiffness, and durability of concrete can result from chemical reactions involving alkali ions from the portland cement, calcium and hydroxyl ions, and certain siliceous constituents in aggregates. Three requirements are necessary for disintegration due to alkali-aggregate reactions: presence of sufficient alkali; availability of moisture [$>80\%$ R.H. (relative humidity) referenced to 23°C (73.4°F)]; and the presence of reactive silica, silicate, or carbonate aggregate material. Primary factors influencing alkali-aggregate reactions include the aggregate reactivity (i.e., amount and grain size of reactive aggregate), alkali and calcium concentrations in concrete pore water, cement content (i.e., alkali content), and presence of water. Although alkali-aggregate reactions typically occur within 5 to 10 years of construction, deterioration has not occurred in some structures until 15 or even 25 or more years following construction. The delay in exhibiting deterioration indicates that there may be less reactive forms of silica that can eventually cause deterioration (Mindress and Young, 1981).

Visual detection of alkali-silica reactions (ASR) is difficult in the early stages due to the fineness of the cracks and may go unrecognized for years. If the concrete member is unrestrained, visible concrete damage starts with small surface cracks exhibiting an irregular pattern (or map cracking). When the expansive forces are restrained (e.g., by reinforcement), the cracking pattern will be modified as the expansion will develop in the direction of least constraint (i.e., parallel surface crack patterns propagating inward from the surface for slabs and cracking parallel to compression forces in columns or prestressed members). Pop-outs and glassy appearing seepage of varying composition can appear as a result of alkali-silica reactions. Expansion reactions also can occur as a result of alkali-carbonate reactions (i.e., dedolomitization). Furthermore, it is quite common that once cracking has developed, the cracks can allow access to the interior of the concrete to enable some other deleterious mechanisms to operate (e.g., leaching by percolating water accompanied by precipitation of calcium carbonate on surfaces, steel reinforcement corrosion, and freeze-thaw attack). It has been shown that alkali-silica reactions occurring in concretes contaminated with NaCl increases the risk of chloride-induced corrosion of steel reinforcement (Kawamura, Takemoto, and Ichise, 1989).

In rare circumstances, ASR expansions can be as much as 2 – 3% (Swamy, 1989). Crack widths up to 15 mm (.591 in.) and crack depths to 300 mm (11.8 in.) have been observed in the field (Ono, 1988). Since structures in service are stressed and cracked, expansive strains from ASR of 0.10 to 0.20% superimposed over load-induced cracks can lead to structural distortion and displacements. However, no concrete structure or part of a structure has been reported to have collapsed due to ASR (Hobbs, 1988). Some of the most significant reported problems resulting from ASR are misalignment of structures, displacement of equipment, and spalling at joints. The effects of ASR on engineering properties often cannot be generalized since both the rate of expansion and the total expansion depend on the reactive aggregate, cement type, cement content, constraint, and environment. For expansive strains of 0.5 to 1.5%, loss in compressive strength can vary from 40 to 60%, whereas loss of tensile strength can be as high as 65 to 80%, with loss of elastic modulus from 60 to 80% (Swamy, 1989). Some guidance to indicate the effects of ASR expansion on the residual compressive strength of concrete (lower bound) has been developed (BRITE/EURAM, 1995) [i.e., for restrained expansions (mm/m) due to ASR of 0.5, 1.0, 2.5, and 5.0%, the percentages of residual compressive strengths are 95, 80, 60, and 60, respectively]. In tests of lapped beams in which the effects of ASR on performance were evaluated, it was found that ASR causes a reduction in bond strength (up to 22% for these tests) and a significant reduction in the fatigue life (Ahmed, Burley, and Rigden, 1999). Other investigators using lapped beams have shown reductions in bond strength in excess of 50% with losses for smooth bars greater than for ribbed bars (Chana and Korobokis, 1991; Majlesi, 1994). Prestress developed by the ASR expansion can enhance the shear strength and stiffness of beams (Jones and Clark, 1998)

To establish that ASR is the primary cause of cracking considerable evidence of the reaction must be found, it must be established that expansion has occurred and, in addition, other causes of cracking (e.g., shrinkage and freeze-thaw attack) must be ruled out because the gel may be simply filling microcracks initiated by some other process (Hobbs, 1988). Petrographic examination of the concrete identifies the presence of ASR gel reaction products, characterizes crack patterns for evidence of distress originating within the aggregate particles and identifies development of reaction rims on aggregate particles (Stark, 1991). Detection of ASR during early stages of gel formation (undetectable by unaided visual inspection) is possible using a rapid, nondestructive test developed at Cornell University (Natesaiyer and Hover, 1992). In this test about 6 mm (.24 in.) of concrete surface is removed by grinding (or a recently obtained concrete core can be used) and a 5% solution of uranyl acetate is applied to wet the area. The solution is permitted to react for three to five minutes and then the area is rinsed with water. The surface is then viewed under light from a UV lamp. If ASR is present, it will fluoresce brightly. It is generally recommended that if ASR is indicated by this test, additional petrographic examinations, field testing, and a condition survey be conducted.

2.1.2 Physical Attack

Physical attack involves the degradation of concrete due to external influences and generally involves cracking due to exceeding the tensile strength of the concrete, or loss of surface material. Concrete attack due to overload conditions is not considered as an aging mechanism.

Salt Crystallization

Salts can produce surface scaling and cracking in concrete through volume changes associated with cycles of salt crystallization and dissolution. Structures in contact with fluctuating water levels or in contact with groundwaters containing large quantities of dissolved salts (e.g., NaCl, CaSO₄, Na₂CO₃ and NaSO₄) are susceptible to this type of deterioration. Susceptibility is also increased if the concrete is of high permeability. The problem of salt crystallization is minimized for low permeability concretes and where sealers or barriers have been effectively applied to prevent water ingress or subsequent evaporation.

Freezing and Thawing Attack

Concrete, when in a saturated or near saturated condition, can be susceptible to damage during freezing and thawing cycles produced by the natural environment or industrial processes. Structures constructed without adequate air entrainment and portions of structures where moisture can accumulate are at greatest risk. One hypothesis is that the damage is caused by hydraulic pressure generated in the capillary cavities of the cement paste while critically saturated as the water freezes. Damage to concrete resulting from freezing and thawing attack can take several forms: scaling, spalling, and pattern cracking (e.g., D-cracking) (Mindress and Young, 1981). The damage is incurred after an extended number of cycles and is observed on exposed surfaces of affected structures. Factors controlling the resistance of concrete to freeze-thaw action include air entrainment (i.e., size and spacing of air bubbles) as opposed to entrapped air, water-cement ratio, curing, strength, and degree of saturation. Selection of durable aggregate materials is also important. Guidelines to evaluate if the concrete was produced to provide resistance to freezing and thawing attack are available (ACI 201.2R, 1992; CSA, 1990; ACI 318, 1995).

Abrasion/Erosion/Cavitation

Progressive loss of material at the concrete surface can occur due to abrasion, erosion, or cavitation. Abrasion generally refers to dry attrition, while erosion is normally used to describe wear by the abrasive action of fluids containing solid particles in suspension. Cavitation relates to the loss of surface material

by formation of vapor bubbles and their subsequent collapse, due to sudden change of direction or pressure in rapidly flowing water, on the surface of the structure. Resistance of concrete to abrasion and erosion is dependent on the quality of the concrete (low porosity, high strength) and in particular the aggregate particles used in the mix. While good quality concrete may show good resistance to abrasion and erosion, it may still suffer severe loss of surface material due to cavitation. The best way to guard against the effects of cavitation is to eliminate the cause(s) of cavitation. Guidelines to evaluate if the concrete was produced to provide resistance to abrasion and erosion are available (ACI 201.2R, 1992; ACI 210, 1993).

Thermal Exposure/Thermal Cycling

Elevated temperature and thermal gradients are important to concrete structures in that they affect the concrete's strength (i.e., ability to carry loads) and stiffness (i.e., structural deformations and loads that develop at constraints). The mechanical property variations result largely because of changes in the moisture content of the concrete constituents and progressive deterioration of the cement paste, aggregate, and bond between the two materials (especially significant where thermal expansion values for cement paste and aggregate are markedly different). The response of concrete in terms of strength loss has been divided into three ranges: 20 to 400°C (68 to 752°F), 400 to 800°C (752 to 1,472°F), and above 800°C (1,472°F) (Chan, Peng, and Chan, 1996). In the first range, it was noted that normal strength concretes [<50 MPa (7.25 ksi)] exhibit a slight loss of strength (~15%), whereas higher strength concretes [80 to 100 MPa (11.6 to 14.5 ksi)] maintain their strengths. In the second range, both concretes lose most of their original strength, especially above 600°C (1,112°F). It is within this range that dehydration of the calcium-silicate hydrate (C-S-H) gel is most significant. Above 800°C (1,472°F) only a small fraction of the original concrete strengths remains. As some aggregates in concrete change color at elevated temperatures (e.g., sedimentary and metamorphic)* (Suprenant, 1997), the color changes can be used to estimate the temperature reached.⁺ It has been indicated that up to 300°C (572°F) the concrete color will be normal, its condition unaffected, with surface crazing around 290°C (554°F); from 300 to 600°C (572 to 1,112°F) the concrete will be pink to red and apparently sound, but its strength will be significantly reduced; from 600 to 900°C (1,112 to 1,652°F) the concrete will be gray to buff, and weak and friable; and above 900°C (1,652°F) it will have a buff color (limestone becomes white) with little to no strength (ASTM C 856; Tucker and Read, 1981). The extent of color change varies with type of fine and coarse aggregate. Knowing the magnitude of thermal exposure, a rough estimate of the residual mechanical properties of concrete can be made. Because concrete's in-situ compressive strength generally exceeds design requirements, the modest strength reductions resulting from temperature exposures up to 300°C (572°F) often can be tolerated. Above 300°C (572°F) an estimate of the residual compressive strength and modulus of elasticity can be obtained from published information (e.g., Freskakis et al., 1979) and ASTM C 856. However, each concrete needs to be evaluated because its residual strength after elevated temperature exposure depends on a number of factors such as the temperature attained, type and porosity of aggregate, rate of heating, permeability, use of pozzolans, moisture state, mix proportions, and loading conditions during heating.

In addition to potential reductions in strength and modulus of elasticity, thermal exposure of concrete can result in cracking, or when the rate of heating is high and concrete permeability low, surface spalling can occur. Elevated temperatures diminish the bond between concrete and steel reinforcement (Concrete

* It should be noted that not all aggregates exhibit color changes as a function of temperature, e.g., igneous aggregates.

⁺ Other methods for indicating the magnitude of concrete thermal exposure include differential thermal analysis, X-ray diffraction, thermoluminescence test, and thin-section petrography (Sarkar, Godbole, and Chakrabarti, 1996).

Society, 1990; CIB, 1989). Figure 2.2 indicates the change in bond strength between concrete and plain round mild steel reinforcement as a function of temperature (in this case resulting from fire exposure). Elevated temperatures also are important in that they affect the volume change and creep of concrete (Uddin and Culver, 1975).

Thermal cycling, even at relatively low temperatures [$<65^{\circ}\text{C}$ (149°F)], can have deleterious effects on concrete's mechanical properties (i.e., compressive, tensile and bond strengths, and modulus of elasticity are reduced). Most reinforced concrete structures are subjected to thermal cycling due to daily temperature fluctuations and are designed accordingly (i.e., inclusion of steel reinforcement). At higher temperatures [200 to 300°C (392 to 572°F)], the first thermal cycle causes the largest percentage of damage, with the extent of damage markedly dependent on aggregate type and is associated with loss of bond between the aggregate and matrix (Bertero and Polivka, 1972). Thermal cycles, also can become important if the deformation of the structure resulting from the temperature variations is constrained.

Codes pertaining to nuclear power plant structures generally handle elevated temperature applications by requiring special provisions (e.g., cooling) to limit the concrete temperature at or below a specified value [e.g., 65°C (149°F)]. A design-oriented approach for considering thermal loads on nuclear power plant reinforced concrete structures is available (ACI 349.1R, 1991). Additional information on the effects of elevated temperature on concrete materials and structures is available (Malhotra, 1956; Cruz, 1966).

Irradiation

Irradiation, either fast and thermal neutrons emitted by the reactor core or gamma rays produced as a result of capture of neutrons by members (particularly steel) in contact with concrete, can affect the concrete. The fast neutrons are mainly responsible for the considerable growth, caused by atomic displacements, that has been measured in certain aggregate (e.g., flint). Nuclear heating occurs as a result of energy introduced into the concrete as the neutrons or gamma radiation interact with the molecules within the concrete. It has been indicated that nuclear heating is negligible for incident energy fluxes less than 10^{10} MeV/cm² (6.5×10^{11} MeV/in.²) per sec (ANS, 1985). Gamma rays produce radiolysis of water in cement paste that can affect concrete's creep and shrinkage behavior to a limited extent and also result in evolution of gas. Prolonged exposure of concrete to irradiation can result in decreases in tensile and compressive strengths and modulus of elasticity. Irradiation has little effect on shielding properties of concrete beyond the effect of moisture loss due to temperature increase. Approximate threshold levels necessary to create measurable damage in concrete have been reported in limited research studies (Hilsdorf, 1978). These levels are 1×10^{19} neutrons/cm² (6.5×10^{19} neutrons/in.²) for neutron fluence and 10^{10} rads of dose for gamma radiation. Additional information on the interaction of radiation and concrete is available (Kaplan, 1989).

Fatigue/Vibration

Concrete structures subjected to fluctuations in loading, temperature, or moisture content (that are not large enough to cause failure in a single application) can be damaged by fatigue. Fatigue damage initiates as microcracks in the cement paste, proximate to the large aggregate particles, reinforcing steel, or stress risers (e.g., defects). Upon continued or reversed load application, these microcracks may propagate to form structurally significant cracks that can expose the concrete and reinforcing steel to hostile environments, produce increased deflections, or lead to debonding of rebar from the concrete. Ultimate failure of a concrete structure in fatigue will occur as a result of excessive cracking, excessive deflections, or brittle fracture. Fatigue failure of concrete is unusual because of its good resistance to fatigue (ACI 215, 1974) and concrete structures are designed using codes that limit design stress levels to values below concrete's endurance limit. However, as structures age, there may be instances of local fatigue damage at

locations where reciprocating equipment is attached, or at supports for pipes that exhibit flow-induced vibrations.

Settlement

All structures have a tendency to settle during construction and early life. Excessive settlement or differential settlement can cause misalignment of equipment and lead to overstress conditions in structures (e.g., cracking). The amount of settlement is dependent on the physical properties of the foundation material at the site, which may range from bedrock (minimal settlement expected) to compacted soil (some settlement expected). Settlement is generally allowed for in the design of the structures and is not expected to be significant. When the structure is sited on soils, the potential for settlement is acknowledged and monitoring programs may be implemented to confirm that design allowables are not exceeded. In general, most of the settlement will occur within a few months after construction and become negligible after this period.

2.2 Mild Steel Reinforcing Systems

Mild steel reinforcing systems are provided in concrete structures to control the extent and width of cracks at operating temperatures, resist tensile and compressive stresses for elastic design, and provide structural reinforcement where required by limit condition design procedures. Potential causes of degradation of the mild reinforcing steel are corrosion, elevated temperature, irradiation, and fatigue. Of these, corrosion is the factor of most concern for aging management of NPP structures. Information on the other potential degradation factors is provided for completeness and special situations that might occur.

2.2.1 Corrosion

Corrosion of conventional steel in concrete is an electrochemical process that can assume the form of either general or pitting corrosion. Both water and oxygen must be present for corrosion to occur (i.e., there is no corrosion in dry concrete or in concrete fully immersed in water that does not contain entrained air). The electrochemical potentials that form the corrosion cells may be generated in two ways: (1) composition cells formed when two dissimilar metals are embedded in concrete, such as steel reinforcement and aluminum conduit, or when significant variations exist in surface characteristics of the steel; and (2) concentration cells formed due to differences in concentration of dissolved ions in the vicinity of steel, such as alkalis, chlorides, and oxygen (Mehta, 1986). As a result, one of two metals (or different parts of the same metal when only one metal is present) becomes anodic and the other cathodic to form a corrosion cell. Other potential causes of corrosion include the effects of stray electrical currents or galvanic action with an embedded steel of different metallurgy.

In good-quality, well-compacted concrete, reinforcing steel with adequate cover should not be susceptible to corrosion because the highly alkaline conditions present within the concrete ($\text{pH} > 12$) causes a passive iron oxide film ($\gamma\text{-Fe}_2\text{O}_3$) to form on the surface (i.e., metallic iron will not be available for anodic activity). The passive film may be relatively thick to inhibit corrosion by providing a diffusion barrier to the reaction products of the reacting species (Fe and O_2), or as is more common, the layer can be very thin. The passive film does not actually stop corrosion, but reduces the corrosion rate to an insignificant level (ACI 222, 1999). Corrosion can occur if this passivating environment is altered by a reduction of the pH of the concrete or by introduction of chlorides that destabilize the passive layer. Figure 2.3 summarizes primary and secondary factors that can depassivate the steel reinforcement (Gonzalez et al., 1996). The discussion below will only address the primary factors.

Reduction of the concrete pH can occur as a result of leaching of alkaline substances by water or carbonation [i.e., calcium hydroxide is converted to calcium carbonate (calcite)].* It has been reported that when the concrete pH falls below about 11.5 (Erlin and Verbeck, 1975), a porous oxide layer (rust) can form on the reinforcing steel due to corrosion. More recent research indicates that the corrosion threshold is considered to be reached once the pH is reduced to 9.5 and there is a steep decrease in the electrochemical corrosion potential indicating decomposition of the passive layer at a pH about 8 (Gonzalez et al., 1983). Carbon dioxide is a minor component of the atmosphere (~0.03% by volume). The penetration of carbon dioxide from the environment is generally a slow process dependent on the concrete permeability, the concrete moisture content, and the carbon dioxide content, temperature, and relative humidity of the ambient medium (i.e., 50 to 75% R.H. with 60-65% being maximum and extremes being capable of preventing carbonation). The rate of carbonation at exposed surfaces is considered to be roughly proportional to the square root of time for concrete kept continuously dry at normal relative humidities (Roberts, 1981). Carbonation generally proceeds in concrete as a front, beyond which the concrete is unaffected, and behind which the pH is reduced. As shown in Figure 2.4, carbonation penetrates more quickly near the corners where reinforcement usually comes closest to the surface, and into concrete where it is cracked and along reinforcement where it is locally unbonded (Pullar-Strecker, 1987). Table 2.3 provides some guidance on expected depths of carbonation for various grades (strengths) of concrete according to time and exposure type (Allen and Forrester, 1983). Table 2.4 indicates expected times to corrosion (in years) for various water/cement ratios and depths of cover (Kobayashi, Suzuki, and Uno, 1990).

Carbonation depth assessments made on 200 bridges chosen to represent a population of nearly 6,000 structures indicated that carbonation depths were generally small [i.e., < 5 mm (.2 in.)] and the main threats to durability were inadequate concrete cover and presence of chlorides (Wallbank, 1989). Carbonation, however, may be accelerated due to the concrete being porous (i.e., poor quality) or the presence of microcracks. If significant amounts of chloride are also present in the concrete, then it is to be expected that the corrosive action on embedded steel will be further enhanced by carbonation of the concrete.+ This occurs because carbonation can result in decomposition of the complex hydrated chloride salts formed by the reaction of chloride with cement components liberating more chloride into solution (Roberts, 1981). In NPPs, carbonation is most likely to occur at inside concrete surfaces exposed to relatively low humidities and elevated temperatures (Clifton, 1991). The extent of carbonation can be determined by treating a freshly exposed concrete surface with phenolphthalein (RILEM, 1988). More precise methods for determining carbonation depth include petrography (microscope), and using X-ray diffraction and differential thermal analysis techniques to analyze drilled powder samples obtained from various depths (Sims, 1994).

The most common cause of initiation of corrosion of steel in concrete is the presence of chloride ions that can destroy the passive iron oxide film on the steel reinforcement even at high alkalinities (pH > 11.5) [e.g., Clifton (1991) notes that at a pH of 13.2 more than 8000 ppm of chloride ions are required to induce

* Carbonation causes the strength of concrete to increase, but this is generally of insignificant consequence because normally only the surface zone becomes carbonated. Although carbonation reduces the concrete permeability, it produces a greater propensity for shrinkage cracking that can negate the positive durability effects of reduced permeability (Sims, 1994).

+ It has been shown that corrosion caused by carbonation increases with increasing chloride ion concentration provided that the carbonation rate itself was not retarded by the presence of chlorides (Roper and Baweja, 1991)

corrosion, however, at a pH of 11.6 only about 71 ppm are required]. The mechanism through which the gamma Fe_2O_3 film is destroyed is not fully understood in that either the chloride ions convert the insoluble iron oxide to soluble iron chloride or they become included in the oxide layer in a manner that makes it permeable to air (Mehta and Gerwick, 1982). Chloride penetration also introduces a source of variation in concentration along the steel, forming concentration cells. Chloride ions are attracted to anodic regions of the steel to increase the local concentration. Increased acidity in the region of the anodic sites also can lead to local dissolution of the cement paste.

Cracks resulting from such causes as direct loading of the structure, or due to chemical or physical causes, can allow the rapid penetration of carbon dioxide or chloride ions to the steel reinforcement, thereby causing local failure of the passive oxide film.* This may lead to concentration of corrosion over a small area resulting in pitting corrosion and can be of concern as it may lead to reduction in bar cross-section. The volume of corrosion products may be so small that no external signs appear. It has been indicated that the presence of the crack is more important than its width, particularly when in the tension zone of a loaded beam [i.e., the crack width influences the speed at which corrosion begins but because this period is short, the influence is limited and the width has only an infinitesimal effect on the spread of corrosion (Francois and Arliguie, 1991)]. Diffusion of chlorides can occur in sound concrete and proceed through the capillary pore structure of the cement paste. Thus cracks in the concrete are not a prerequisite for transporting chlorides to the reinforcing steel. The rate of diffusion is strongly dependent on a number of factors (e.g., water/cementitious material ratio, type cement, temperature, and maturity of concrete). Some of the chlorides react chemically with cement components (e.g., calcium aluminates) and are effectively removed from the pore solution. The fraction of total chlorides available in the pore solution to cause a breakdown of the passive film is a function of a number of parameters [e.g., C_3A and C_4AF content, pH, and source of chlorides (mix or environment)].⁺ The threshold value of chloride concentration below which significant corrosion does not occur is also dependent on these parameters. Different organizations have proposed various values: BS 8110 (1985) and European Standard ENV 206 (1992) (0.4% Cl by mass cement); and ACI 318 (1995) (0.15% water soluble Cl by mass cement). Investigators have reported minimum threshold values for chloride ion contents to initiate corrosion in the range of 0.026 to 0.033% [approximately 0.6 to 0.8 kg/m^3 (0.0375 to 0.0499 pcf)] total chloride ion content by mass of concrete (ACI 222R-9X). The threshold acid-soluble chloride contents reported by various investigators to initiate steel corrosion range from 0.15 to 1.0% (Hussain, 1996). However, as shown in Figure 2.5, the critical chloride content can be higher or lower than the proposed values depending on whether the concrete is carbonated or not and the environment (i.e., relative humidity) (CEB, 1992).

Chlorides may be present in concrete due to external sources (seawater effects, deicing salts, etc.) or may be naturally introduced into the concrete via aggregate or mix water transport. Furthermore, when large amounts of chloride are present, concrete tends to hold more moisture, which also increases the risk of steel corrosion by lowering concrete's electrical resistivity. Once the passivity of the steel is destroyed, the electrical resistivity of concrete and availability of oxygen control the rate of corrosion. Oxygen availability at cathodic sites is essential for corrosion to occur. In some instances where the oxygen

* In tests where cracked reinforced concrete beams were exposed to a marine environment, it was found that corrosion was somewhat accelerated in the regions of flexural cracks, however, longitudinal cracking produced by corrosion dominates corrosion occurrence with the initiation and growth of the longitudinal cracks controlled by the restraining action of transverse reinforcement (Misra and Uomoto, 1991). Once the longitudinal cracking exceeded a critical length, the corrosion rate accelerates.

⁺ A distinction needs to be made between chlorides added during the mix and those acquired by diffusing into the concrete from the environment. Added chlorides can combine with C_3A and ferric compounds in cement to give Friedel's salt, whereas chlorides resulting from diffusion cannot. Chlorides from diffusion therefore are potentially more hazardous (González et al., 1998)

supply is limited at active anodes the resulting corrosion products may be green, white or black in color (Arya and Wood, 1995). The green product probably is a chloride complex while the black product is magnetite (Fe_3O_4). Corrosion under oxygen-deficient conditions such as this is considered to be more serious than haematite ($\text{Fe}_2\text{O}_3 \cdot 3 \text{H}_2\text{O}$), or normal red-brown rust, since it may go on some time before any visible evidence.

The transformation of metallic iron to ferric oxide (rust) is accompanied by an increase in volume that can cause cracking and spalling of the concrete. Corrosion of reinforced concrete structures can be visible in the form of rust spots, cracks in the concrete cover along the line of bars, and spalling. Generally, because the corrosion is fairly uniform, cracking of the cover concrete in normally reinforced structures usually occurs prior to a particular structural cross-section becoming excessively weak, thus giving visual warning of the deterioration (BRE, 1982). Occasionally, however, cover spalling occurs before any visible sign of deterioration at the concrete surface is apparent. Figure 2.6 presents a summary of effects and visible signs of corrosion on reinforced concrete structures (Gonzalez, 1996). Structural strength and serviceability are only reduced and jeopardized when corrosion of reinforcement causes a significant loss of steel cross section and/or there occurs a loss of bond between the steel and concrete (Rasheeduzzafar, Al-Saadoun and Al-Gahtani, 1992). This is supported by results of tests of corrosion affected beams detailed with adequate development length and shear stirrups (Al-Sulaimani et al., 1990). In these tests there was no significant loss of bond up to about 5% corrosion, as measured by loss of metal mass. After 5% corrosion, only a 12% reduction was observed in the load-carrying capacity which was attributed to loss of steel section. As a reference, cracking of the concrete cover was first observed at 0.75% metal loss.

In addition to cracking and spalling, corrosion will result in a reduction in effective steel cross-section (e.g., load capacity), a decrease in ductility, and loss of composite interaction between concrete and steel due to bond deterioration. Figure 2.7 provides an indication of the significance of corrosion (weight loss) on the steel reinforcement yield point, tensile strength, and elongation (Morinaga, 1990). These results were obtained by testing steel reinforcement that had been removed from the slab of a building that suffered severe corrosion damage due to chloride attack. Data on loss of steel reinforcement cross-sectional area as a function of time for homogeneous corrosion (e.g., carbonation) and pitting corrosion (e.g., chloride attack) at a current intensity of $1 \mu\text{A}/\text{cm}^2$ ($6.45 \mu\text{A}/\text{in.}^2$) [$\mu = 1 \times 10^{-6}$] is presented in Figure 2.8 (Rodriguez, 1996). Reductions in elongation at maximum load of 30 and 50% have been reported for cross-section losses of 15 and 28%, respectively. Although reduced, the elongation reductions generally still exceeded the minimum code requirements.

Loss of bond to concrete due to the formation of expansive corrosion products has been identified as the primary cause of flexural strength loss of corroding reinforced concrete beams (Al-Sulimani et al., 1990). Bond pullout data for 150-mm (5.91 in.) concrete cubes containing bars having diameters of either 10, 14, or 20 mm (.394, .551, or .787 in.) indicate that up to 1 percent corrosion (loss of bar weight), the bond strength increases (up to about 50%) with increasing corrosion (Al-Sulaimani et al., 1990). This can be explained on the basis of increased surface roughness of the bars with the growth of firm rust that tends to enhance the holding capacity. However, with further corrosion the bond stress declines consistently until it becomes negligible for about 8.5, 7.5, and 6.5 percent corrosion for the 10, 14, and 20-mm (.394, .551, and .787 in.) bars, respectively. The significant degradation of bar lugs and reduction of section, as well as the heavy layer of corroded material adhering to the concrete at these corrosion levels contribute to the significant decline in bond stress (e.g., loss of mechanical interlocking between ribs and deterioration of concrete, and influence of lubricating effect of flaky corroded material between bars and concrete).

The interrelationship of cover concrete, bar diameter, and corrosion was investigated (Morinaga, 1988). Cylindrical specimens either 100- or 150-mm (3.94 or 5.91 in.) diameter by 100-mm (3.94 in.) high containing either a 9-, 19-, or 25-mm (.354, .748, or .984 in.) diameter bar with an embedment length of 100 mm (3.94 in.) were subjected to different degrees of corrosion (i.e., rebar weight loss). Test results

indicate that the concrete-rebar bond strength increased (up to 200 or 300%) with increasing corrosion until sufficient corrosion was induced to produce concrete cracking. With increasing surface cracking the bond strength decreased. It was found for constant bar diameter that the bond strength increased as the cover thickness increased. Also, for constant cover thickness it was found that the bond strength increased as the bar diameter decreased. Results of bond tests using cubic specimens reinforced with four bars at the corners indicated that if the cover is cracked by reinforcement corrosion, neither the concrete quality nor the C/d ratio influenced the residual bond strength (Rodriguez, 1996).

Bond test results have also been presented using 100-mm (3.94 in.) diameter by 1-m (3.28 ft) long concrete specimens containing a single longitudinal No. 20 bar ($C/d = 2$) that was corroded to levels representing weight loss of bar material ranging from 0 to 17.5% (Amleh and Mirza, 1999). Average surface concrete crack widths obtained for corrosion levels (weight loss) of 4, 5.5, 11, 11.5, 12, and 17.5% were 0.15, 0.2, 6.0, 1.5 to 3.0, 1.5 to 4.0, and 9.0 mm, (.00591, .00787, .236, .0591 to .118, .0591 to .157, and .354 in.) respectively. Tensile force-elongation results for these specimens indicated that as the level of corrosion increased, spacing of the transverse cracks increased (i.e., fewer cracks formed) indicating a decrease in bond capacity between the corroded steel and the concrete. At 4% weight loss there was a 9% decrease in bond strength relative to an uncorroded control specimen while at a 17.5% weight loss there was a 92% loss of bond.

Bond characteristics of corroding reinforcement in concrete beams loaded in flexure have also been evaluated (Mangat and Elgarf, 1999). Reinforced concrete beams 910-mm (35.8 in.) long by 150-mm (5.91 in.) deep by 100-mm (3.94 in.) wide containing two 10-mm (.394 in.) diameter steel bars as tensile reinforcement [20 mm (.787 in.) cover] ($C/d = 2$) and a steel hinge at the mid-beam compression face were tested using a RILEM test procedure (RILEM, 1973). Prior to loading in four-point bending, corrosion was induced representing different levels of steel reinforcement diameter loss up to 5%. Surface crack widths prior to loading corresponding to corrosion losses of 0.3, 0.4, 0.5, 1.0, 2.0, and 5.0% were 0.05, 0.05, 0.20, 0.30, 0.40, and 0.55 mm (.00197, .00197, .00787, .0118, .0157, and .0217 in.), respectively. Results obtained indicated that the bond strength increased by about 25% for corrosion losses of 0.4%, and then decreased for greater corrosion losses.

2.2.2 Elevated Temperature

The properties of mild steel reinforcement of most importance to design are the yield stress and modulus of elasticity. Almost all of the information available on elevated temperature effects addresses the residual strength of reinforcing bars after fire exposure, and is somewhat controversial. One source reports that the mechanical properties of steels that have been heat treated are largely unaffected by heating and normal cooling as long as the maximum temperature does not exceed 704°C (1,299°F) (AISC, 1980). Another reference indicates that temperatures up to 500°C (932°F) do not degrade the yield stress or ultimate strength of hot-rolled bars, but 700°C (1,292°F) causes significant reductions in both [e.g., yield stress may be reduced by 50% (Malhotra, 1982)]. Tests in which a number of ASTM A615 Grade 60 12-mm (.472 in.) diameter reinforcing bars were heated to temperatures up to 802°C (1,476°F), held at temperature for one hour, and then permitted to slowly cool to room temperature indicate that the general nature of the stress-strain curve does not change in that all test results exhibited sharply defined yield points followed by a yield plateau followed by strain hardening (Edwards and Gamble, 1986). Reductions in both the yield and ultimate stress were observed at temperatures above 500°C (932°F) with the largest reductions being 27 per cent [749°C (1,380°F)] and 17% [700°C (1,292°F)], respectively. At 700°C (1,292°F) elongations [203-mm (7.99 in.) gage length] increased about 40 per cent. Data for German reinforcing steels (Schneider, 1981) indicate that for temperatures up to ~200°C (392°F), the yield strength is reduced by 10% or less, and at 500°C (932°F) it falls to about 50% its reference room temperature value. Hot-rolled steels tend to resist the effects of temperature better than cold drawn or

twisted steel. With cold-worked steel, the work hardening effect that increases the strength of the reinforcement under normal exposure conditions suffers regression if exposed to high temperatures [e.g., >400°C (752°F)] (El-Nesr, 1995). With temperatures lower than 400°C (752°F) a residual hardening due to aging may be observed. The steel modulus of elasticity exhibits similar reductions with increasing temperature to that of the yield stress. Other data (Smith, 1978) confirm the effects of temperatures above 200°C (392°F) on the mild steel reinforcing as well as providing a threshold temperature of about 300°C (572°F) for loss of bond properties with the concrete.

2.2.3 Irradiation

Neutron irradiation produces changes in the mechanical properties of carbon steels (e.g., increased yield strength and rise in the ductile-to-brittle transition temperature). The changes result from the displacement of atoms from their normal sites by high-energy neutrons, causing the formation of interstitials and vacancies. A threshold level of neutron fluence of 1×10^{18} neutrons per square centimeter (6.5×10^{18} neutrons per square in.) has been cited for alteration of reinforcing steel mechanical properties (Cowen and Nichols, 1968). Fluence levels of this magnitude are not likely to be experienced by the safety-related concrete structures in NPPs, except possibly in the concrete primary biological shield wall over an extended operating period (SAIC, 1977).

2.2.4 Fatigue

Fatigue of the mild steel reinforcing system would be coupled with that of the surrounding concrete. The result of applied repeated loadings, or vibrations, is generally a loss of bond between the steel reinforcement and concrete. For extreme conditions, the strength of the mild steel reinforcing system may be reduced or failures may occur at applied stress levels less than yield. However, there have been few documented cases of fatigue failures of reinforcing steel in concrete structures and those published occurred at relatively high stress/cycle combinations (ACI Committee 215, 1974). Because of the typically low normal stress levels in reinforcing steel elements in NPP safety-related concrete structures, fatigue failure is not likely to occur.

2.3 Anchorage Embedments

Anchorage to concrete is required for heavy machinery, structural members, piping, ductwork, cable trays, towers, and many other types of structures. An anchorage might have to meet certain requirements for ease of installation, load capacity, resistance to vibration, preload retention, temperature range, corrosion resistance, post-installation or pre-installation, and ease of inspection and stiffness (Meinheit and Heidbrink, 1985). There are three basic principles upon which concrete anchorages work: (1) friction locking – the working principle of expansion anchors; (2) mechanical interlock – cast-in-place, headed studs or undercut anchors; and (3) bonding – resin or chemical anchors.

In meeting its function, loads that the anchor must transfer to the concrete vary over a wide combination of tension, bending, shear, and compression. Several potential factors related to failure or degradation of the anchorage systems include design detail errors, installation errors (improper embedment depth or insufficient lateral cover, improper torque), material defects (low anchor or concrete strengths), shear or shear-tension interaction, slip, and preload relaxation (Meinheit and Heidbrink, 1985). Of the features affecting the load-bearing behavior of anchors, one of the most important is the state of the material into which the anchor is secured – namely whether the concrete is cracked or not. Torque-controlled expansion anchors fail due to concrete breakout when anchored in uncracked concrete, but fail due to pull-out when anchored in cracked concrete because their expansion forces are reduced by the opening of the cracks making further expansion impossible. The load-bearing capacity of resin or chemical anchors

also is strongly affected by cracks in concrete, due mainly to variations in cracks over the circumference of the drilled hole. In structural elements having a high percentage of reinforcement, additional reduction in the ultimate load an anchor can resist may occur due to decrease in the volume (or area) of the concrete available to transmit load into the concrete element. Failures of anchors in uncracked concrete take the form of a breakout cone in the concrete. In cracked concrete failure is due to pull-out. Aging effects that could impair the ability of an anchorage to meet its performance requirements would be primarily those that result in deterioration of concrete properties or cracking, because if a failure did occur, it would most likely initiate in the concrete.

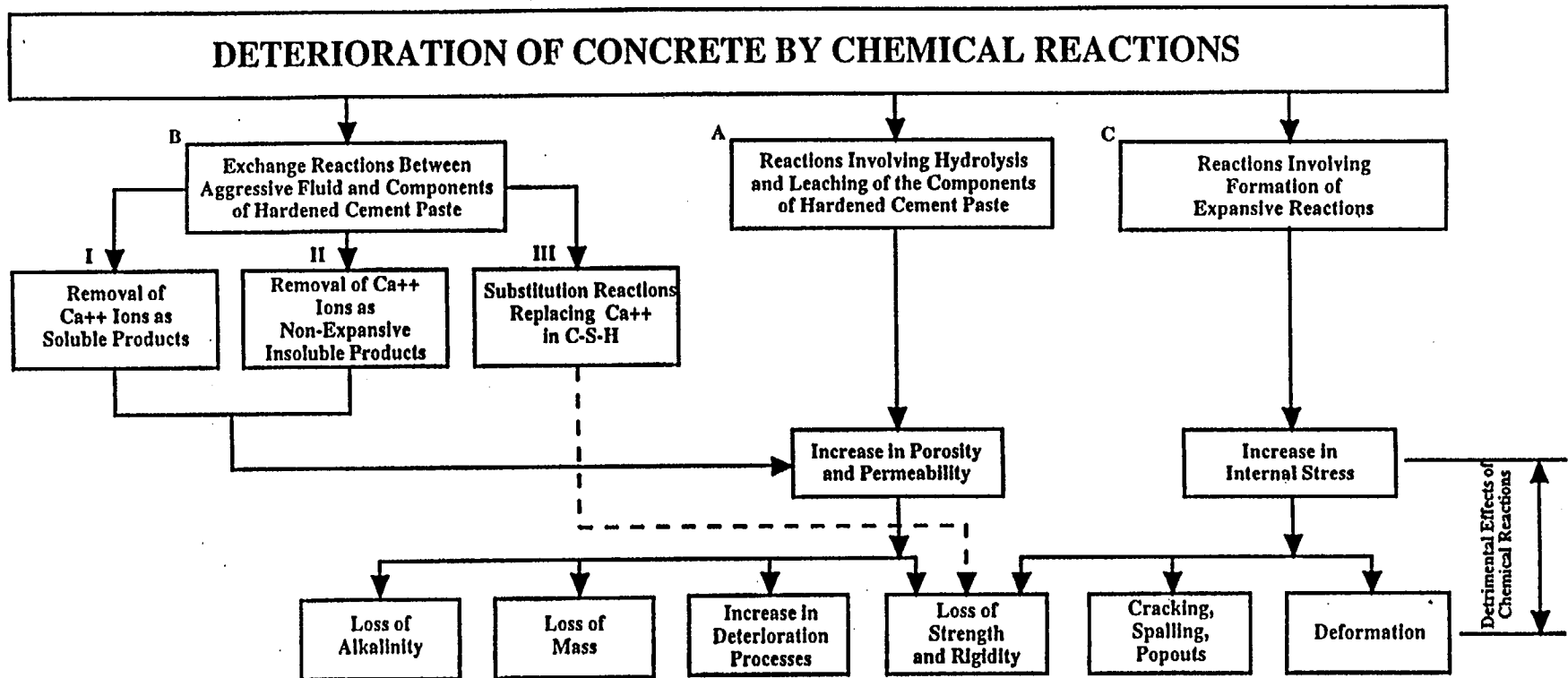
2.4 Important Aging Effects for Use in this Study

The previous sections contain discussions of those factors which can degrade the performance of reinforced concrete structures (these are summarized in Table 2.1). Based on experience, the predominant aging mechanisms/effects that should be considered are corrosion of embedded steel reinforcement, cracking, and spalling of concrete cover due either to corrosion or freezing and thawing. Most of the other degradation mechanisms would have resulted in observable damage early in the plant life and actions would probably have been taken to resolve any identified problems. The factors in Table 2.1 which are placed into this category are: exposure to aggressive acids and bases; cyclic loads/vibration; consolidation or movement of soil; and cyclic load effects on steel.

Second, many of the degradation mechanisms are the result of improper concrete mix design or construction practices. The QA/QC procedures employed during the design and construction of NPPs together with the review process undertaken during plant licensing make it unlikely that improper concrete mixes or construction practices would be used. The following factors listed in Table 2.1 which are eliminated from further consideration for this reason are: percolation of fluid through concrete; exposure to alkali and magnesium sulfates; combination of reactive aggregate, high moisture levels, and alkalis; thermal exposure; irradiation; elevated temperature of steel; and irradiation of steel.

The remaining degradation mechanisms which are considered during the study are:

- Exposure to flowing gas or liquid carrying particulate and abrasive components - This is likely to affect intake structures and result in abrasion of the concrete surface.
- Exposure to thermal cycles at low temperature (freeze thaw) - This can occur on any exterior surfaces in locations where freezing temperatures are found. It is most likely to occur on horizontal surfaces which can hold surface water allowing it to penetrate into the concrete or on buried portions of concrete structures which are below the water table but above the freeze depth. Its effect is spalling of the concrete.
- Exposure to water containing dissolved salts - This mechanism is likely to affect intake structures in areas where water levels can fluctuate and concrete structures in contact with soils having high sulfate contents. Its manifestation is cracking and scaling of the concrete.
- Depassivation of steel due to carbonation or presence of chloride ions - This can occur in any concrete structure but is more likely in those structures subjected to some external source of chlorides or locations where concrete carbonation can occur. The result is a corrosion of the steel with subsequent loss of steel area, concrete spalling resulting from the expansion of the steel as it corrodes, and loss of bond strength as the steel surface changes and the concrete cracks.



- A: Softwater attack on calcium hydroxide and C-S-H present in hydrated portland cements;
 B(I): acidic solution forming soluble calcium compounds such as calcium sulfate, calcium acetate, or calcium bicarbonate;
 B(II): solutions of oxalic acid and its salts, forming calcium oxalate;
 B(III): long-term seawater attack weakening the C-S-H by substitution of Mg^{++} for Ca^{++} ;
 C(1): sulfate attack forming ettringite and gypsum;
 C(2): alkali-aggregate attack;
 C(3): corrosion of steel in concrete; and
 C(4): hydration of crystalline MgO and CaO.

Figure 2.1 Types of Chemical Reactions Responsible for Concrete Degradation (Mehta and Gerwick, 1982)

Permission to use this copyrighted material is granted by the above author(s).

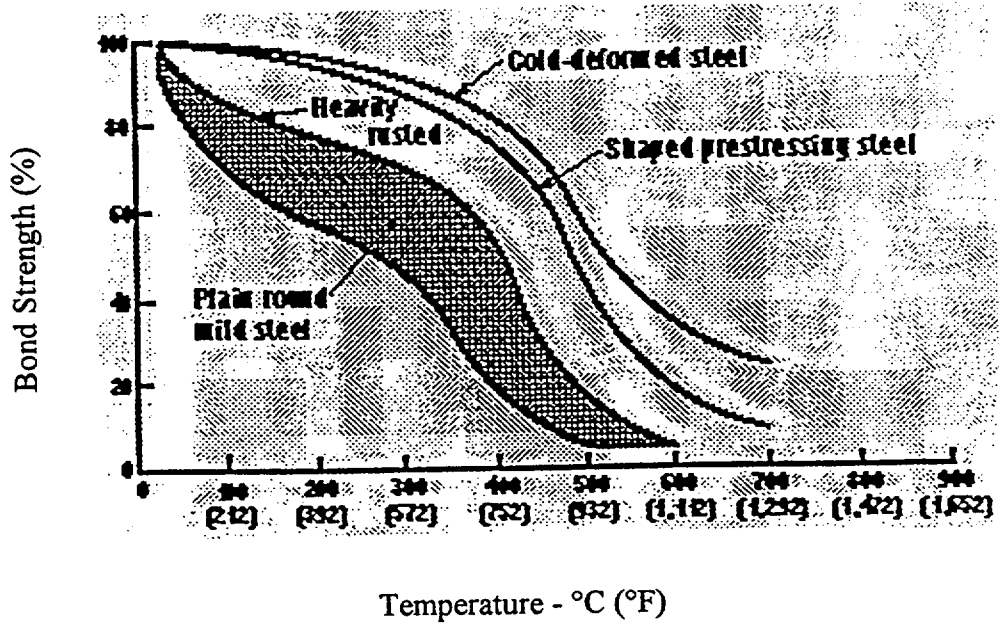


Figure 2.2 Bond Strength Between Concrete and Steel.
 (CIB Report No. 111, "Repairability of Fire-Damaged Concrete Structures").
 Permission to use this copyrighted material is granted by CIB.

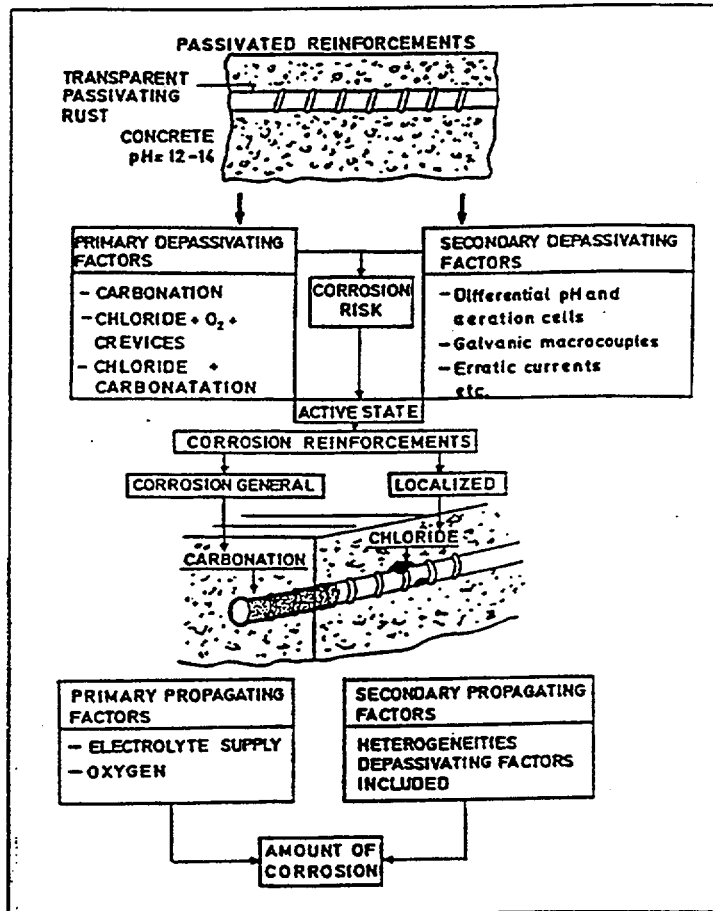
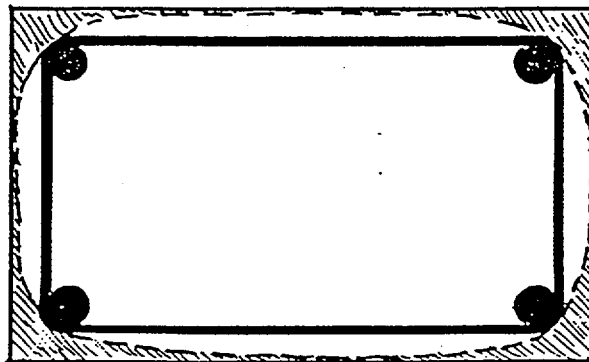


Figure 2.3 Factors Leading to Depassivation of Steel in Concrete (Gonzalez et al., 1996).
Permission to use this copyrighted material is granted by the above author(s).



Carbonation penetrates more quickly near corners—usually where the main reinforcement comes closest to the surface.



Carbon dioxide can penetrate into concrete where it has cracked, and along the reinforcement where is locally debonded.

Figure 2.4 Carbonation Penetration (Pullar-Strecker, 1987).
Reproduced by kind permission of CIRIA.

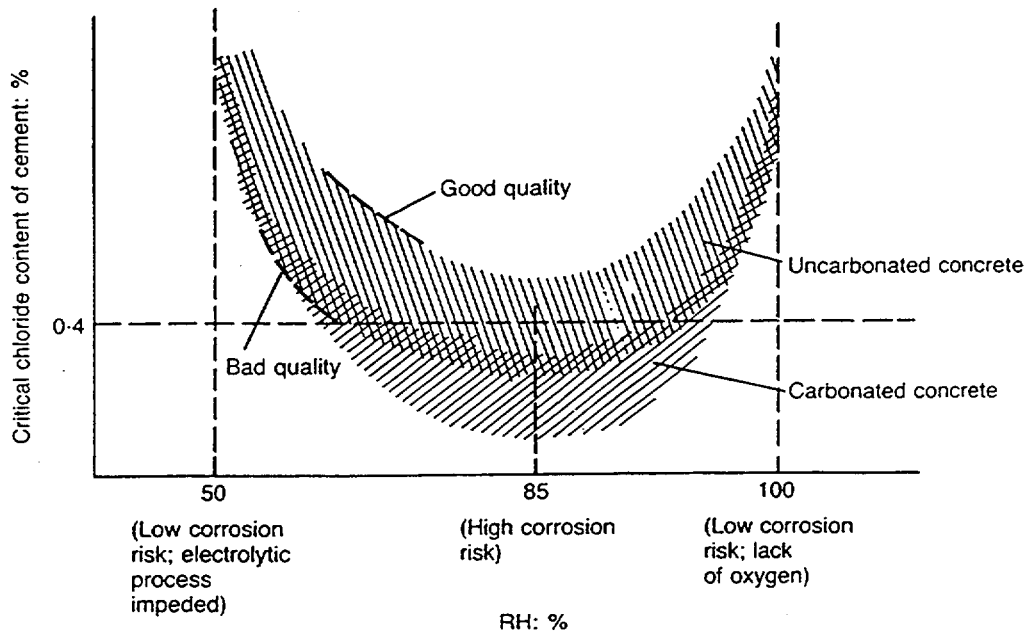


Figure 2.5 Variation of Critical Chloride Content with Environment (CEB, 1992). Reprinted with permission of *fib*, Federation Internationale du Beton (CEB-FIB).

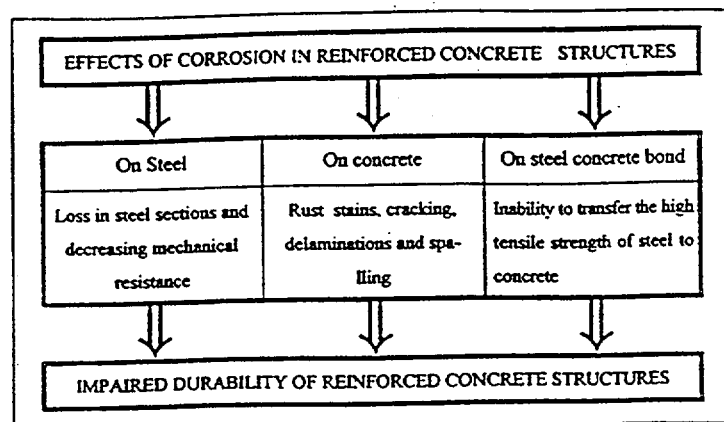
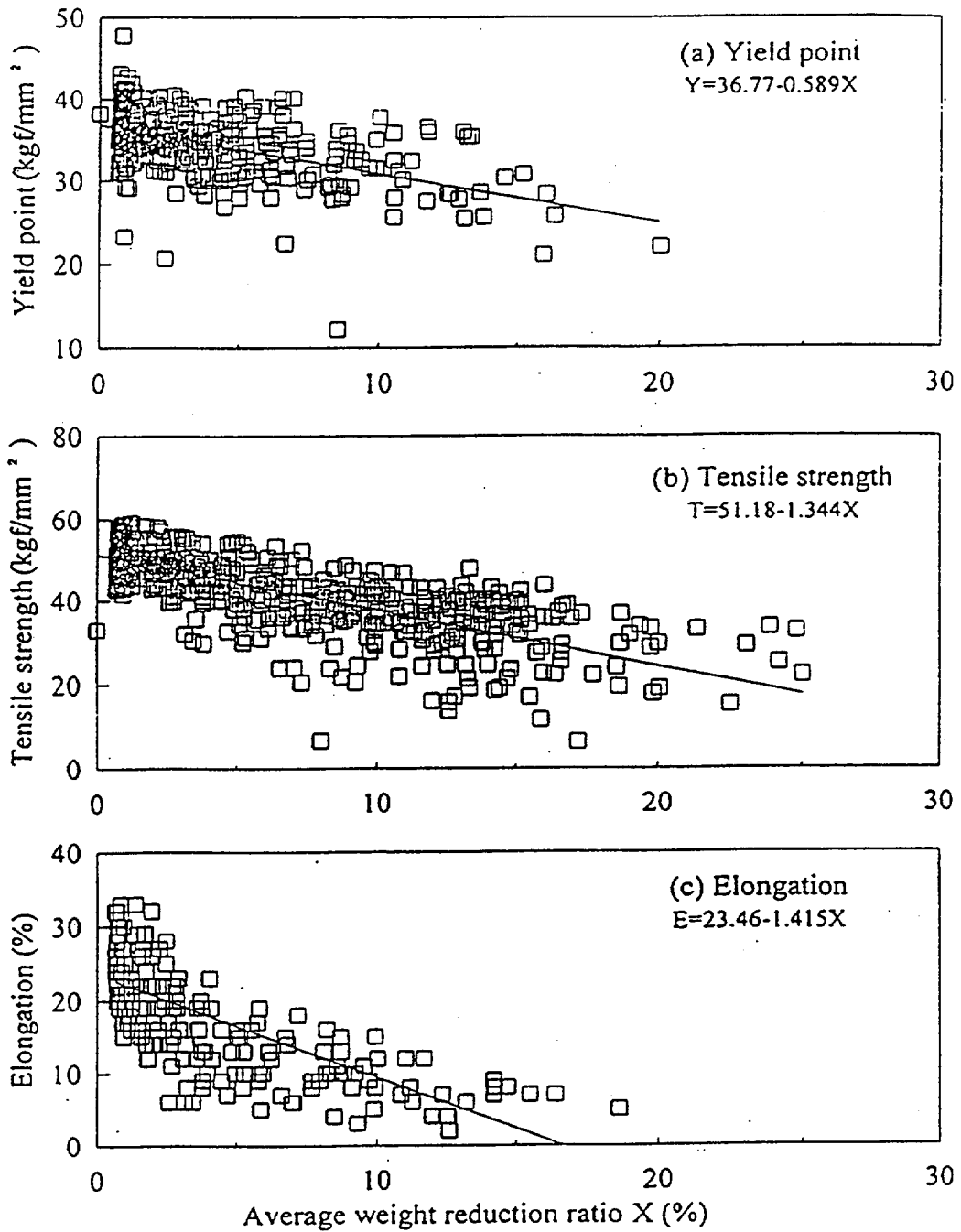


Figure 2.6 Effects and Visible Signs of Corrosion on RC Structures (Gonzalez, 1996). Permission to use this copyrighted material is granted by the above author(s).



Note: $1 \text{ kgf/mm}^2 = 1,422 \text{ psi}$

Figure 2.7 Properties of Corroded Steel Reinforcement (Morinaga, 1990).
 Permission to use this copyrighted material is granted by the above author(s).

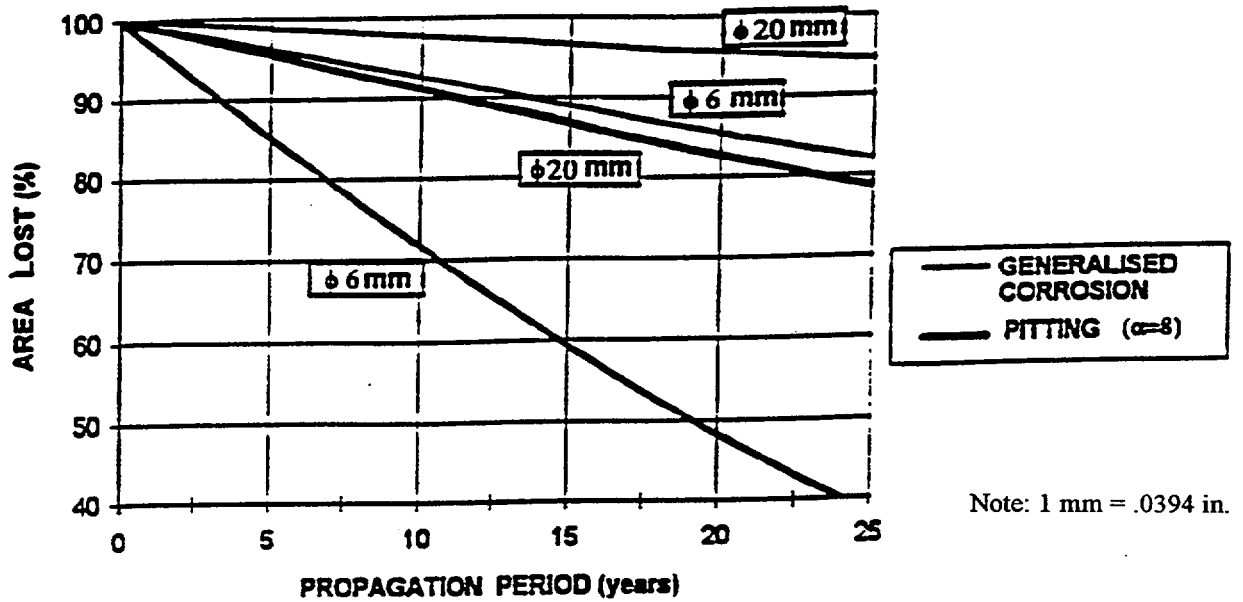


Figure 2.8 Loss of Steel Section Due to Corrosion ($I_{\text{corr}} = 1 \mu\text{A}/\text{cm}^2$) (Rodriguez, et al., 1996). Proceedings of the 7th International Conference on the Durability of Building Materials and Components, Stockholm, Sweden, 1996. Permission to use this copyrighted material is granted by the above author(s).

Table 2.1 Degradation Factors that can Impact the Performance of Safety-Related Concrete Structures (IAEA, 1998).

Permission to use this copyrighted material is granted by IAEA.

a. Concrete

Ageing Stressors/ Service Conditions	Ageing Mechanism	Ageing Effect	Potential Degradation Sites	Remarks (e.g., Significance)
Percolation of fluid through concrete due to moisture gradient	Leaching and efflorescence	Increased porosity and permeability; lowers strength	Near cracks; Areas of high moisture percolation	Makes concrete more vulnerable to hostile environments; may indicate other changes to cement paste; unlikely to be an issue for high quality, low-permeability concretes
25 Exposure to alkali and magnesium sulfates present in soils, seawater or groundwater	Sulfate attack	Expansion and irregular cracking	Subgrade structures and foundations	Sulfate-resistant cements or partial replacement of cements used to minimise potential occurrence
Exposure to aggressive acids and bases	Conversion of hardened cement to soluble material that can be leached	Increased porosity and permeability	Local areas subject to chemical spills; adjacent to pipework carrying aggressive fluids	Acid rain not an issue for containments
Combination of reactive aggregate, high moisture levels, and alkalis	Alkali-aggregate reactions leading to swelling	Cracking; gel exudation; aggregate pop-out	Areas where moisture levels are high and improper materials utilised	Eliminate potentially reactive materials; use low alkali-content cements or partial cement replacement
Cyclic loads/vibration	Fatigue	Cracking; strength loss	Equipment/piping supports	Localised damage; fatigue failure of concrete structures unusual

Table 2.1 (cont.) Degradation Factors that can Impact the Performance of Safety-Related Concrete Structures (IAEA, 1998).

Permission to use this copyrighted material is granted by IAEA.

a. Concrete (cont.)

Ageing Stressors/ Service Conditions	Ageing Mechanism	Ageing Effect	Potential Degradation Sites	Remarks (e.g., Significance)
Exposure to flowing gas or liquid carrying particulates and abrasive components	Abrasion; Erosion; Cavitation	Section loss, loss of cover concrete to expose rebar to corrosion	Cooling water intake and discharge structures	Unlikely to be an issue for containment, intake structures at most risk
Exposure to thermal cycles at relatively low temperatures	Freeze/thaw	Cracking; spalling	External surfaces where geometry supports moisture accumulation	Air-entrainment utilised to minimise potential occurrence
26 Thermal exposure/ thermal cycling	Moisture content changes and material incompatibility due different thermal expansion values	Cracking; spalling; strength loss; reduced modulus of elasticity	Near hot process and steam piping	Generally an issue for hot spot locations; can increase concrete creep that can increase prestressing force losses
Irradiation	Aggregate expansion; hydrolysis	Cracking; loss of mechanical properties	Structures proximate to reactor vessel	Containment irradiation levels likely to be below threshold levels to cause degradation (i.e., $<10^{19}$ neutrons/cm ² or $<10^{10}$ rads)
Consolidation or movement of soil on which containment is founded	Differential settlement	Equipment alignment, cracking	Connected structures on independent foundations	Allowance is made in design; soil sites generally include settlement monitoring instrumentation
Exposure to water containing dissolved salts (e.g., seawater)	Salt crystallisation	Cracking and scaling	Surfaces subject to salt spray; intake structures; foundations	Minimised through use of low permeability concretes, sealers, and barriers

Table 2.1 (cont.) Degradation Factors that can Impact the Performance of Safety-Related Concrete Structures (IAEA, 1998).

Permission to use this copyrighted material is granted by IAEA.

b. Mild Steel Reinforcing

Ageing Stressors/ Service Conditions	Ageing Mechanism	Ageing Effect	Potential Degradation Sites	Remarks (e.g., Significance)
Depassivation of steel due to carbonation or presence of chloride ions	Composition or concentration cells leading to corrosion	Concrete cracking and spalling; loss of reinforcement cross-section	Outer layer of steel reinforcement in all structures where cracks or local defects (e.g., joints) are present	Prominent potential form of degradation; leads to reduction of load-carrying capacity
Elevated temperature	Microcrystalline changes	Reduction of yield strength and modulus of elasticity	Near hot process and steam piping	Of significance only where temperatures exceed ~200°C
Irradiation	Microstructural transformation	Increased yield strength; reduced ductility	Structures proximate to reactor vessel	Containment irradiation levels likely to be below threshold levels to cause degradation
Cyclic loading	Fatigue	Loss of bond to concrete; failure of steel under extreme conditions	Equipment/piping supports	Localised damage; fatigue failure of concrete structures unusual

Table 2.2 Reactivity of Various Materials with Concrete and Steel

Material	Effect on concrete	Effect on steel
Acetone	Liquid loss by penetration (may cause slow disintegration)	None
Acidic Water (less than 6.5 pH)	Disintegrates concrete slowly	May attack rebar and embedments
Boric Acid	Negligible effect unless immersed	Severely corrosive to liner and reinforcing steel
Borated Water (and boron)	Negligible effect unless immersed	Very corrosive at high concentration
Chlorine Gas	Concrete (moist) slowly disintegrates	Highly corrosive
Demineralized Water	Leaches	Slight
Deicing Salts	Scaling of non-air entrained concrete	Highly corrosive
Diesel Exhaust Gases	May disintegrate moist concrete by action of carbonic, nitric, or sulphurous acid; minimal effect on hardened dry concrete	Minimal
Hydrochloric Acid	Disintegrates concrete rapidly	Highly corrosive
Hydroxides	At low concentrations, slow disintegration; at high concentrations, greater disintegration	Unknown
Nitric Acid	Disintegrates rapidly	Highly corrosive
Lubricating Oil	Fatty oils, if present, slowly disintegrate concrete	Minimal
Seawater	Disintegrates concrete with inadequate sulfate resistance	Highly corrosive
Sodium Hydroxide	Not harmful below 20% concentration, disintegrates at concentrations above 20%	Minimal
Sodium Pentaborate	Disintegrates at varying rates depending on concentration	Dependent on concentration
Sulphates	Disintegrates at varying rates with concentration (concretes with low sulfate resistance such as Type I Portland cement concrete)	Harmful at certain concentrations
Sulphuric Acid (sulphurous)	Disintegrates rapidly in concentration between 10 and 80%	Very corrosive

Table 2.3 Expected Carbonation Depths (Allen and Forrester, 1983).
 © 1983 Society of Chemical Industry/Ellis Horwood Ltd., reprinted with permission.

Concrete strength	Storage conditions	Constant B	Carbonation depth (mm) after				
			1 year	2 years	5 years	10 years	25 years
Low	Outdoors (moist)	0.6	6	9	13	19	30
	Indoors	1.0	10	14	22	32	50
Medium	Outdoors (moist)	0.2	2	3	4	6	10
	Indoors	0.5	5	7	11	16	25
High	Outdoors (moist)	0.1	1	1.5	2	3	5
	Indoors	0.2	2	3	4	6	10

Note: 1 mm = .0394 in.

Table 2.4 Expected Times to Corrosion (Years) (Kobayashi et al., 1990).
 Reprinted from Cement and Concrete Research 24(1), pp. 619-622, Kobayashi, K., Suzuki, K., and Uno, Y., "Carbonation of Concrete Structures and Decomposition of C-S-H," copyright 1990, with permission from Elsevier Science.

Water/cement ratio	Cover (mm)					
	5	10	15	20	25	30
0.45	19	75	100+	100+	100+	100+
0.50	6	25	50	99	100+	100+
0.55	3	12	27	49	76	100+
0.60	1.8	7	16	29	45	65
0.65	1.5	6	13	23	36	52
0.70	1.2	5	11	19	30	43

Note: 1 mm = .0394 in.

3 STRUCTURAL IMPACT OF REINFORCED CONCRETE DEGRADATION AND REVIEW OF EXPERIMENTAL EVIDENCE

Primary mechanisms (factors) that, under unfavorable conditions, can produce premature concrete deterioration include (1) freezing and thawing, (2) aggressive chemical exposure, (3) abrasion, (4) corrosion of steel reinforcement and other embedded metals, (5) chemical reactions of aggregates, and (6) other factors (e.g., unsound cement and shrinkage cracking). Table 3.1 summarizes interacting factors for mechanisms producing premature concrete deterioration (Mather, 1979). As shown in this table, the most prevalent manifestation of concrete degradation is cracking.

Cracking occurs in virtually all concrete structures and, because of concrete's inherently low tensile strength and lack of ductility, can never be totally eliminated. Cracks are significant from the viewpoint that they can indicate major structural problems (active cracks); provide an important avenue for ingress of hostile environments (active or dormant cracks); and inhibit a structure from meeting its performance requirements (e.g., water retaining or biological shielding). Figure 3.1 presents a summary of crack types that can form in concrete and when they form (i.e., plastic or hardened state). Examples of intrinsic cracks in a hypothetical concrete structure and cracks that form due to load or imposed deformations are presented in Figure 3.2. Additional information on classification of intrinsic cracks is presented in Table 3.2 (e.g., location, causes, and time of appearance). Intrinsic cracks are generally controlled by appropriate measures of concrete technology, such as mix design and composition, and proper placing and curing. Table 3.3 presents a listing of common defects observed in reinforced concrete buildings and possible causes (Pinjarkar, 1984). Control of cracking due to loads or imposed deformations is addressed through minimum bonded steel reinforcement requirements. In the present study, cracking and its relationship to corrosion of embedded steel reinforcement, and the performance of degraded reinforced concrete structures are of primary interest.

3.1 Cracking and Corrosion

A review of the performance of NPP reinforced concrete structures indicates that concrete cracking and corrosion of embedded steel reinforcement are the primary manifestations of degradation that have been reported (IAEA, 1998). The present study will restrict itself to the relation between concrete cracking and corrosion of embedded steel reinforcement.

The relation between crack characteristics and corrosion needs to be addressed from two aspects. The first relates to the crack characteristics and corrosion occurrence; the second addresses the relation between corrosion significance and crack characteristics (e.g., visual features or indicators).

3.1.1 Crack Characteristics and Corrosion Occurrence

Crack characteristics identified to be of importance to corrosion include width, orientation or type, propagation status, frequency, and shape.

Two viewpoints, or theories, have been proposed relative to the significance of crack width (or presence of a crack) and corrosion (Darwin, 1985). Theory one believes that cracks significantly reduce the service life of structures by permitting access of carbon dioxide, chlorides, water, and oxygen to the reinforcing steel. The cracks thus accelerate corrosion initiation and provide space for the deposition of the corrosion products. Several researchers studying the effects of cracks transverse to steel reinforcement seem to confirm that this theory is correct and found a relation between crack width, exposure condition, and corrosion (Arya and Wood, 1995). Information in support of this is provided in Figure 3.3 which presents data relating surface crack width, carbonation, and corrosion of reinforcement (Yoda and Yokomuro,

1987). In this figure the triangular points represent steel reinforcement at pour joints and the circular points represent steel reinforcement not located at pour joints. Theory one is embodied in many national codes (ACI 318, 1995; BS8110, 1985) in which crack widths at the concrete surface are limited based on exposure conditions. A comparison of code requirements for crack control in reinforced concrete structures is available (Halvorsen, 1987).

In theory two it is accepted that crack widths may accelerate corrosion initiation, but the subsequent rate of corrosion is minimal and confined to zones where the cracks cross the reinforcing bars. It is important to note that theory two does not suggest that cracks do not cause corrosion. Cracks do act as corrosion initiators and, after years of exposure there is likely to be some corrosion at points where the cracks cross the reinforcement (Beeby, 1979). The reasoning behind theory two is that, provided the reinforcement is properly located and the quality of the surrounding concrete is adequate, then the steel will not corrode. However, the formation of a crack in the concrete cover will allow ingress of carbon dioxide or chlorides to depassivate the steel and set up an electrolytic cell at or near the crack where corrosion can occur.

Although it would appear as if differences between theories one and two are irreconcilable, they both can be justified based on the type of crack – coincident and intersecting. Coincident cracks (e.g., plastic settlement or due to corrosion) follow the line of the steel reinforcement and intersecting cracks (e.g., load induced and not normally due to corrosion) cross the steel reinforcement. With coincident cracks the passivity of the reinforcing steel may be lost at several locations with the same crack being able to readily transmit oxygen and moisture to the cathodic areas of the steel. Since there is no way of inhibiting or confining the corrosion process, corrosion may then proceed unchecked and possibly accelerate. Intersecting cracks (e.g., result of loads) will also increase the rate of penetration of aggressive substances to the reinforcing steel and hence accelerate corrosion initiation. However, since the cathodic sites are mainly confined to the crack-free regions of the concrete, any oxygen and moisture that penetrate the crack will not significantly affect the rate of corrosion.

Where a crack is generally transverse to the reinforcement, only localized corrosion may occur. It has been suggested that corrosion is limited to about three bar diameters away from the crack, but relatively recent laboratory studies on cracked concrete with 10-mm (.394 in.) diameter rebar found significant corrosion as far as 130 mm (5.12 in.) away from the crack location (Krauss, 1994). Evidence indicates that there is a relationship between surface crack width and corroded length of bar, but not to the amount of corrosion (Tremper, 1947). For specimens containing initial surface crack widths of 0.13 to 1.3 mm (.00512 to .0512 in.) stored outdoors for 10 years it was found that corrosion occurred in all cases. A significant increase in the corroded area was observed with increasing crack width, but no effect of the crack width could be found with regard to the maximum corrosion depth. Table 3.4 presents data on the relationship between concrete surface crack width, depth of corrosion, and average corroded length of steel reinforcement (Beeby, 1979). Figure 3.4 presents additional information on the effect of crack width on corrosion length (Halvorsen, 1966). Results from cracked specimens exposed to various environments for 1 and 2 years indicates a linear increase in the degree of corrosion with increasing surface crack width (Rehm and Moll, 1964). Using the same data reported by Rehm and Moll (1964) but including results for 4 and 10 years exposure, it was found that the crack width did not have a significant influence on corrosion (Schiessl, 1975). It was suggested that the difference in these two conclusions was related to the initiation time and that as the time increased the influence of crack width on the amount of corrosion becomes negligible. Figure 3.5 presents the mean reduction in area of an 8-mm (.31 in.) bar plotted against crack width for marine exposure (Beeby, 1983). Considering that there was a substantial scatter in the data used to determine the mean values plotted and absence of a definite trend for the means, it can be concluded that crack width had a negligible influence on corrosion for these results. In another study involving loaded concrete specimens confined in a salt fog for 12 years (Francois and Arliguie, 1999), it was concluded that development of steel reinforcement corrosion was not influenced by crack width [up to 0.5 mm (.02 in.)], but load applied to the beams played a significant role in the penetration of the

aggressive agents and the ensuing corrosion. The explanation for an increase in chloride penetration due to loading is that, first the loading causes paste-aggregate interface damage, and secondly, loads encourage the development of corrosion on the tensile reinforcement because of damage to the steel-concrete interface.

Comparing results of a number of researchers, including some of the information presented above, it was concluded that there is little evidence to support the idea that wide cracks will promote corrosion faster than narrow cracks (Beeby, 1978, 1978a). The reason proposed for this is that in order for corrosion to proceed, oxygen must be supplied to the cathodic regions of the reinforcement and there must be an electrical path between the anode and the cathode. Since both of these factors are independent of crack width, it was concluded that the corrosion rate is also independent of crack width. Information presented above seems to indicate that larger crack widths increase the probability of corrosion (Beeby, 1979a), however values of crack width are not always reliable indicators of corrosion and deterioration expected (ACI Committee 224, 1984). Other investigators have produced similar evidence to support the general conclusion that corrosion does not exhibit a relationship to crack width (O'Neill, 1980; Raphael and Shalon, 1971; Houston, Atimtay, and Ferguson, 1972). Thus, except for larger crack widths that are likely to cause a breakdown of the passivity of the reinforcement and hence cause corrosion to start earlier, there is no reason to expect the rate of corrosion to be influenced by cracks (Beeby, 1979b; Schiessl, 1976). Unfortunately, at present there are no alternatives to describing cracks other than by crack width at the surface. Therefore, until recently, most code provisions address durability by limiting crack width at the concrete surface.

In addition to the cause of a crack, the time-dependent behavior of the crack must be determined in order to judge the significance of a crack (Nielsen, 1978). Dormant cracks have widths that do not vary with time and as a result may be blocked by the deposition of extraneous substances. Dormant cracks also may self-heal through filling with stationary or slowly moving water leading to cement hydration products and $\text{Ca}(\text{OH})_2$ crystals being precipitated in the crack (Concrete Society, 1992). Active cracks on the other hand have widths that vary with time and are more likely to provide access to the steel reinforcement.

As the frequency or number of cracks increases, the number of sites at which steel reinforcement corrosion can occur increases so there is an increasing risk that a crack will have a significant amount of corrosion. Exposure tests on cracked reinforced concrete beams showed that for any given crack width, the depth of corrosion was generally fairly small (Figure 3.6) (Beeby, 1978a). Detailed analysis of this data, presented in Figure 3.7, indicate that the distributions of the corrosion depths vary exponentially, perhaps suggesting that the higher the frequency of cracking the greater the risk of a particular amount of corrosion. Conversely, for a given environment, if a structure has only a few cracks, the risk of obtaining a crack with a high degree of corrosion is low because of the distribution.

As noted previously, most codes have dealt with crack width at the surface of the structure. It may be demonstrated that some cracks may: (a) taper quickly from the surface (e.g., plastic shrinkage cracks), (b) remain approximately parallel throughout the section (e.g., thermal contraction cracks in thin walls), and (c) widen within the section (e.g., thermal gradient cracks within deep foundations) (Concrete Society, 1992). However, crack width at the surface may not be a good indicator of crack width at the reinforcement as shown in Figure 3.8. Thus a wide surface crack may not imply a wide internal crack. The crack width at the steel reinforcement is a function of several factors (including the crack origin): amount of concrete cover, steel stress, reinforcement ratio, reinforcement arrangement, diameter of the reinforcement bars, and depth of tensile zone (Manning, 1985).

3.1.2 Corrosion Significance and Cracking Occurrence

The other important aspect of the relationship between concrete cracking and corrosion significance relates to the extent of concrete cracking that occurs as a result of corrosion of the embedded steel reinforcement. In other words – What is the relation between characteristics (e.g., width) of cracks formed at the concrete surface resulting from corrosion and the extent of corrosion (e.g., loss of steel reinforcement section or loss of bond between the steel reinforcement and concrete)? Occurrence of concrete cover cracking due to corrosion of the steel reinforcement is important not only because it affects the functional and structural properties of reinforced concrete but, after cracking of the cover concrete, the rate of corrosion increases significantly (Morinaga, 1990). Although structural properties are not damaged significantly at the time of initial cover concrete cracking, spalling of cover concrete will follow shortly thereafter. It has been noted that in studies involving deterioration of bridge decks that the cracking period, or time between corrosion initiation and concrete cracking, ranges between two and five years (Cady and Weyers, 1984). Concrete cover depth, reinforcing steel spacing and size, and concrete strength were found to have little influence on the length of the cracking period. The most significant parameter with respect to the length of the cracking period was the corrosion rate.

In the corrosion process, higher bursting forces causing cracking of concrete are signified by an increasing bar diameter, whereas the thickness and quality of concrete cover over the reinforcement characterize the resistance to the splitting-corrosion forces.* Cover to bar diameter (C/d) therefore is a significant corrosion protection parameter (Al-Sulaimani et al., 1990). For steel in concrete the passive corrosion rate is typically on the order of $1 \mu\text{m}/\text{yr}$ ($0.000039 \text{ in.}/\text{yr}$), but without the passive film the rate would be at least three orders of magnitude higher (Foley, 1975). Once the chloride ions reach the bar, cracks appear relatively soon in high quality concrete with low C/d values. In low quality concrete with high C/d values, it has been reported that about $60 \mu\text{m}$ (0.0024 in.) of bar loss may be required for cracking because the corrosion products can easily diffuse through the concrete cover due to the high porosity of the low quality concrete (Rodriguez et al., 1996). Table 3.5 provides an indication of the expected time periods needed to develop a crack width of either 0.05 to 0.1 mm ($.002$ to $.0039 \text{ in.}$) (visible) or 0.2 to 0.3 mm ($.0079$ to 0.012 in.) in the concrete cover for several corrosion rates having magnitudes typical of maximums found under field conditions (Andrade, Alonso, and Molina, 1993). Prismatic specimens 150 cm (59.1 in.) by 150 cm (59.1 in.) by 380 cm (15.0 in.) long containing a single 16-mm ($.63 \text{ in.}$) diameter bar and either 2 or 3 mm ($.079$ or $.12 \text{ in.}$) of cover were used in the study. Visible cracks are generated after a negligible bar cross-section loss of only $10\text{-}20 \mu\text{m}$ ($.00039 - .00079 \text{ in.}$) ($\sim 0.1\%$ loss of section).** Assuming generalized corrosion, it has been concluded from results presented in the literature that for $C/d > 2$ reinforcement radius losses of around $50 \mu\text{m}$ ($.002 \text{ in.}$) induce crack widths of about 0.05 mm ($.002 \text{ in.}$), while for $C/d < 2$ radius losses of only $15\text{-}30 \mu\text{m}$ ($.00059 - .0012 \text{ in.}$) are required (Alonso, Andrade, Rodriguez, and Diez, 1998). Furthermore, for $C/d > 2$ crack widths of 0.3 mm ($.012 \text{ in.}$) appear for radius losses of $100\text{-}200 \mu\text{m}$ ($.0039 - .0079 \text{ in.}$), and of 1 mm ($.0039 \text{ in.}$) for losses of about $300 \mu\text{m}$ (0.012 in.). At larger crack widths definitive conclusions cannot be

* It has been reported that smooth bars are more likely to suffer corrosion damage than deformed bars (Soretz, 1967; Martin and Schiessl, 1969). Other research (Mohammed, Otsuki, and Hisada, 1999) reports that deformed bars corrode more than plain bars. This study also indicates that the orientation of the steel bars influences steel corrosion in concrete. Due to the formation of gaps below the bottom of the horizontal steel, significant macrocell and microcell corrosion takes place and the presence of stirrups increases the macrocell activity. Other research (González, 1996a) has noted that for a given corrosion penetration, larger reinforcement diameters will provide improved performance (longer service life) because the relative reduction in cross section for the larger diameter bars will be less.

** Reinforcement radius losses of 15 to $50 \mu\text{m}$ ($.00059$ to $.002 \text{ in.}$) have been reported by another source as being necessary to produce a visible crack (width $< 0.1 \text{ mm}$ ($.0039 \text{ in.}$)) (Alonso, Andrade, Rodriguez and Diez, 1998).

drawn because scatter is very high as the oxides diffuse out of concrete to reduce the pressure resulting from development of the corrosion products. It should be noted, however, that the corrosion rate has a significant effect on these limits as a slower corrosion rate will produce earlier cracking for the same attack penetration. After generation of the crack, the increase in crack width shows a linear relationship to corrosion penetration until levels of 200 to 300 μm (0.0079 to 0.012 in.). Prediction of evolution of crack width as a function of corrosion penetration after these levels is difficult because the geometry and size of the structural element start to dominate. (Alonso, Andrade, Rodriguez, and Diez, 1998). Laboratory studies show that for a given diameter of rebar and concrete cover, the crack width appears to increase linearly with the amount of corrosion product developed (JCI, 1996). Data in support of this are provided in Figure 3.9 in which results from 300-mm (11.8 in.) concrete cubes containing either a 9- or 10-mm (.35 or .39 in.) diameter rebar with 25 mm (.98 in.) of concrete cover are presented (Maruyama, Shimomura, and Hamada, 1999).

3.2 Performance of Degraded Structures

Although somewhat limited, data are available from exposure tests involving the effects of degradation on the performance of reinforced concrete structural members. Interpretation of this data and information however can be difficult because exposure conditions for each test are different, test parameters are inconsistent (e.g., specimen geometry), and the extent of damage is assessed in different ways by different researchers. For example, with respect to corrosion, interpretation of end-of-service life is viewed in different ways by different researchers. Also, many investigators have used impressed currents to induce corrosion in embedded steel reinforcement, but it has been noted that the electrolyte corrosion product is different from the natural electrochemical corrosion product with respect to constitution and microstructure (Okada, Kobayashi, and Miyagawa, 1988).

The seismic performance of a reinforced concrete component may be characterized or quantified by a combination of parameters such as the following: stiffness, strength (bending and shear), energy absorbing capacity, ductility, and failure mode. On the other hand, the type of structural degradation that may affect these performance parameters may include: direction of concrete cracks (vertical or horizontal with regard to component axis), pattern of cracks (with respect to the crack pattern due to seismic forces), amount of cracks (size and number), and degree of corrosion of rebars (Park, 1998). Provided below are summaries of structural tests in which the performance of degraded reinforced concrete structures has been investigated. Although corrosion of embedded steel reinforcement has been noted as the major threat to NPP reinforced concrete structures, information has also been included on the performance of reinforced concrete structures subjected to ASR. Information from tests involving these two degradation mechanisms will be of assistance in trying to assess the significance of degradation of reinforced concrete structures and how it relates to the limit states such as noted above, or more specifically, the remaining structural margins.* That is, attempting to identify visual effects or characteristics that can be used as indicators of the degradation significance.

* Although structural tests involving other potential age-related degradation mechanisms identified in Section 2.1 were not identified, information on potential manifestations of each of the degradation mechanisms that may be of use in structural evaluations was included as part of the description (e.g., concrete compressive strength versus temperature).

3.2.1 Tests Involving Corrosion-Damaged Structures

Reinforced Concrete Beams and Slabs

A two-phase test program related to the residual capacity of concrete beams damaged by salt attack has been conducted (Kawamura, 1999). In the first phase 100 x 150 x 1200 mm (3.94 x 5.91 x 47.2 in.) beams containing a single 13-mm (.512 in.) diameter rebar were tested to investigate the fundamental behavior of damaged beams in flexure (Figure 3.10). Corrosion was accelerated by incorporating chloride solution (simulate sea water) into the concrete mix. Electrolytic corrosion was used to accelerate the degradation process with longitudinal crack width controlled through the accumulated current. One longitudinal crack was initiated along the rebar. Two control specimens and eleven specimens having crack widths up to 1 mm (.039 in.) were tested under static loading to failure (flexure or diagonal tension). Results indicate that as the corrosion-induced crack width increased, the flexure capacity decreased, but the decrease was less than 10%. When the crack width was small [i.e., 0.3 mm (.012 in.)], the stiffness of the beam as well as its ultimate capacity increased slightly relative to the uncorroded specimen. This indicates that a modest amount of corrosion (i.e., negligible loss of rebar cross section) may improve performance in flexure. In the second phase a companion series of 10 beams having the same geometry as the beams used in the static tests was tested. Reinforcement in eight of the beams was corroded using the accelerated procedure. Longitudinal crack widths were limited to 0.5 mm (.02 in.). The beams were cyclically loaded at four load ranges, with the highest load-range corresponding to about 70% of ultimate load. After a predetermined number of load applications, the beams were statically loaded to failure in flexure. Both the fatigue life and stiffness of beams were reduced as the longitudinal crack width increased. Beams having longitudinal crack widths of 0.125 or 0.5 mm (.00492 or .0197 in.) failed prior to the fatigue life predicted by the Japanese Society of Civil Engineers Code. Reduction of fatigue life was attributed to reduction of the fatigue life of the rebars due to corrosion and deterioration of the bond due to longitudinal cracking.

Three series of test have been conducted: an electrochemical test to establish the relationship between the amount of corrosion and average crack width, a static loading test, and a fatigue loading test (Maruyama and Shimomura, 1999). Figure 3.11 presents the specimens used in the tests. In the electrochemical tests it was found that after initiation of longitudinal cracks due to corrosion there was a linear relationship between the amount of corrosion and crack width (Figure 3.12). The presence of stirrups and its spacing did not influence the relationship between crack width and corrosion. In the second test series it was found that in specimens without splices that as long as anchorage of longitudinal bars was sufficient, the reduction in flexural capacity due to corrosion was relatively insignificant, even up to crack widths of 0.5 mm (.02 in.) (Figure 3.13). When splices are present at midspan, the load-deflection behavior depends on the amount of corrosion and stirrup spacing (Figure 3.14). Although the effect of the presence of stirrups up to maximum capacity is relatively small, the presence of stirrups does affect the energy absorption capacity. In the third series of tests the specimens were cyclically loaded up to about 65% of the ultimate static flexural capacity of a beam without corrosion. It was found that corrosion of the longitudinal bars significantly affected the fatigue life of the beams with the beams failing either by rupture of the rebars or failure of the concrete-steel reinforcement bond. As the amount of corrosion increased, the number of cycles to failure decreased. Although a definite relationship between stirrup spacing and performance could not be developed, the beams with stirrups exhibited a significant improvement in performance relative to the beam without stirrups (i.e., four orders of magnitude increase in number of cycles to failure).

The effects of rebar corrosion on the strength of reinforced concrete members was evaluated in three series of tests: tension test of rebars, pull-out tests, and static load test of beams (Lee, Tomosawa and Noguchi, 1996). The tension tests utilized specimens 80 x 160 x 50 mm (3.15 x 6.3 x 1.97 in.) and contained 10-mm (.394 in.) diameter rebars. Corrosion in each test series was induced by impressed

current and the amount of corrosion was determined by weight loss. Figure 3.15 presents the relationships between corrosion percentage and yield point and elastic modulus. Results are presented in terms of reduction in cross-sectional area of the steel and show that as the reduction in area increases both the yield point and elastic modulus decrease. The pull-out test series used specimens 100 x 100 x 150 mm (3.94 x 3.94 x 5.91 in.) with an embedded 10-mm (.394 in.) rebar. As the corrosion percentage increased, the maximum bond stress decreased and the free-end slip at maximum bond stress decreased. With the onset of concrete cover cracking, the bond strength decreased rapidly due to a reduction in restraint. In the third series of tests static load tests were conducted on 100 x 100 x 800 mm (3.94 x 3.94 x 31.5 in.) beams containing two 10-mm (.394 in.) rebars (Figure 3.16). Cracking of the concrete cover occurred in all beams, with the crack width increasing as the amount of corrosion increased. After the onset of flexural cracks, the control beams without corrosion failed in compression with high toughness. On the other hand, although the strength of beams with cover concrete cracks due to rebar corrosion retained much of the initial stiffness, there was a significant decrease in capacity as well as toughness in beams where the longitudinal reinforcement was not hook anchored. Beams with hook anchored longitudinal rebars performed much better than the beams with non hook anchored longitudinal bars (Figure 3.17).

In an investigation taking into account longitudinal cracks due to reinforcement corrosion as the limit state in durability design (Okada, Kobayashi, and Miyagawa, 1988), beams 100 x 200 x 1600 mm (3.94 x 7.87 x 63.0 in.) were tested (Figure 3.18). Two 10-mm (.394 in.) diameter rebars having 25 mm (.984 in.) of concrete cover ($C/d = 2.5$) were located in both the tension and compression regions of the beam. Corrosion was induced by spraying the beams once a day with a 3.13% NaCl solution. Microcracks occurred in the concrete cover after about 13 weeks of spraying, with longitudinal cracks occurring in the concrete cover after about 20 weeks [0.05 to 0.15 mm (.00197 to .00591 in.) wide]. The longitudinal cracks occurred most frequently at the concrete surface where two steels were in contact with each other (e.g., stirrup locations). It was noted that half-cell potential measurements indicated a significant increase just before longitudinal crack appearance suggesting that this measurement may have the ability to predict the appearance and location of the longitudinal cracks). Three patterns were used to load the beams (Figure 3.19). Flexure test results showed that fewer flexural-shear cracks formed in the beams that had corroded reinforcement than in the control beams (uncorroded), indicating that the bond in the corroded beams had decreased. Elastic performance (yield strength) of the corroded and uncorroded beams was similar, however, there was a slight decrease in ultimate performance (i.e., <10% difference).

Pull-out and beam specimens have been tested to study the influence of reinforcing bar corrosion and cracking on the bond behavior and strength of reinforced concrete members (Al-Sulaimani et al., 1990). Twelve beam specimens 150 x 150 x 1000 mm (5.91 x 5.91 x 39.4 in.) containing two 10-mm (.394 in.) diameter top bars and one 12-mm (.472 in.) diameter bottom bar with a concrete cover of 29 mm (1.14 in.) were tested.* Impressed current was used to induce corrosion amounts up to 4.1% (by weight). Results showed that corrosion up to about 1.5% did not affect the ultimate load. Thereafter, the ultimate load was reduced to the extent of about 10% for about 4.1% loss due to corrosion. Figure 3.20 presents a summary of ultimate load versus percentage corrosion data for the beam tests.

The effect of reinforcement corrosion on the flexural strength, ductility, and mode of failure of one-way slabs was investigated (Almusallam et al., 1996). The test specimens were 305 x 711 x 63.5 mm (12 x 28 x 2.5 in.) (Figure 3.21). Five 6-mm (.236 in.) diameter rebars were placed in the slab with a 57 mm (2.24 in.) center-to-center spacing and 9.5 mm (.374 in.) clear cover. Corrosion was accelerated by impressing direct current into each of the bars while the specimen was partially immersed in a 5% NaCl solution. The reinforcement remained totally above the solution. Corrosion amounts up to 75% (determined by

* Results to evaluate effects of corrosion on bond were summarized earlier.

gravimetric loss in weight) were produced in the rebars. The slabs were tested in flexure using a simply supported system having a total span of 610 mm (24 in.). The load was uniformly distributed. Figures 3.22 and 3.23 present loss in ultimate strength and load-deflection curves, respectively, for slabs with bars of varying degrees of corrosion. A slight increase in ultimate strength was obtained for 1% corrosion, but as the corrosion amount increased there was a sharp reduction in ultimate strength. This sharp reduction was attributed to loss in cross-sectional area of steel, and degradation of bond of the rebar to concrete. Slabs with corroded bars exhibited progressively reduced ductile behavior with an increasing magnitude of reinforcement corrosion. A sudden failure without considerable deflection was the typical mode of failure for the corroded slabs. This behavior was attributed to loss in cross-sectional area of steel at points of concentrated corrosion, and degradation of bond of the rebar to concrete (i.e., crack formation and with increasing corrosion the corrosion products can act as a lubricant between the rebars and concrete). Ultimate deflections decreased with increasing magnitude of reinforcement corrosion, leading to a marked and progressive reduction in the ductility of the slabs. With respect to mode of failure, it was found that the mode of failure of reinforced concrete slabs containing corroded rebars is dependent on the degree of reinforcement corrosion. In the precracking stage, performance of slabs with corroded rebars is somewhat similar to that of slabs with uncorroded rebars. In the post-cracking stage, the failure mode of slabs with corroded rebars was characterized by the formation of flexural cracks at low load. With increasing load these cracks propagated and merged with longitudinal cracks caused by corrosion of the rebars, ultimately leading to sudden longitudinal splitting along the reinforcing bar.

An extensive study was carried out to investigate how the behavior of concrete beams and columns was affected by corrosion (Uomoto and Misra, 1988). Two beam sizes were utilized: 100 x 100 x 700 mm (3.94 x 3.94 x 27.6 in.) (Type A) with steel reinforcement percentages from 0.57 to 5.67, and 100 x 200 x 2100 mm (3.94 x 7.87 x 82.7 in.) (Type B) with a steel reinforcement percentage of 2.28. Type A beams primarily used 10-mm (.394 in.) diameter rebars and Type B beams used a combination of 6- and 16-mm (.236 and .63 in.) diameter rebars. Type A beams did not contain stirrups and Type B beams contained 6 mm (.24 in.) ties at 170-mm (6.69 in.) spacing. Columns 100 x 100 x 400 mm (3.94 x 3.94 x 15.7 in.) also were tested and contained 6 mm (.24 in.) ties at 75-mm (2.95 in.) spacing. Concrete cover was either 10 or 20 mm (0.394 or 0.787 in.). Accelerated corrosion was produced by adding NaCl [0 to 6.3 kg/m³ (0 to .393 pcf) of concrete] to the mixing water and applying an impressed current to the reinforcement. Cracks that formed in the beams and columns as a result of corrosion are presented in Figure 3.24. Cracks occurred much earlier along the stirrups and ties than along the longitudinal reinforcement because there was less concrete cover. Type A beams primarily failed when both flexure and shear cracks were connected to the cracks caused by corrosion, and the cover concrete spalled. Most of the Type B beams failed in flexure accompanied by crushing of the compression concrete. Corroded columns collapsed either after spalling of cover concrete or after buckling of the reinforcement. The number of cracks that formed in the columns prior to failure was relatively small. For Type B beams that experienced reinforcing bar weight losses of 1.0, 1.2, and 2.4% of the main 16-mm (.63 in.) diameter bars, corresponding losses in capacity of 4, 8, and 17% occurred. Although the reduction in the yield and maximum strength of the rebars due to corrosion was 5 to 10%, the decrease in the maximum load-carrying capacity of the beams and columns was higher. This indicates that the reduction in capacity is not caused simply by reduction of effective rebar area or reduction in the rebar strength, but by the cracks formed by the corrosion process. These results were used to provide a qualitative representation of damage in reinforced concrete structures in terms of loss of load-carrying capacity and corrosion regimes (Figure 3.25).

The influence of corrosion on the performance of concrete elements, in terms of Ultimate and Serviceability Limit States, has been investigated by testing concrete beams with corroded rebars (Rodriguez, Ortega, and Casal, 1995; Rodriguez et al., 1996). Thirty-one beams, mostly 2300 x 200 x 150 mm (90.6 x 7.87 x 5.91 in.) were fabricated and tested to evaluate the effects of level of corrosion, detailing of reinforcement, and interaction between corrosion and loading. In the tests to investigate the

interaction between corrosion and loading, the beams were corroded while loaded. Beams in which the reinforcement was to be corroded contained 3% (by weight of cement) calcium chloride in the mix. Impressed current was used to accelerate the corrosion process. The reinforcing bars were intentionally corroded up to $600\ \mu\text{m}$ (.0236 in.), with heavy pitting in some cases. After inducing the required amount of corrosion the beams were loaded in four-point bending. The loading was done in two phases: (1) load was increased until the calculated service load was reached, and (2) load increased to failure. Beams with low ratio of tensile steel (0.5%) failed by rupture of the steel with significant concrete cracking at the tensile surface. Beams with high ratio of tensile reinforcement (1.5%) and high amount of shear reinforcement [6-mm (.24 in.) diameter stirrups at 85-mm (3.35 in.) spacing] failed by crushing of the concrete at the compression face with associated buckling of the compression reinforcement. Several conclusions were derived from this study. Corrosion of reinforcement affects the performance of concrete beams by increasing both the deflections and crack widths at the service load and reducing the strength at ultimate load. Corrosion of reinforcement modifies the type of failure in concrete beams in that uncorroded beams failed in bending while corroded beams primarily failed in shear. Pitting at stirrups and cracking and spalling of top cover concrete, due to corrosion of reinforcement, are the most relevant types of damage affecting load-carrying capacity in the beams. With respect to columns containing corroded rebars that were tested as part of the overall program (BRITE/EURAM, 1995), three main aspects were identified as affecting the behavior of corroded columns: deterioration of the concrete section, increase in load eccentricity due to asymmetric deterioration of the concrete cover, and likely reduction of reinforcement strength due to premature buckling. The most relevant deterioration having consequences relative to column strength produced by corrosion is damage at the concrete cover (e.g., cracking, delamination, and spalling).

Flexure tests have been conducted using beam specimens in which corrosion was accelerated (Yokota, M. et al., 1994). Prior to loading to failure, the beams were first loaded in bending to loads sufficient to cause cracking. Then accelerated corrosion was achieved by applying alternating cycles (up to 21 cycles) of wetting and drying using salt water. This induced axial cracks from 0.01 to 0.4 mm (.00039 to .016 in.) wide along the longitudinal reinforcement. Figure 3.26 presents the pattern of precracks and the corrosion of rebars for four specimens before loading. As noted in Figure 3.27, the amount of corrosion, expressed in terms of corroded area ratio, increased faster in the specimens designated Crack III and Crack IV, than for Crack I or Crack II specimens due to higher applied bending load. Bending strengths of beams normalized to that of an uncracked beam show that the bending strength tends to decrease as the amount of corrosion increases (Figure 3.28). The moderate increase in bending strength after four cycles of wetting and drying was due to an increase in the concrete reinforcement bond due to moderate corrosion. Normalized bending strength as a function of corroded area ratios is presented in Figure 3.29. The peak improvement in bond strength for this data appears to occur at a corroded area ratio of about 20%.

Reinforced Concrete Walls

Six reinforced concrete structural wall specimens (Figure 3.30) having a width of 800 mm (31.5 in.), height of 950 mm (37.4 in.), and thickness of 80 mm (3.15 in.) were fabricated (Yamakawa, T., 1995). Steel reinforcement consisted of 6-mm (.24 in.) diameter bars in a double-layered mesh arrangement with or without end anchorage. Two of the specimens were used as control tests (no corrosion) while the remaining specimens were degraded by electrolytic corrosion. Three of the specimens were fabricated with a 3.3% solution of sodium chloride to simulate local construction. Three concrete cylinders and a 800 x 500 x 50 mm (31.5 x 19.7 x 1.97 in.) wall panel were cast with each structural wall test specimen. The cylinders were tested to provide concrete compressive strength data. The smaller wall panels were also subjected to electrolytic corrosion to investigate the corrosion loss and mechanical properties of the damaged steel reinforcing bars. Electrolytic corrosion produced cracks in concrete of the structural walls, mainly along the steel reinforcing mesh (Figure 3.31). In general the maximum crack widths increased as the product of applied current and elapsed time. A maximum crack width of 3.0 mm (.118 in.) was

reported. The structural walls were tested by subjecting them to cyclic shearing forces while maintaining a constant axial force (Figure 3.30). Instrumentation was utilized to provide data on applied forces, horizontal and vertical displacements, rotation of upper edge beam, and strains of the steel reinforcing bars in the wall panels. Figure 3.32 summarizes results for the shear walls presented in Figure 3.31 as well as for two walls not degraded by electrolytic corrosion prior to testing. Results of the cyclic load tests showed that the ultimate load capacities and energy absorbing capacities (areas of hysteresis loops) of the corroded and uncorroded walls were almost the same. The cracks caused by corrosion did not affect the strength (or initial stiffness) because they did not coincide with the diagonal cracks produced by the lateral loads. Also, the amount of corrosion induced in the specimens was less than 20% which has been noted by other researchers to be the point at which the improvement in bond between concrete and reinforcement is maximum (Yamada, 1992; Yokota, M. et al., 1994). Although the corrosion-damaged walls exhibited a higher initial stiffness, they exhibited a significant deterioration in ductility relative to the uncorroded walls. In the corroded shear walls the spalling of cover concrete was more significant, which was believed to be the reason for the reduced ductility. The uncorroded walls exhibited a flexure-compression type failure, whereas the corroded walls tended to lose the corrosion damaged cover concrete near the bottom of the wall panel with associated buckling of the vertical reinforcing bars. After electrolytic corrosion of the monitoring panels, the reinforcing bars were removed from the panels, corrosion products removed, and the bars weighed. Stress-strain results for the steel bars indicated that the yield stress and strain at ultimate stress decreased as the corrosion increased.

Reinforced Concrete Columns

Several reinforced concrete columns (Figure 3.33) damaged by corrosion have also been tested (Yamakawa, 1998). Three specimens 250 x 250 x 750 mm (9.84 x 9.84 x 29.5 in.) high were tested. The longitudinal reinforcement was 1.37% and the shear reinforcement was 0.85%. One of the specimens was used as a control and the other two were exposed to a saline environment to induce corrosion. One of the exposure-test specimens contained sodium chloride in the concrete mix. Cracking of the specimens was monitored at three-month intervals since the exposure tests initiated. The number of cracks and crack widths increased as the exposure period increased, with the cracks along the longitudinal reinforcement being dominant. Cracking was most significant for the specimen containing sodium chloride. After about three-years exposure, the columns were tested under a combination of cyclic lateral forces and constant axial compression load. Figure 3.34 presents the crack patterns at different drift angles up to 3% for the three specimens. Applied forces and horizontal and vertical displacements were monitored during each test. After the cyclic load tests were completed, concrete cores were taken from the stub at the top of the column to examine for total chloride content. Chloride ions were found to permeate the concrete about 70 mm (2.76 in.) and exceeded the Japanese Government guideline of 0.3 kg/m³ (.0187 pcf). A comparison of the results between the corrosion-damaged concrete columns and the control column indicated little difference in behavior. It was concluded that in the corroded columns there was a type of chemical prestressing occurring as a result of the rebar corrosion. This chemical prestressing tended to improve the bond strength and transverse confining effect despite the deterioration of the flexural capacity and shear strength resulting from concrete cracking and pitting corrosion of the rebar.

3.2.2 Tests Involving AAR-Damaged Structures

A series of cyclic loading tests of uncracked and precracked concrete beams has been conducted (Akiyama et al., 1987). Initially the influence of alkali-aggregate reactions on the shear strength of reinforced concrete beams was considered. Although a cement with a high alkali content, in conjunction with high temperature and high relative humidity, was investigated in an attempt to induce cracks, results obtained were not controllable and the cracks only formed near the surface. The cracking procedure was then changed to incorporate a static fracture agent. Holes were drilled into the concrete and a chemical was inserted into each hole that expanded to produce the lattice cracking. Twelve beams 200 x 400 x

1400 (major span) mm (7.87 x 15.7 x 55.1 in.) were fabricated from 360 kg/cm² (5,120 psi) concrete and contained 2.17% longitudinal rebar (Figure 3.35). Variables in the investigation included percent stirrup rebar (0.09 or 0.28%) and shear span ratio (1.5, 2.5, or 4). Six of the specimens were precracked using the static fracture agent. All specimens were cyclically loaded in flexure with each subsequent loading cycle increased in magnitude. The effect of the cracks on the ultimate load and ductility was shown to be dependent on the failure mode (e.g., sliding shear and compressive shear) as determined by the test parameters. Vertical precracks reduced the bending stiffness and precracks reduced the shear strength that in turn altered the failure mechanism. General conclusions provided were that at formation of diagonal cracks the cracked beams showed increased deflections (1.3 to 2.3) relative to uncracked beams, and the shear strength of every cracked beam was about equal to that of its corresponding uncracked beam as long as the average shear stress was less than about 37 kg/cm² (526 psi).

Thirty beam specimens were fabricated and tested to determine the influence of alkali-aggregate reaction on the flexural yield strength and ultimate shear strength of reinforced concrete members (Abe et al., 1989). The study consisted of three series of tests where the tension reinforcement ratios were equal to 0.75%, 1.17%, and 1.76%. Ten specimens were contained in each series: three specimens unaffected by alkali-aggregate reactions, five affected by alkali-aggregate reactions, and two that were repaired after alkali-aggregate reactions by injecting cracks with epoxy. The specimens and companion control prisms, with dimensions 100 x 100 x 400 mm (3.94 x 3.94 x 15.7 in.), were cured under a constant temperature of 40°C (104°F) and high humidity. Expansions of the beams (two directions) and prisms were measured over a 500-day period. The amount of expansion was dependent on confinement with the greatest expansion obtained from the prismatic specimens (about 0.53%), followed by the beam depth direction (about 0.31 to 0.45%), and beam length direction (<0.1%). Expansion decreased along the beam length as the amount of steel reinforcement increased. The beams were tested in flexure. Failure of Series AI and AII specimens, except for an unaffected specimen that failed by diagonal tension, was flexural crushing of concrete after flexural yield. In Series AIII, the failure mode of unaffected specimens was diagonal shear tension after flexural yield. Several of the affected specimens in this series failed by horizontal slip failure that incorporated the horizontal cracks generated by the alkali-aggregate reactions. Comparing load-deformation responses for unaffected and affected beams shows that at the early elastic stages the performance is similar, but after that the stiffness of the affected beams was higher. The ultimate shear strength of affected specimens was slightly higher than that of unaffected specimens. Also the deflection at ultimate shear strength of affected specimens was larger than that of unaffected specimens. Compressive strength results obtained from companion cylinders cast in conjunction with the beams indicated that the strength of affected cylinders was about 23% lower at 513 days age relative to the 28-day strength, however, cores removed from the beams showed only a slight reduction for the affected specimens. The modulus of elasticity of affected specimens was about 46% lower at 513 days age relative to the 28-day modulus.

Long-term expansion characteristics and structural behavior of reinforced concrete beams fabricated using reactive aggregates have been investigated and compared to beams using non-reactive coarse aggregates (Inoue et al., 1989). Six beams 200 x 200 x 1700 mm (7.87 x 7.87 x 66.9 in.) containing tensile reinforcement ratios of either 0.77%, 1.20%, or 1.74% were fabricated and tested. Three of the beams contained reactive aggregate. All beams, after an initial 14-day cure at 20°C (68°F) and 80% R.H., were cured at 40°C (104°F) and 100% R.H. for 178 days. Following this the beams were stored at 20°C (68°F) and 70% R.H. in the laboratory for an additional two years to monitor the chemical prestress resulting from the alkali-aggregate reactions. Strains up to about 7000×10^{-6} developed at the upper face of the beams cast with reactive aggregate as compared to strains of 500×10^{-6} or less developed by the beams not containing reactive aggregate. The beams were then tested in four-point bending to failure. Flexural cracking strength of the affected beams was larger than the unaffected beams, irrespective of the reinforcement ratio, because of the chemical prestress effect of the alkali-aggregate reactions. The

reduction in measured yield strength and ultimate flexural strength of the affected beams was less than 10% relative to unaffected beams. At the time of the beam tests, the compressive strength, tensile strength, and elastic modulus were determined for the affected and unaffected materials using 100-mm (3.94 in.) diameter by 200-mm (7.87 in.) long cylinders. The affected materials had these values reduced to approximately 64%, 59%, and 48%, respectively, of the unaffected material values.

Two series of tests utilizing beams 200 x 200 x 1700 mm (7.87 x 7.87 x 66.9 in.) were conducted to examine the effects of alkali-aggregate reactions on performance (Fujii et al., 1987). In the first series static load tests were conducted. Test variables included tension steel ratio (0.77 to 1.77%), compression steel ratio (0.43 to 1.3%), and shear steel ratio (0.2 to 0.3%). In beams with alkali-silica reactions, initial cracks occurred along the longitudinal steel at about 200 microstrain. Expansion essentially stopped in the affected beams at an age of about 100 days. The beams were tested to failure at an age of about 150 days using symmetric two-point loading with a shear span to effective depth ratio of 2.5. In the alkali-aggregate affected beams it was observed that up to flexural cracking caused by applied load that the deflection of the affected beams was similar to unaffected beams, but after cracking the deflection was less. The ratio of the strength of the affected beams to the unaffected beams ranged from 0.95 to 1.10. Fewer flexural cracks and no shear cracks formed in the affected beams with failure occurring by yielding of the main reinforcement and concrete crushing (i.e., prestress induced by alkali-aggregate expansions increased the shear strength by more than the strength reduction* caused by the reactions). It was concluded that the alkali-aggregate reactions did not have an adverse effect on the strength or stiffness of the beams. In the second series of tests both the static (two tests) and fatigue (eight tests) behavior of reinforced concrete beams were studied. The beams were tested under symmetric two-point loading with a shear span/effective depth ratio of 2.5. A minimum load of one ton was used in the fatigue tests with the maximum load increased in steps of one ton until failure occurred. At each load, 10^5 cycles of loading were applied to the beams. Failure of the affected beams occurred by yielding of the main reinforcing bars and concrete crushing. One of the unaffected beams failed in shear with the other failing in flexure. The number of cycles to failure of the affected beams was found to be greater than that for the unaffected beams.

In Denmark a project was initiated in 1984 to investigate the load-carrying capacity of structural members subjected to alkali-silica reactions (Danish Ministry of Transport Directorate, 1986). Eight beams 180 x 360 x 4300 mm (7.09 x 14.2 x 169 in.) were fabricated containing three 18-mm (.709 in.) diameter bars as tensile reinforcement and two 12-mm (.472 in.) bars as compression reinforcement. Stirrups, 7-mm (.28 in.) diameter, were contained in the bending and anchorage regions of each beam. Six of the beams were affected by alkali-silica reactions. Loading tests showed that the alkali-silica expansion resulted in a significant increase in the shear capacity of the beams. This was attributed to the induced compressive stress resulting from restraint of the alkali-silica reactions by the reinforcement. The compressive strength of cores taken from affected beams indicated that the concrete strength had been reduced by 20% at the lowest level of alkali-silica expansion, and about 55% at the highest level of expansion. The elastic modulus was reduced to about one-third the value of comparable sound concrete.

* The reductions in cylinder compressive strength, tensile strength, and elastic modulus due to alkali-aggregate reactions were 40, 50, and 65%, respectively.

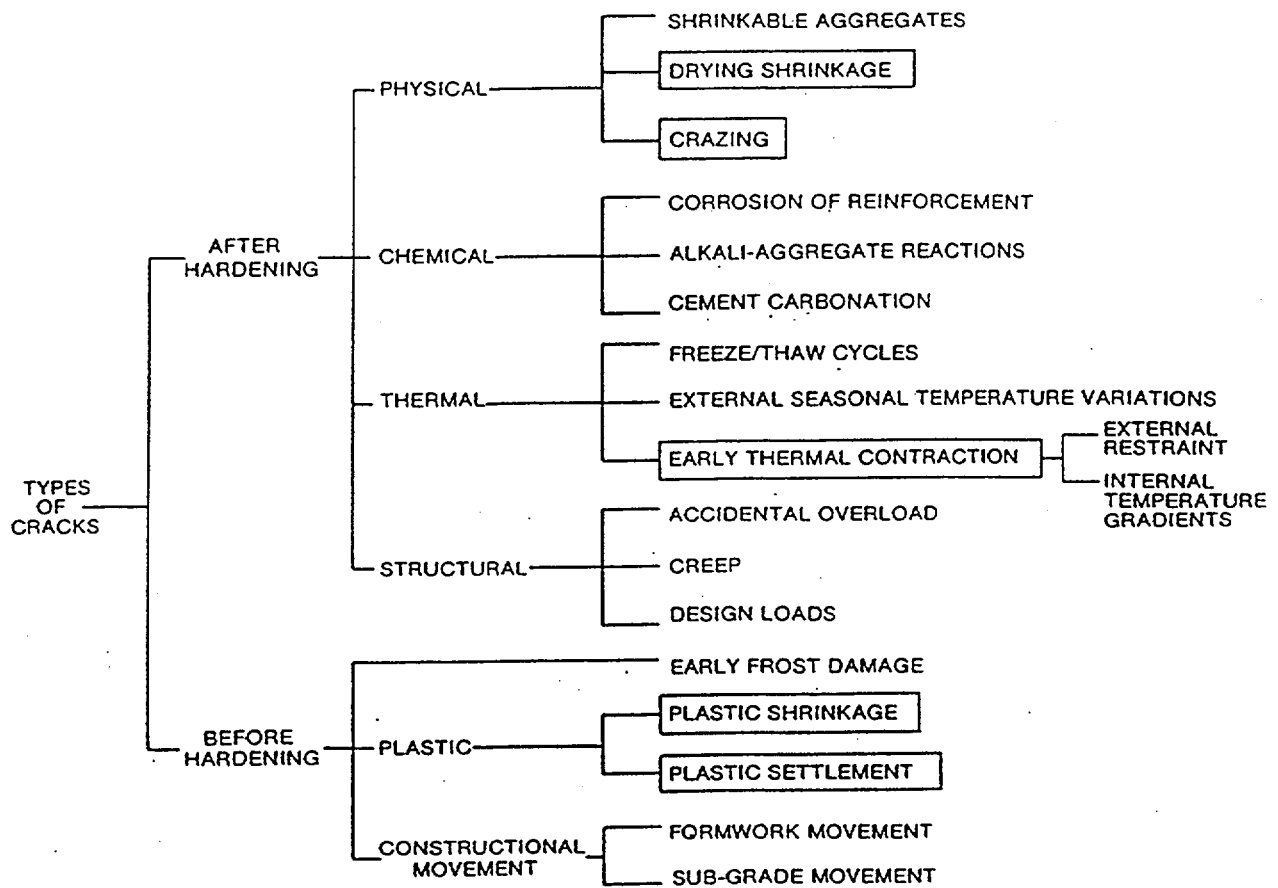
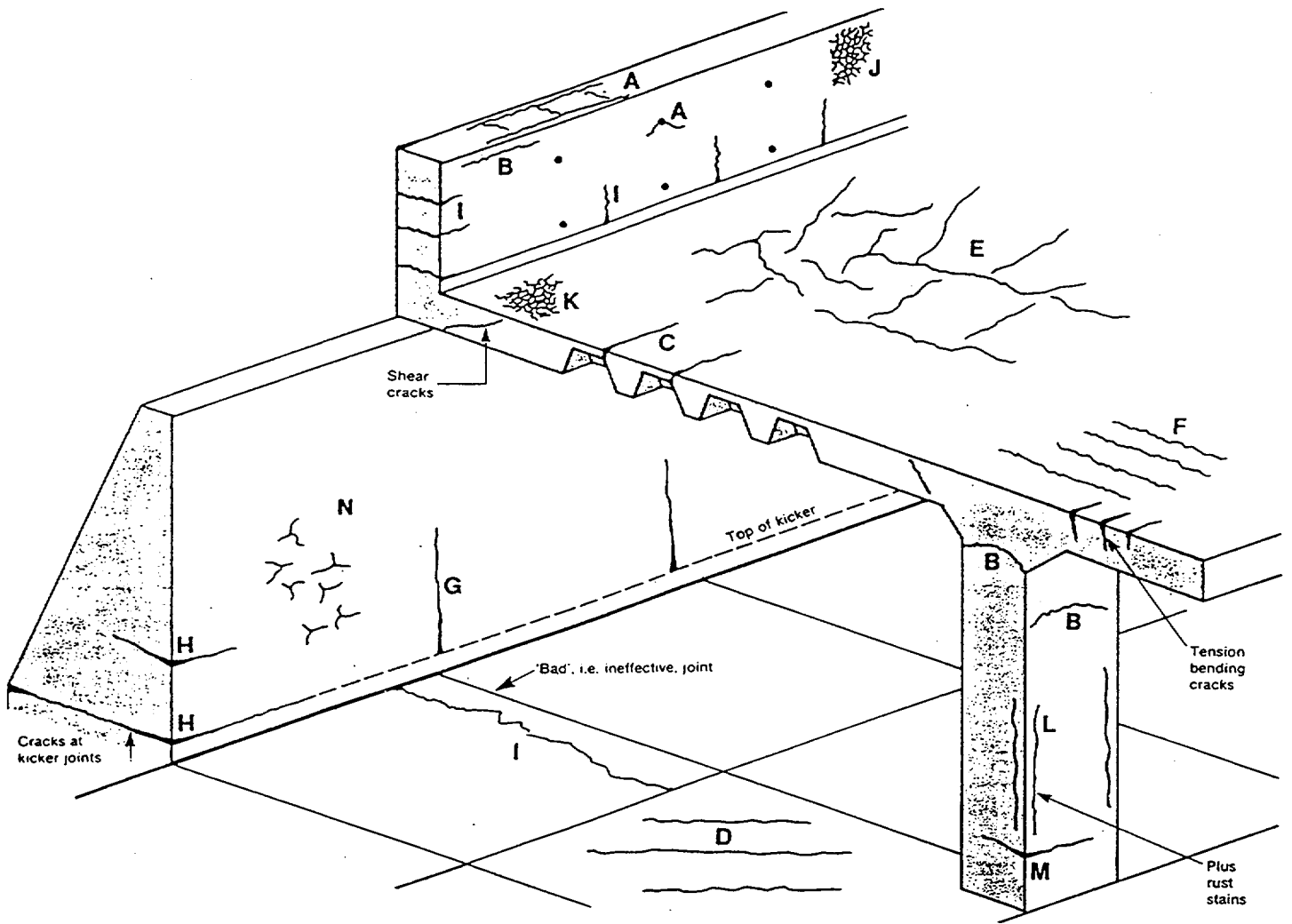


Figure 3.1 Summary of Concrete Crack Types (CEB-FIB, 1992)
 Reprinted with permission of *fib*, Federation Internationale du Beton (CEB-FIB).

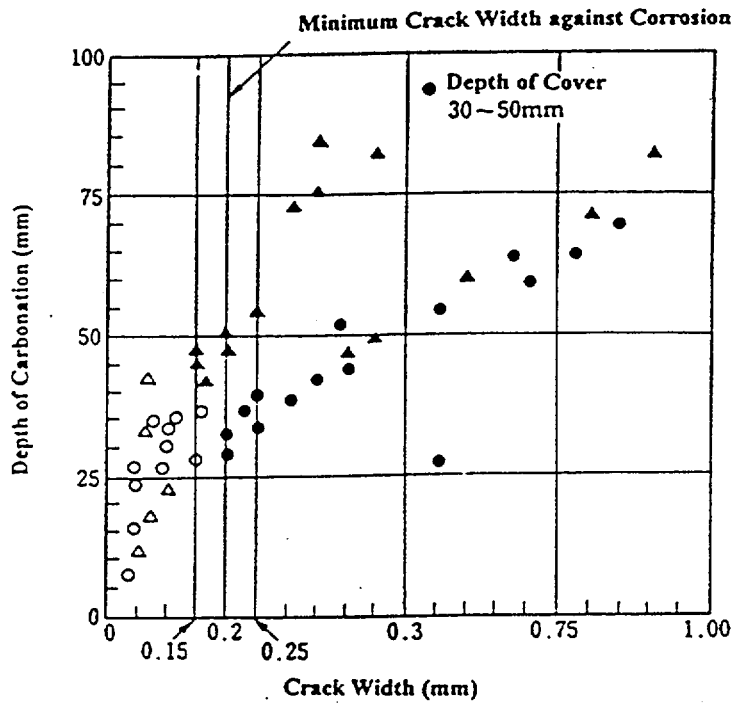


(a) Intrinsic Cracks (See Table 3.2) (CEB-FIB, 1992)
 Reprinted with permission of *fib*, Federation Internationale du Beton (CEB-FIB).

Cracks caused by load/Imposed deformation	Pure flexure		Direction of cracks transverse to tensile reinforcement
	Shear		Cracks develop from those due to flexure (Line 2a)
	Pure tension		Cracks cross the full cross-section
	Bond failure		Cracks may form in the anchorage zone; they are parallel to the reinforcing bars

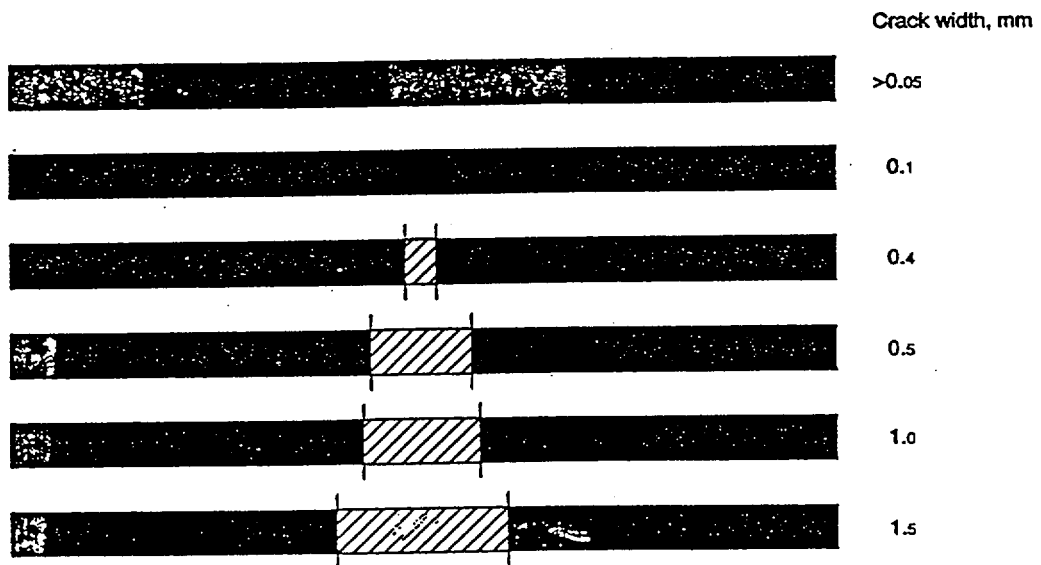
(b) Cracks Due to Load or Deformation (Litzner and Becker, 1999)
 Permission to use this copyrighted material is granted by RILEM.

Figure 3.2 Examples of Crack Types that can Form in Concrete Structures



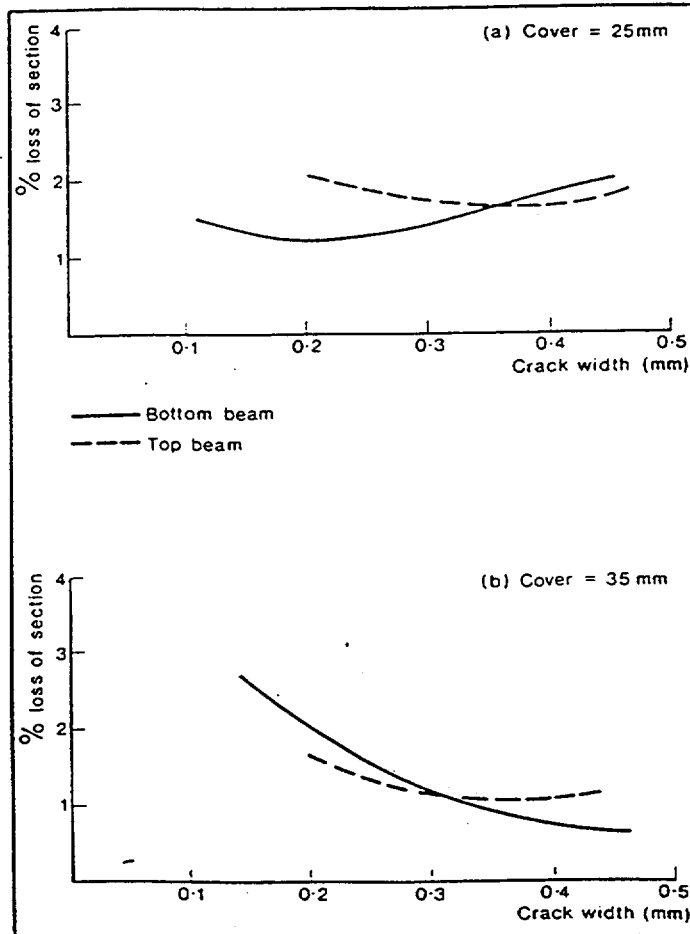
Note: 1 mm = .0394 in.

Figure 3.3 Surface Crack Width, Carbonation Depth, and Corrosion (Yoda and Yokomuro, 1987)
 Permission to use this copyrighted material is granted by the above author(s).



Note: 1 mm = .0394 in.

Figure 3.4 Effect of Crack Width on Corrosion Length (Halvorsen, 1966).
 Permission to use this copyrighted material is granted by Lund Institute of Technology, Sweden.



Note: 1 mm = .0394 in.

Figure 3.5 Crack Width and Corrosion of 8-mm ϕ Bar in Marine Environment (after 10-year exposure) (Beeby, 1983). Permission to use this copyrighted material is granted by the American Concrete Institute.

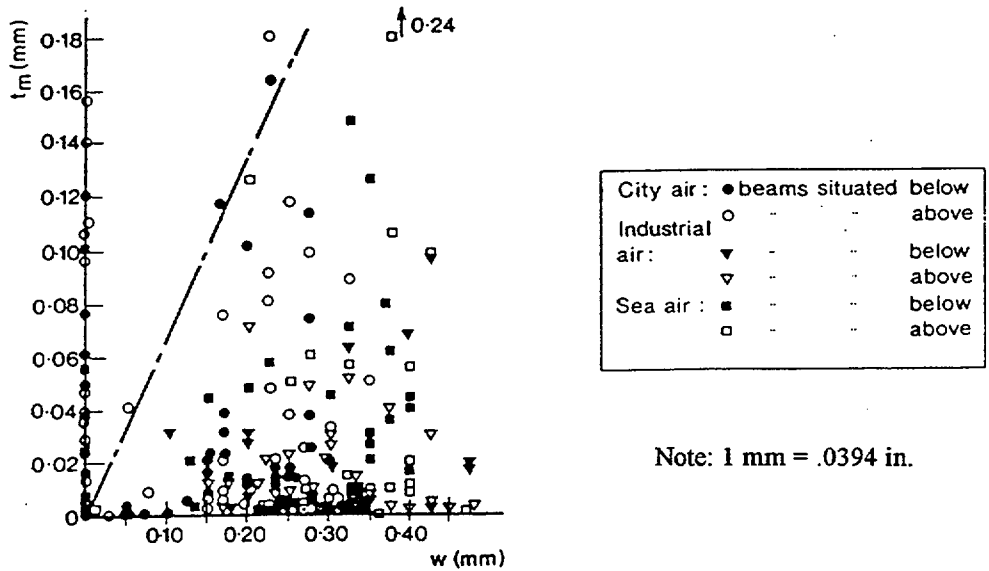


Figure 3.6 Corrosion Depth vs Crack Width After 10-Year Exposure (Beeby, 1978a).
 Permission to use this copyrighted material is granted by the British Cement Association.

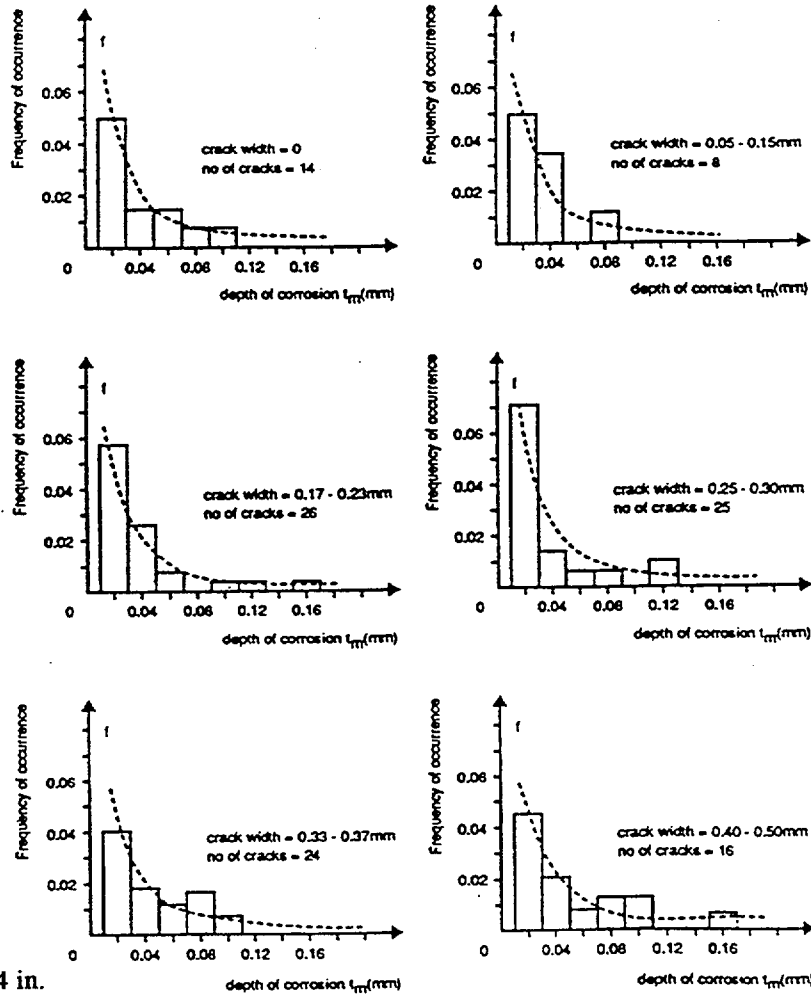
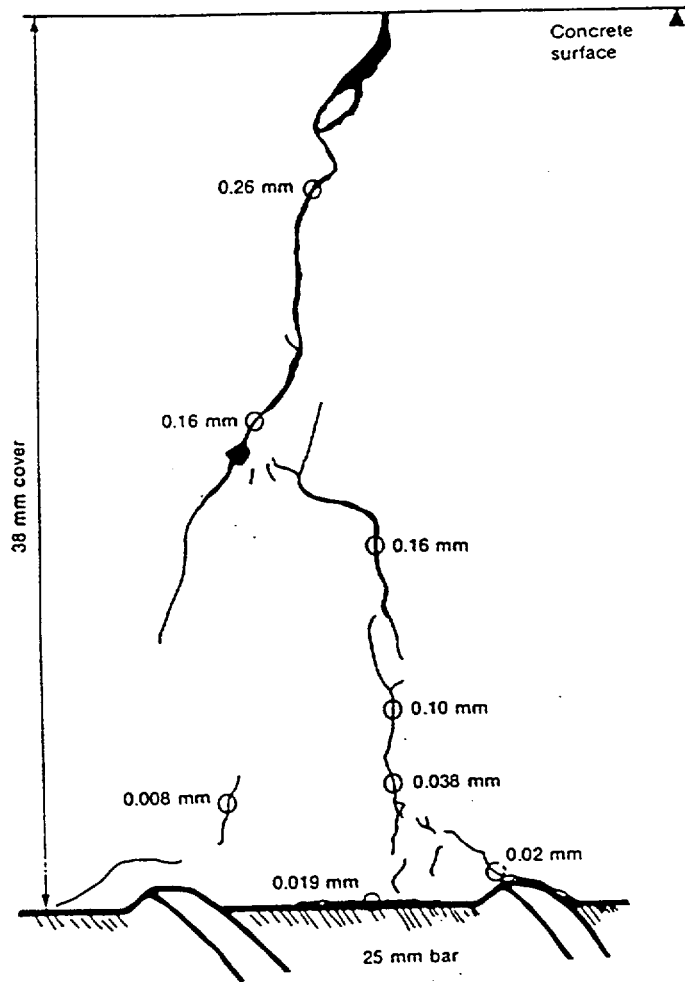
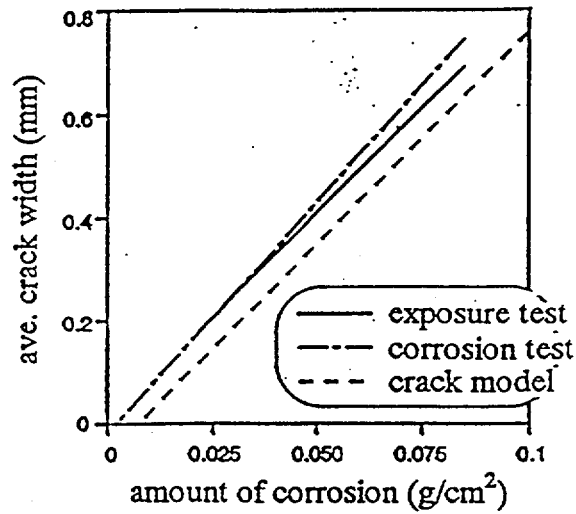


Figure 3.7 Distribution of corrosion Depths in Figure 3.6 (Beeby, 1978a).
 Permission to use this copyrighted material is granted by the British Cement Association.



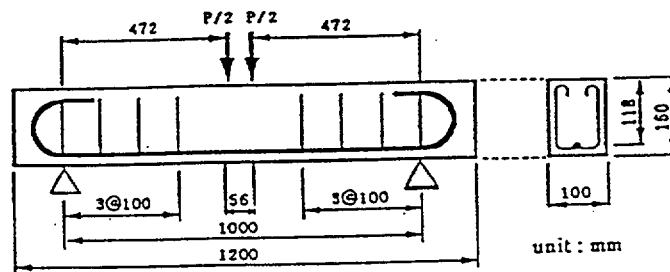
Note: 1 mm = .0394 in.

Figure 3.8 Variation of Crack Width with Depth (Beeby, 1978).
 Reprinted by kind permission of the Institute of Structural Engineers (www.istructe.org.uk).



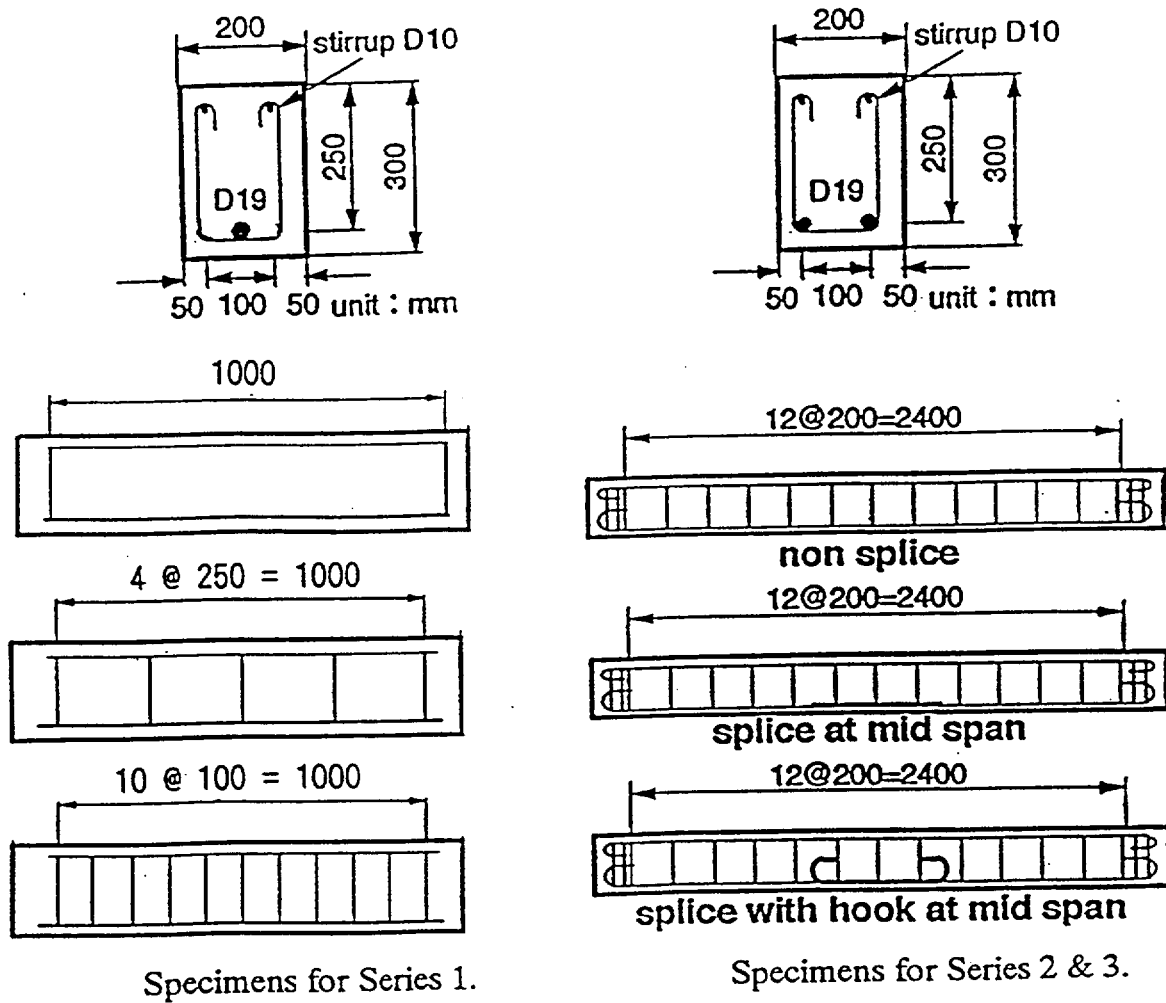
Note: 1 mm = .0394 in., 1 g/cm² = .0142 psi

Figure 3.9 Crack Width vs Corrosion (Maruyama, Shimomura, and Hamada 1999)
 Permission to use this copyrighted material is granted by the above author(s).



Note: 1 mm = .0394 in.

Figure 3.10 Beam Test Specimen (Kawamura et al., 1999).
 Permission to use this copyrighted material is granted by Nagaoka University of Technology, Japan.



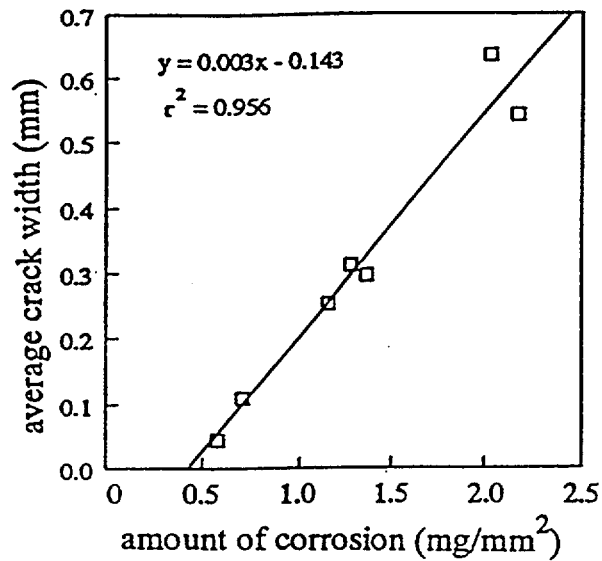
Specimens for Series 1.

Specimens for Series 2 & 3.

Note: 1 mm = .0394 in.

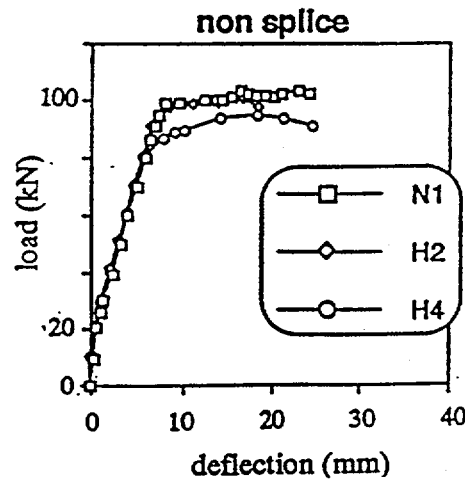
Figure 3.11 Beam Test Specimens (Maruyama and Shimomura, 1999).

Permission to use this copyrighted material is granted by the above author(s).



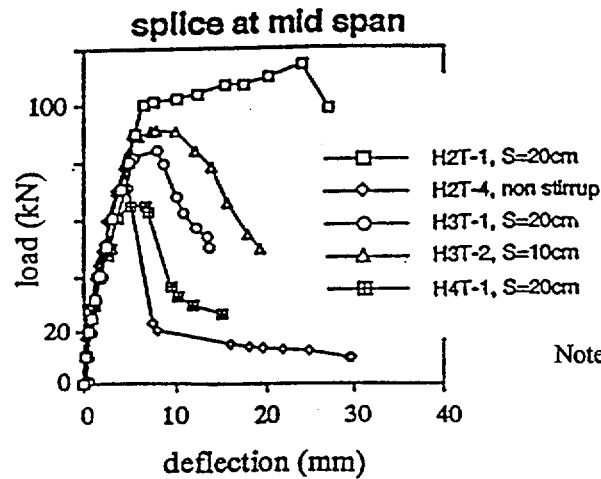
Note: 1 mm = .0394 in.,
1 mg/mm² = .00142 psi

Figure 3.12 Crack Width vs Corrosion (Maruyama and Shimomura, 1999). *



Note: 1 mm = .0394 in.,
1 kN = 225 lbs.

Figure 3.13 Load vs Deflection Curves (w/o Splices) for Static Loading (Maruyama and Shimomura, 1999). *



Note: 1 mm = .0394 in.,
1 kN = 225 lbs.

Figure 3.14 Load vs Deflection Curves (w Splices) for Static Loading (Maruyama and Shimomura, 1999). *

* Permission to use this copyrighted material is granted by the above author(s).

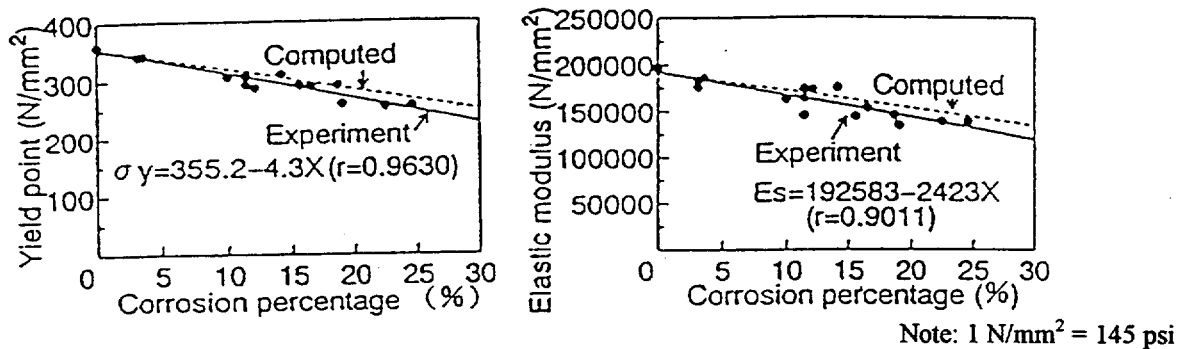
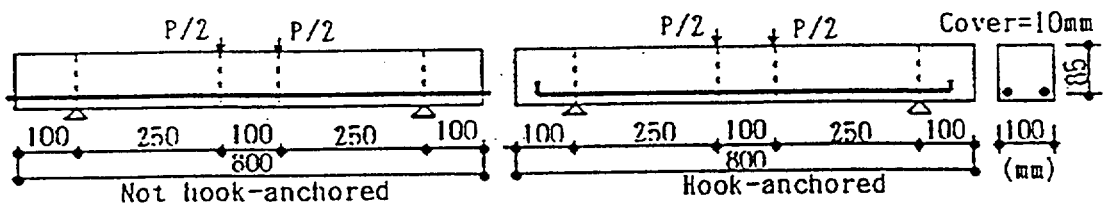


Figure 3.15 Effect of Corrosion on Steel Properties (Lee et al., 1996). *



Note: 1 mm = .0394 in.

Figure 3.16 Beam Test Specimens (Lee et al., 1996). *

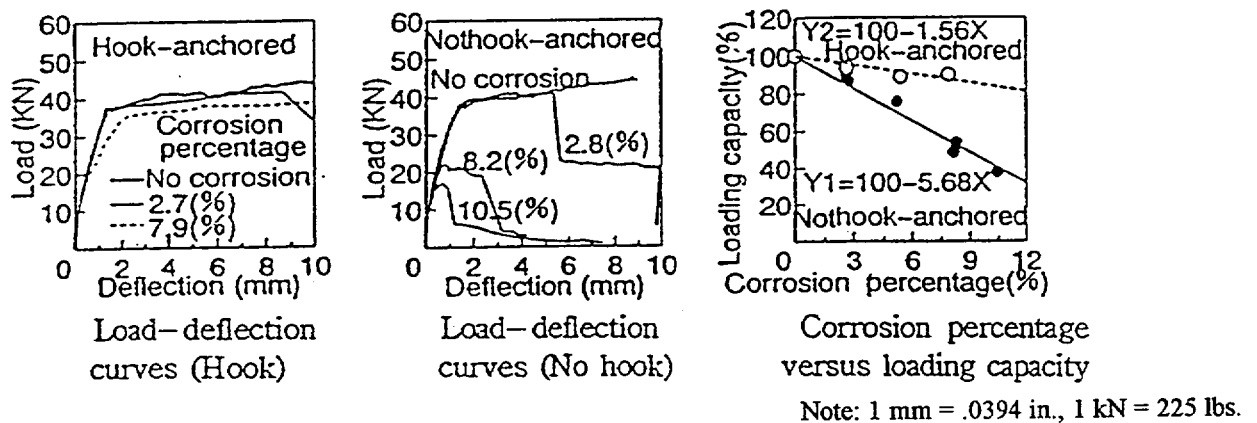


Figure 3.17 Performance of Beams w and w/o Hooked Anchors (Lee et al., 1996). *

* Permission to use this copyrighted material is granted by the International Thomson Publishing Services, Ltd., England.

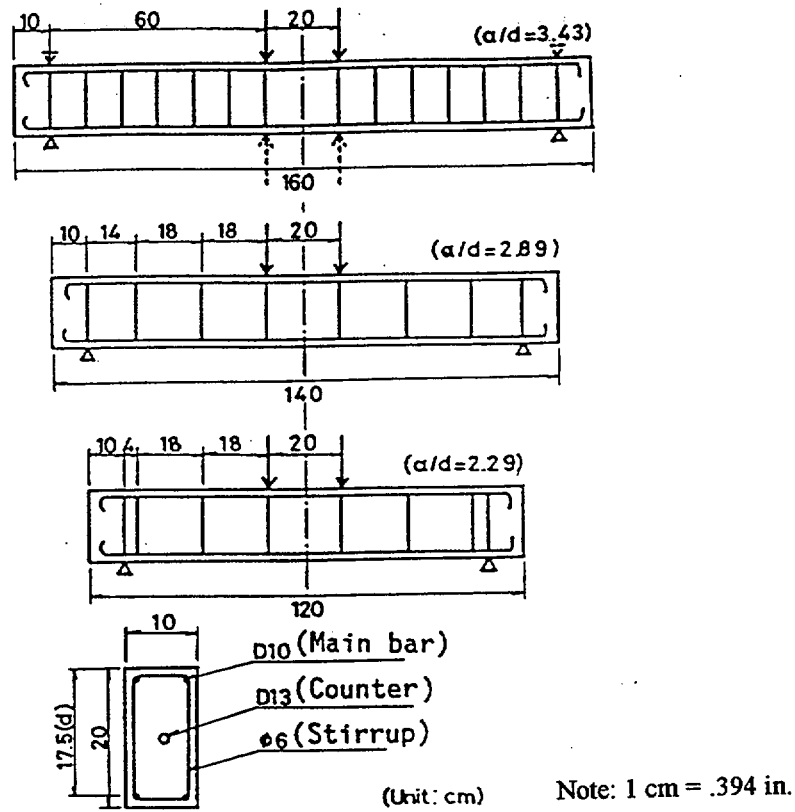


Figure 3.18 Details of Test Specimens (Okada et al., 1988).
 Permission to use this copyrighted material is granted by the American Concrete Institute.

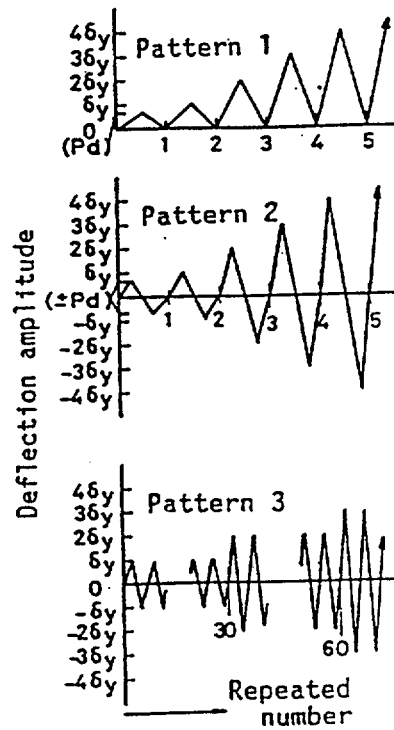
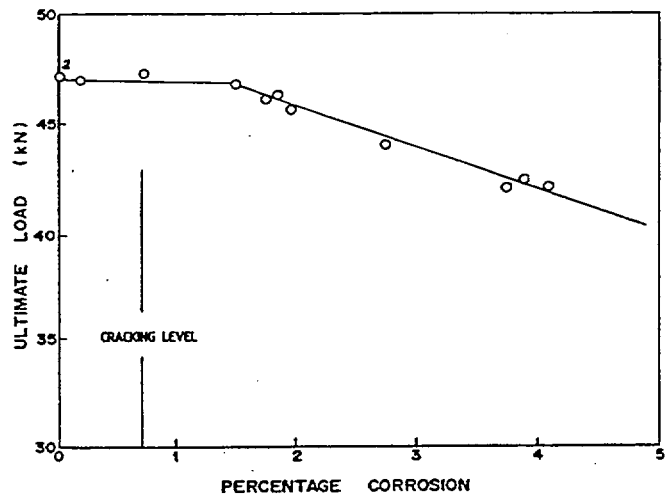
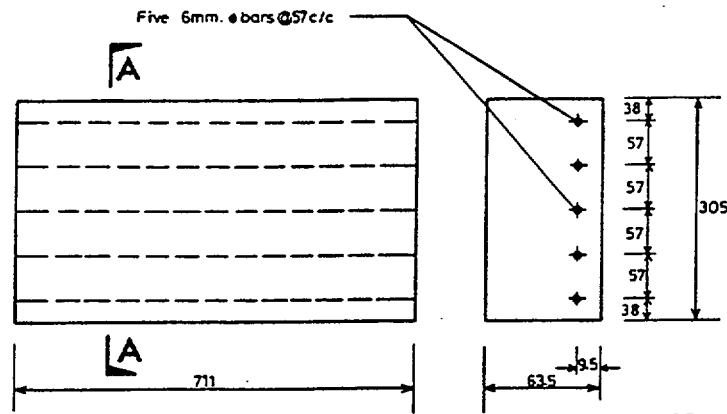


Figure 3.19 Loading Patterns (Okada et al., 1988).
 Permission to use this copyrighted material is granted by the American Concrete Institute.



Note: 1 kN = 225 lbs.

Figure 3.20 Effect of Corrosion on Ultimate Load of Beams (Al-Sulaimani et al., 1990).
 Permission to use this copyrighted material is granted by the American Concrete Institute.



Note: 1 mm = .0394 in.

PLAN & SECTION A-A
DIMENSIONS IN mm.

Figure 3.21 Slab Test Specimens. (Almusallam, et al., 1996 "Effect of Reinforcement Corrosion on Flexural Behavior of Concrete Slabs," *Journal of Materials in Civil Engineering* 8(3), American Society of Civil Engineers (ASCE), pp. 123-127, August 1996; reprinted with permission of ASCE.)

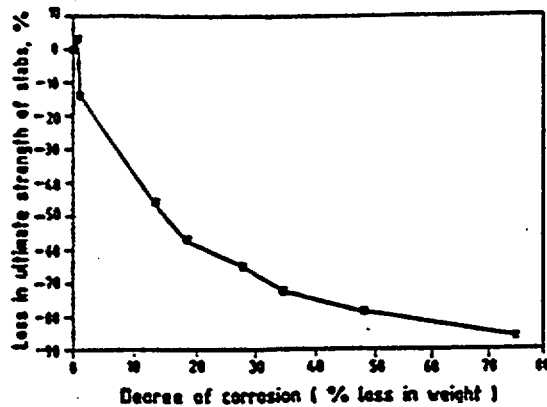
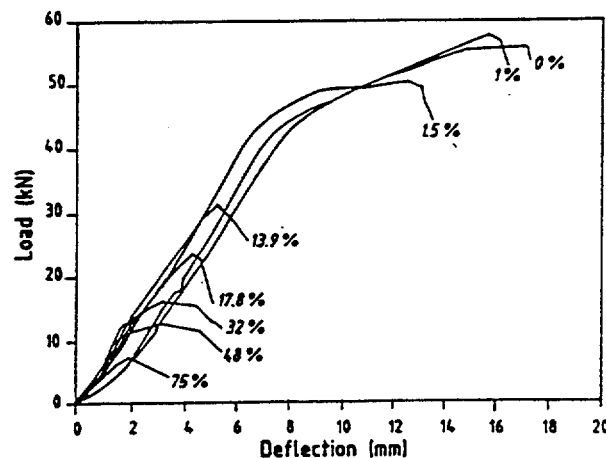


Figure 3.22 Effect of Corrosion on Strength. (Almusallam, et al., 1996 "Effect of Reinforcement Corrosion on Flexural Behavior of Concrete Slabs," *Journal of Materials in Civil Engineering* 8(3), American Society of Civil Engineers (ASCE), pp. 123-127, August 1996; reprinted with permission of ASCE.)



Note: 1 mm = .0394 in.,
1 kN = 225 lbs.

Figure 3.23 Effect of Corrosion on Load vs Deflection. (Almusallam, et al., 1996 "Effect of Reinforcement Corrosion on Flexural Behavior of Concrete Slabs," *Journal of Materials in Civil Engineering* 8(3), American Society of Civil Engineers (ASCE), pp. 123-127, August 1996; reprinted with permission of ASCE.)

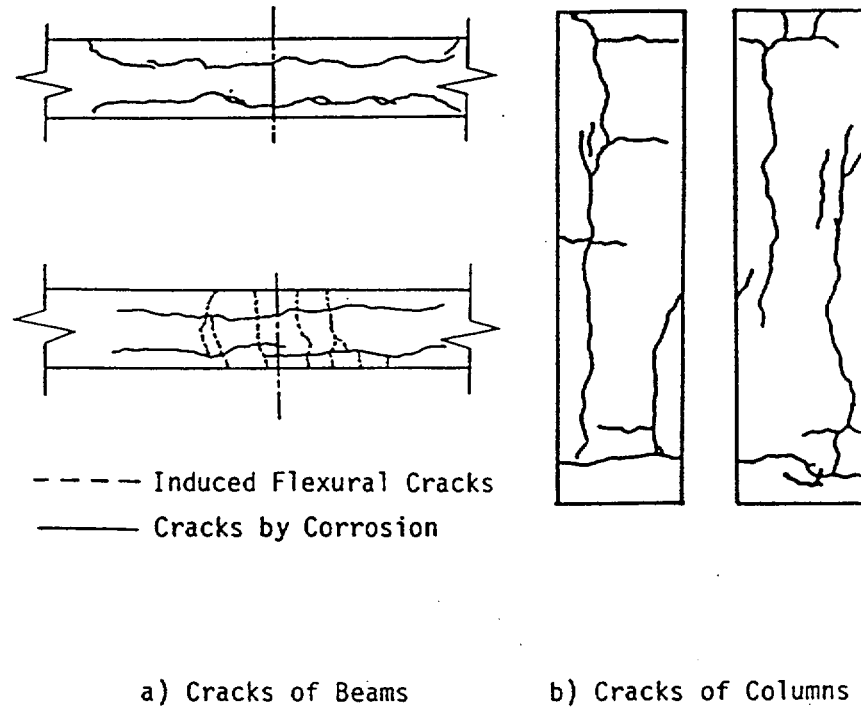


Figure 3.24 Cracking in Beams and Columns Due to Corrosion (Uomoto and Misra, 1988).
 Permission to use this copyrighted material is granted by the American Concrete Institute.

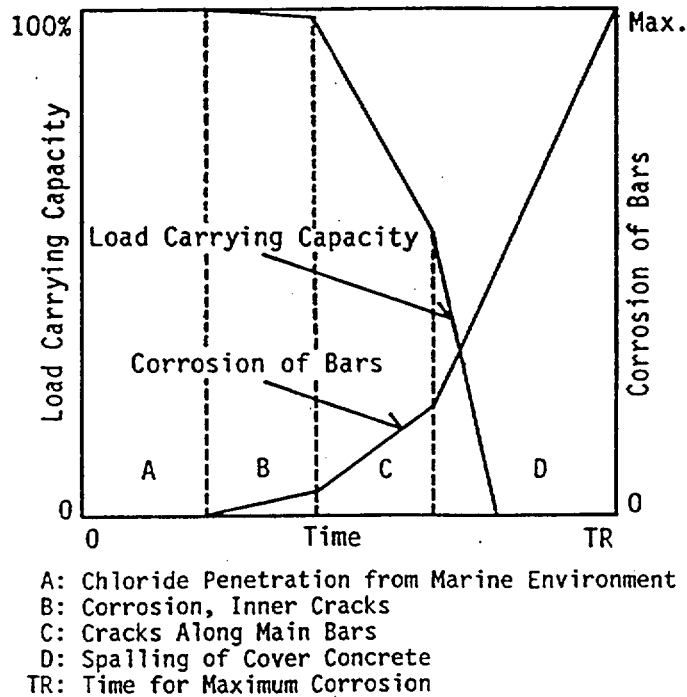


Figure 3.25 Qualitative Representation of Damage in RC Structures Due to Corrosion (Uomoto and Misra, 1988).
 Permission to use this copyrighted material is granted by the American Concrete Institute.

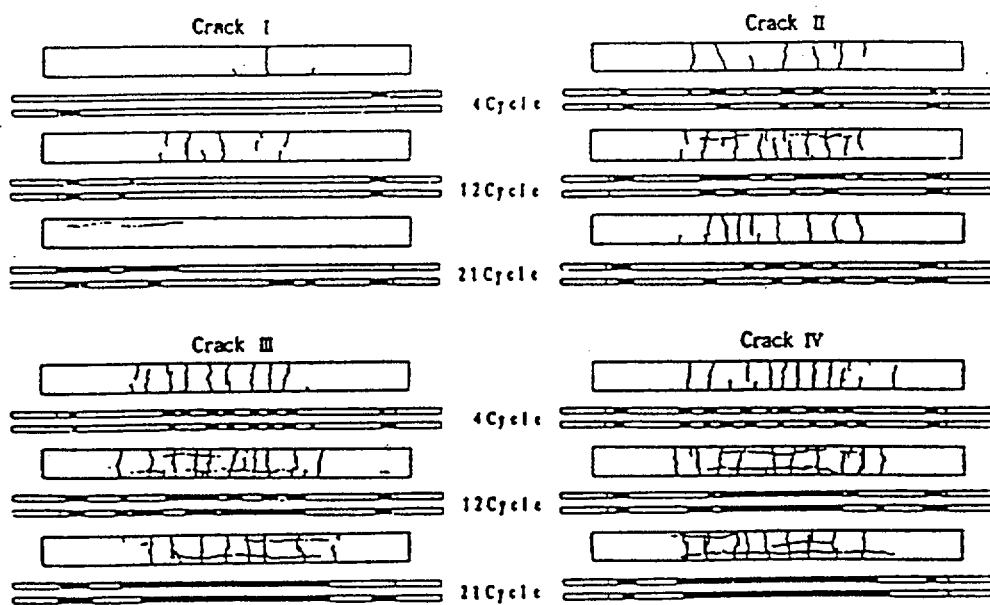


Figure 3.26 Pattern of Precracks and Rebar Corrosion Before Loading (Yokota, et al., 1994).
 Permission to use this copyrighted material is granted by the Japan Cement Association.

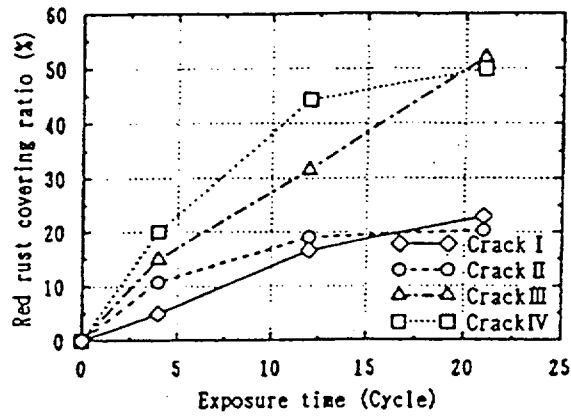


Figure 3.27 Corrosion Formation vs Exposure Cycles (Yokota et al., 1994).
 Permission to use this copyrighted material is granted by the Japan Cement Association.

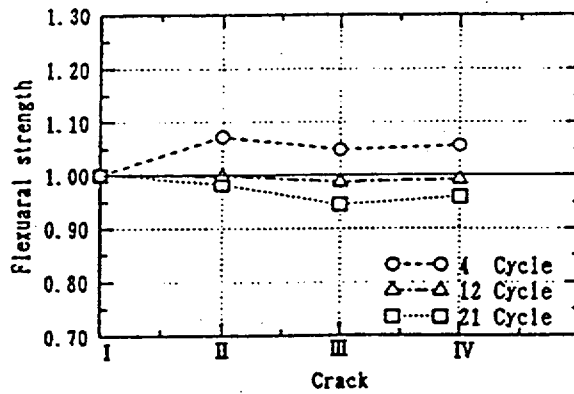


Figure 3.28 Normalized Flexural Strength vs Exposure Cycles (Yokota et al., 1994).
 Permission to use this copyrighted material is granted by the Japan Cement Association.

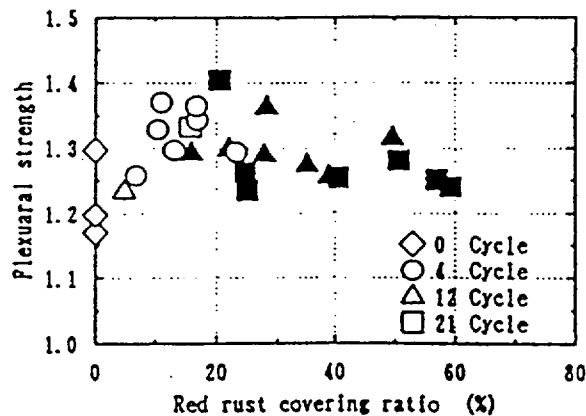


Figure 3.29 Normalized Flexural Strength vs Amount Corrosion (Yokota et al., 1994).
 Permission to use this copyrighted material is granted by the Japan Cement Association.

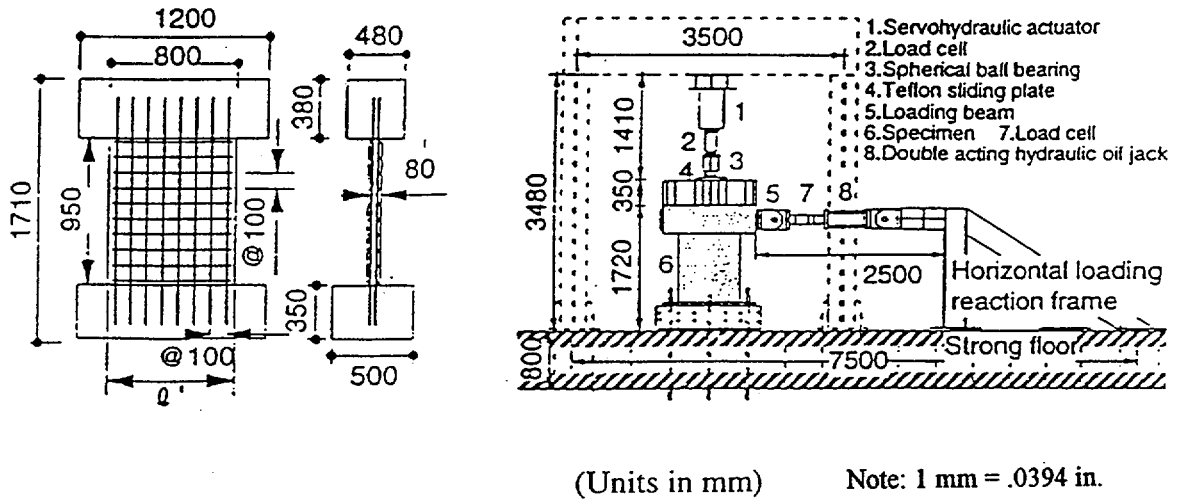


Figure 3.30 RC Structural Wall Specimen and Test Set Up (Yamakawa, 1995).
 Permission to use this copyrighted material is granted by the above author(s).

Specimen	RCW-SCe-1	RCW-SCe-2	RCW-SCe-3	RCW-SCe-4
Corrosion (%)	7	14	10	9
Free Side				
Electrode Side				
Max. crack width	0.15mm	3.0mm	0.8mm	0.7mm

Note: 1 mm = .0394 in.

Figure 3.31 Cracks in RC Structural Wall Specimen Due to Corrosion (Yamakawa, 1995).
 Permission to use this copyrighted material is granted by the above author(s).

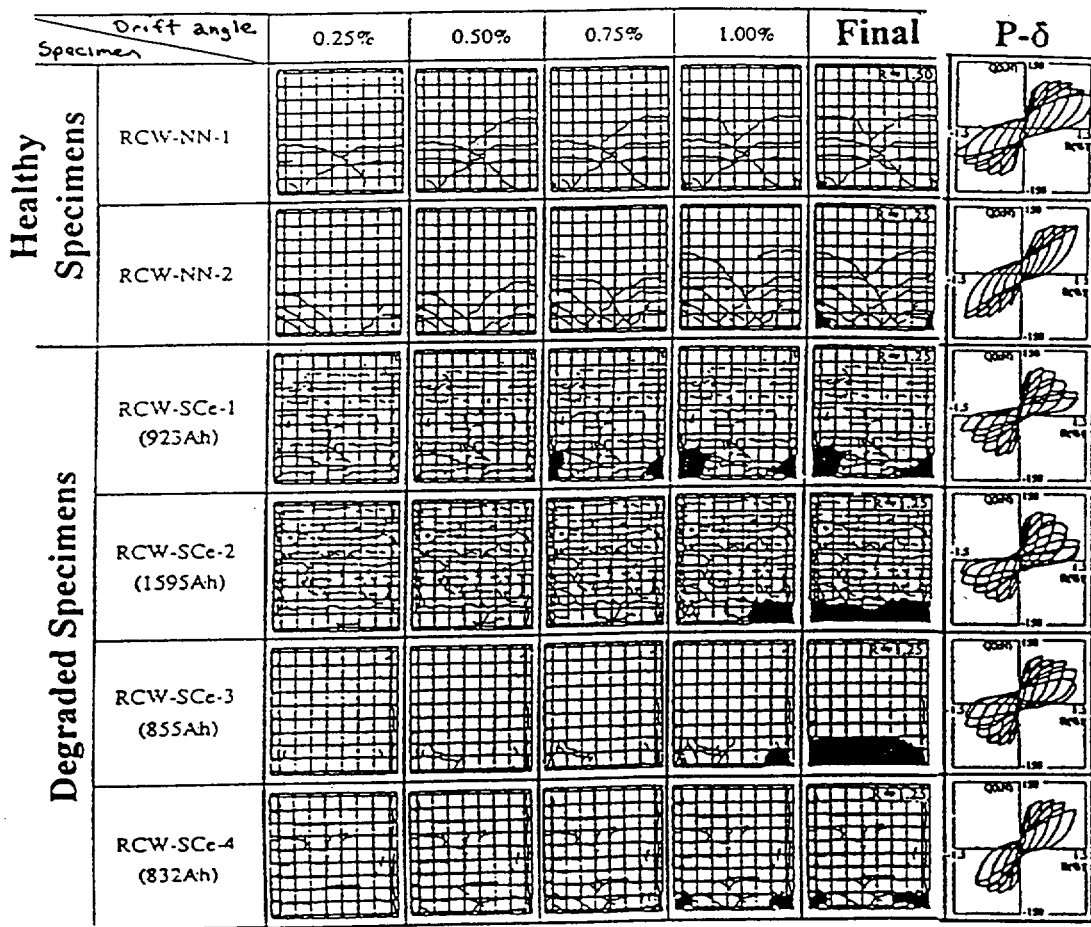
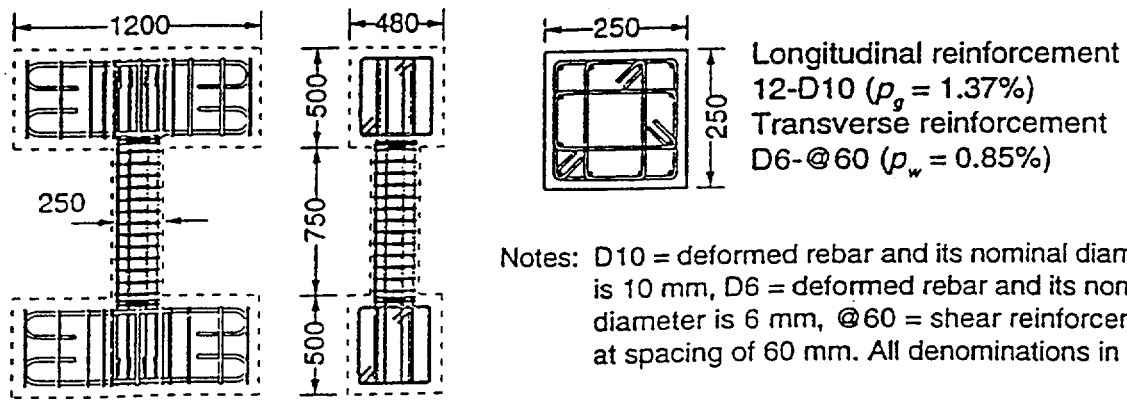


Figure 3.32 Summary of Shear Test Results (Yamakawa, 1995).
 Permission to use this copyrighted material is granted by the above author(s).



Note: 1 mm = .0394 in.

Figure 3.33 Detail of RC Column Specimen (Yamakawa, 1998).
Permission to use this copyrighted material is granted by the above author(s).

		R=0.5%		R=1.0%		R=2.0%		R=3.0%	
		Web	Flange	Web	Flange	Web	Flange	Web	Flange
Normal test	RCC-NN-6 (Non salt)								
Exposure test	RCC-NC-1 (Non salt)								
	RCC-SC-1 (Salt)								

Figure 3.34 Crack Patterns at Different Drift Angles for Column Specimens (Yamakawa, 1998).
Permission to use this copyrighted material is granted by the above author(s).

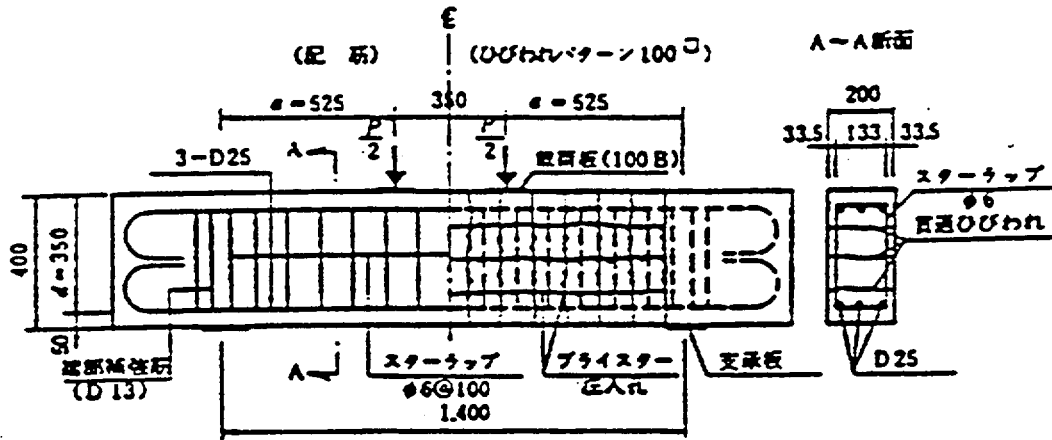


Figure 3.35 Specimen Configuration and Initial Crack Pattern (Akiyama, 1987).
 Permission to use this copyrighted material is granted by the Japan Concrete Institute/Kajima
 Technical Research Institute, Japan.

Table 3.1 Interacting Factors for Mechanisms Producing Premature Concrete Degradation (Mather, 1979). Permission to use this copyrighted material is granted by the American Concrete Institute.

Factor that may induce premature deterioration	Characteristic of the concrete	Characteristic of the environment	Manifestation of deterioration
Freezing and thawing	Lack of entrained air in the cement paste or excessively porous aggregate, or both, in saturated concrete	Moisture and freezing and thawing	Internal expansion and cracking
Aggressive chemical attack			
Sulfate attack	Excessive amounts of hydrated calcium aluminates in the cement paste	Moisture containing dissolved sulfates in excessive concentration	Internal expansion and cracking
Leaching	Excessive porosity	Moisture of low pH and low dissolved lime content	Dissolution and removal of soluble constituents
Abrasion	Lack of resistance to abrasion	Abrasive, often in or under water	Removal of material
Corrosion of embedded metal	Corrodible metal and (usually) corrosion-inducing agents in the concrete	Moisture (or moisture and corrosion-inducing agents)	Internal expansion and cracking
Alkali-silica reaction	Excessive amounts of soluble silica in the aggregate and (usually) alkalis in the cement	Moisture (or moisture and alkalis)	Internal expansion and cracking
Other			
Unsound cement	Excessive amounts of unhydrated CaO or MgO in the cement	Moisture	Internal expansion and cracking
Plastic shrinkage cracking	Lack of maintained moisture content during specified curing period	High evaporation rate for moisture	Cracking at very early ages

Table 3.2 Classification of Intrinsic Cracks (CEB-FIB, 1992).
 Reprinted with permission of *fib*, Federation Internationale du Beton (CEB-FIB).

Type of cracking	Letter (See Fig. 3.2)	Subdivision	Most common location	Primary cause (excluding restraint)	Secondary causes/factors	Remedy (assuming basic redesign is impossible) in all cases reduce restraint	Time of appearance
Plastic settlement	A	Over reinforcement	Deep sections	Excess bleeding	Rapid early drying conditions	Reduce bleeding (air entrainment) or revibrate	Ten minutes to three hours
	B	Arching	Top of columns				
	C	Change of depth	Trough and waffle slabs				
Plastic shrinkage	D	Diagonal	Roads and slabs	Rapid early drying	Low rate of bleeding	Improve early curing	Thirty minutes to six hours
	E	Random	Reinforced concrete slabs	Ditto plus steel near surface			
	F	Over reinforcement	Reinforced concrete slabs				
Early thermal contraction	G	External restraint	Thick walls	Excess heat generation	Rapid cooling	Reduce heat and/or insulate	One day to two or three weeks
	H	Internal restraint	Thick slabs	Excess temperature gradients			
Long-term drying shrinkage	I		Thin slabs (and walls)	Inefficient joints	Excess shrinkage Inefficient curing	Reduce water content Improve curing	Several weeks or months
Crazing	J	Against formwork	'Fair faced' concrete	Impermeable formwork	Rich mixes Poor curing	Improve curing and finishing	One to seven days, sometimes much later
	K	Floated concrete	Slabs	Over-trowelling			
Corrosion of reinforcement	L	Natural	Columns and beams	Lack of cover	Poor quality concrete	Eliminate causes listed	More than two years
	M	Calcium chloride	Precast concrete	Excess calcium chloride			
Alkali-silica reaction	N		(Damp locations)	Reactive aggregate plus high-alkali cement		Eliminate causes listed	More than five years

Table 3.3 Identification of Concrete Defects (Pinjarkar, 1984).
 Permission to use this copyrighted material is granted by the Author(s).

No.	Type of Defect	Most Common Structural Element	Plausible Causes	Suggested Investigations
1	Diagonal cracks generally at or near ends	Beams	Overloading in shear Missing or improper placement of stirrups Error in design	Check existing loading Check design Verify stirrup locations
2	Transverse cracks at the bottom of beams within span and/or excessive deflections	Beams	Overloading Inadequate prestress Low concrete elastic modulus	Check existing loading Check design and prestressing records Test concrete modulus
3	Vertical or inclined cracks at beam-column interfaces	Monolithic beam-column connections	Forces due to restrained volume changes of concrete	Verify reinforcement details Check building movements due to temperature, creep, shrinkage, and elastic shortening
4	Vertical or inclined cracks in support member below the seat and beam ends. Spalling of concrete from the face of column or corbel or beam face below the seat.	Sliding beam-column or slab-beam connections.	Lack of free movement at the sliding surface. Inadequate shear-friction reinforcement. Deficiencies in reinforcement placement and detailing. Inadequate surface preparation.	Check design and shear-friction reinforcement details for forces due to restrained volume changes of concrete. Check building movements due to temperature, shrinkage, creep, and elastic shortening Determine reinforcement location by pachometer or by chipping.

Table 3.3 (Cont.) Identification of Concrete Defects (Pinjarkar, 1984).
 Permission to use this copyrighted material is granted by the Author(s).

No.	Type of Defect	Most Common Structural Element	Possible Causes	Suggested Investigations
5	Excessive deflections or damaged partitions, window and door frames	Slabs Beams	Overload or design deficiencies. Low strength or low modulus concrete. Load too soon or forms removed too soon. Inadequate prestress.	Check loading history Check design Test concrete strength and modulus
6	Cracking in slab over and around columns	Flat Slabs	Insufficient effective depth Design deficiencies Misplaced reinforcement Possible overload	Check concrete cover and effective depth Check design and loading history
7	Corner cracking in slabs near the intersection of support beams or walls	Slabs Walls	Forces caused by restrained volume change deformations of concrete Excessive drying shrinkage or inefficient curing	Check restraints and building movements due to shrinkage, creep, temperature, and elastic shortening
8	Horizontal (in slabs) or vertical (in walls) cracks	Slabs or walls	Lack of contraction or control joints or excessive joint spacing, inefficient curing	Check joint locations Test concrete quality

Table 3.3 (Cont.) Identification of Concrete Defects (Pinjarkar, 1984).
 Permission to use this copyrighted material is granted by the Author(s).

No.	Type of Defect	Most Common Structural Element	Possible Causes	Suggested Investigations
9	Honeycomb and voids	Footings Columns Walls	Inadequate consolidation, poor mix design, placement deficiencies	Review concrete placement methods and test concrete quality
10	Cracking or rust stains parallel to the direction of longitudinal steel. Cracks or rust stains directly over the reinforcement	Slabs Walls Beams Columns	Corrosion of embedded reinforcement Lack of sufficient cover Excessive chlorides in concrete or exposure to corrosive environment	Check as-built concrete cover Test concrete quality and chloride content Measure half-cell potentials Expose and determine extent of steel corrosion Test grout and condition of post-tensioning conduits, if any.
11	Delaminations	Slabs Walls Columns	Corrosion of embedded reinforcement Excessive chlorides in concrete or exposure to corrosive environment	Test concrete quality and chloride content Conduct delamination survey Measure half-cell potentials
12	Spalls and popouts over pre-stressing steel anchors, or other embedded steel items	Slabs	Corrosion of embedded steel Lack of sufficient cover	Test concrete quality and chloride content Check sources of corrosion. Check waterproofing requirements

Table 3.3 (Cont.) Identification of Concrete Defects (Pinjarkar, 1984).
 Permission to use this copyrighted material is granted by the Author(s).

No.	Type of Defect	Most Common Structural Element	Plausible Causes	Suggested Investigations
13	Random shallow cracks on the surface	Slabs	Plastic shrinkage cracking due to rapid early drying Inefficient curing	Test concrete quality Check curing procedures Check environmental conditions during construction such as temperature, humidity, and wind
14	Cracks in thick or massive concrete members	Walls Pedestals Slabs	Thermal contraction Excess heat generation and/or temperature gradients External or internal restraints Rapid cooling	Check restraints Check temperature gradients and rate of cooling. Test concrete quality
15	Scaling	Slabs	Lack of entrained air Deficiencies in concrete quality Over troweling	Test concrete quality and air void system Check exposure conditions
16	Leakage and efflorescence	Slabs Walls Beams	Plastic shrinkage Leakage through cracks	Test concrete quality Evaluate causes of cracking

Table 3.4 Relation Between Crack Width and Corrosion (Beeby, 1979).

Permission to use this copyrighted material is granted by the British Cement Association.

Surface crack width (mm)	Average depth of corrosion (mm)	Average corroded Length (mm)
0.13	0.16	9.2
0.25	0.16	12.9
0.51	0.18	12.8
1.27	0.21	15.0

Note: 1 mm = .0394 in.

Table 3.5 Expected Time Periods to Develop Visible Crack Width (Andrade et al., 1993).

Permission to use this copyrighted material is granted by the above author(s).

Corrosion rate per year	Time period (years)	
	Crack width of 0.05–0.1 mm (20 µm) ^a	Crack width 0.2–0.3 mm (100–150 µm)
1 µm	20	> 100
10 µm	2	10–15
100 µm	0.2	1–2
1 mm	0.02	0.1–0.2

^a Bar cross-section loss given in brackets.

Note: 1 mm = .0394 in.

4 DEGRADATION DETECTION AND CONDITION ASSESSMENT

Reinforced concrete structures in NPPs are subjected in use to many environmental influences that can impact their ability to continue to meet functional and performance requirements. Continuing satisfactory performance of the reinforced concrete structures over an extended period of time is dependent in large measure on the durability of its basic components. Techniques for detection of degradation should therefore concentrate on these elements (i.e., concrete and reinforcing steel). Due to the significant safety as well as economic influences that could result if these structures were to deteriorate to unacceptable performance levels, it is important that they be inspected at regular intervals.

There is a vast variety of test methods available for use in performing inspections of reinforced concrete structures and their materials of construction. Information provided below focuses on methods most commonly used and on those that represent good practice for the detection of degradation of elements used in the construction of reinforced concrete structures. Additional information to that provided below is available elsewhere (e.g., ACI 228.1R, 1989; ACI 228.2R, 1999; Malhotra and Carino, 1991; Lew, 1988; Bungey, 1996). Often the most effective approach to detecting aging effects is to use a combination of testing methods.

4.1 Detection Methods for Concrete

Primary manifestations of distress that are present or can occur in concrete used to fabricate NPP reinforced concrete structures include cracking, voids, and delaminations; and strength losses.* Methods used to detect discontinuities in concrete structures generally fall into two categories: direct and indirect. Direct methods involve a visual inspection of the structure, removal/testing/analysis of material(s), or a combination of the two. The indirect methods generally measure some parameter from which an estimate of the extent of degradation can be made through existing correlations. Most nondestructive testing methods for concrete are indirect. Quite often, however, evaluation of concrete structures and materials requires use of a combination of test methods since no single testing technique is available that will detect all potential degradation factors. For discussion purposes, testing methods are grouped into categories of nondestructive and destructive testing. Assessments of inaccessible concrete components would be done either through removal of material to expose the component of interest and applying the methods described below, or indirectly through environmental evaluations (i.e., quantification of the aggressiveness of the ambient environment).**

4.1.1 Nondestructive Testing

Nondestructive test methods can be used to indicate the strength, density and quality of concrete; locate and characterize voids or cracks in concrete; and locate steel reinforcement and indicate depth of concrete cover. Tables 4.1 and 4.2 present nondestructive test methods for determining material properties of hardened concrete in existing structures, and to determine structural properties and assess conditions of concrete, respectively (ACI 228.2R, 1999). Nondestructive testing methods can be grouped under several categories (1) visual, (2) stress wave, (3) nuclear, (4) magnetic, (5) infrared thermography, (6) radar, (7) audio, (8) rebound hammer, and (9) penetrability.

* Corrosion of embedded steel reinforcement, which is the primary mode of degradation of concrete structures that is of interest in this study, is addressed in Section 4.2.

** If the ambient environment is determined to be potentially aggressive, additional testing and evaluation is required that may involve removal of material to expose the component for direct inspection and testing.

4.1.1.1 Visual Inspection

Visual inspection generally is the basic method used as a first step in a typical inspection program. A high quality visual inspection of exposed concrete is able to detect and define areas of age-related distress that result in visible effects on the surface of the structure (e.g., cracking, moisture movement, mechanical degradation, spalling, volume change, or cement-aggregate interactions). Visual inspections also include periodic mapping and measurements to provide a history of crack appearance and development that can assist in identifying the cause and establish whether the crack is active or dormant. Tools that can aid in performing a visual inspection include items such as field book, clipboards, markers, flashlight, camera, measuring tapes, calipers, optical magnification device, mirror, feeler gages, crack comparator, straight edge, level, pocket knife, wire and paint brushes, screwdriver, pliers, chipping hammer, binoculars, and sounding line. Fiberscopes and borescopes allow inspection of regions that might otherwise be inaccessible to the naked eye. Also, video cameras provide a means of recording current conditions for future reference.

The primary limitation of this method is that it cannot reveal internal degradation of the concrete structure when there are no visible symptoms on the surface (e.g., subsurface cracking, voids, and delaminations; and extent of cracking). Broad knowledge in structural engineering, concrete materials, and construction methods is needed in order to extract the most information from the visual inspection. Useful guides are available to help recognize and classify different types of damage as well as the probable cause (ACI 201.1R, 1968; ACI 207.3R, 1979; ACI 224, 1989; ACI 311.4R, 1988; and ACI 349.3R, 1996).

4.1.1.2 Stress Waves

Stress waves occur when pressure or deformation is suddenly applied to the surface of a material. The disturbance is propagated in a manner analogous to how sound travels through air. The speed of stress-wave propagation in an elastic solid is a function of the modulus of elasticity, Poisson's ratio, density, and geometry. This dependence is used to infer characteristics about the solid by monitoring wave propagation. Several test methods based on stress-wave propagation can be used for nondestructive testing of concrete structures. Ultrasonic methods can be used for locating discontinuities or abnormalities in concrete structures. The stress-pulse echo methods are useful for flaw detection and thickness determinations, and spectral analysis of surface waves is useful for thickness determinations of layered media.

Ultrasonic pulse velocity methods are commonly used to examine homogeneous materials such as metals. Basic components of the equipment include a means for producing and introducing a pulse into the material examined, and a means of accurately measuring the time required for the pulse to travel through the material to a receiver [Figure 4.1(a)]. The condition of the material is assessed through determination of the pulse velocity and the amplitude of the stress wave at the receiver (ASTM C 597). When displaying the travel time of the stress waves between the generator and receiver versus the location, there will be a deviation in the curve at the position of the subsurface defect. Figure 4.1(b) indicates the effects of different defects on the travel time of the ultrasonic pulse. Ultrasonic pulse velocity equipment for examination of concrete materials is essentially the same as that used for metallic materials except a 30 to 200 kHz transducer is used instead of a 0.1 to 25 MHz transducer because of the greater attenuation characteristics of concrete materials. By using this method it is possible to determine the concrete dynamic modulus of elasticity, Poisson's ratio, thickness, and estimate in-situ compressive strength. The method also can be used to detect concrete internal structure changes, cracking or voids, and changes due to freezing and thawing or other aggressive environments. For detecting internal structural changes, the method is limited by segregation/inhomogeneity of the concrete and quality of the acoustical contact. For strength and related properties, the test must be calibrated to the specific concrete as the results are influenced by aggregate size, type, and gradation; cement type; water-cementitious materials ratio;

admixtures; degree of compaction; curing conditions and age of the concrete; acoustical contact; concrete temperature; moisture content; size and shape of specimen; and presence of reinforcement. Despite the dependence on so many variables, the ultrasonic pulse velocity method can be used effectively. It is most useful when carrying out comparative surveys of concrete quality in or between similar concrete structures. Changes in signal amplitude or attenuation characteristics can be used to indicate changes in material properties that occur with time (e.g., detection of the action of frost or alkali-silica reactions through measurement of frequency-dependent attenuation of direct transmission ultrasonic pulses).

Ultrasonic pulse echo involves the use of transmitting and receiving transducers that are normally placed close to each other on the testing surface (Figure 4.2). This method thus overcomes the drawback of the ultrasonic pulse velocity methods that require access to both surfaces. Rapid-hardening cement is used to effectively attach the transducers to the concrete surface. The transmitter also may be designed as a receiver. The pulsed signal inputs may be produced by a piezoelectric transducer. The echo signals are analyzed and their transmission times may be converted to velocities if the wave speed is known. In this way it is possible to measure the depth to reflectors (e.g., cracks or large voids). Because of the heterogeneity of concrete, it may be difficult to distinguish actual defects. Large aggregates have a significant scattering effect on the signals thus restricting the method to relatively low frequency inputs. Modern pulse-echo equipment has achieved some success in this respect by using transducer "arrays" of up to twelve transducers. Signals are transmitted and received between combinations of these transducers and by averaging the response it is possible to more clearly define relevant reflectors. The pulse-echo method is the acoustic method most similar to conventional ultrasonic testing such as used for examining metallic materials. It has the potential to locate and identify discrete defects or objects if sufficient focusing is achieved by the transducers. Concrete made with aggregates of 16-mm (.63 in.) maximum size has been tested successfully and cylindrical voids with a 100-mm (3.94 in.) diameter can be detected at depths to 600 mm (23.6 in.). Reflected signals from large planar surfaces can be detected at depths to 1300 mm (51.2 in.).

The impact-echo method involves striking the concrete surface with a small ball of given diameter to produce a transient stress wave that propagates into the concrete (Wiberg, 1993). In a true pulse-echo mode the transmitter and receiver are one transducer, however, there are technical problems associated with this setup relative to development of a suitable transducer for concrete. Current applications primarily place the impact source and receiving transducer adjacent to each other on the concrete surface (pitch-catch method). Some control of the input can be achieved by varying the size of the impactor thus determining the frequency of the input signals (i.e., smaller diameter impactors create higher frequency waves that are more sensitive to small reflectors at shallower depths, and vice versa). The sound pulse or compression wave is reflected from the back side of the concrete element, internal reflectors (e.g., cracks), or from other objects that may cause changes in the acoustic impedance and material density along the path of pulse propagation (Figure 4.3). Information is obtained related to the complete, or a significant volume of the concrete (i.e., the signal can not be focused as with the ultrasonic pulse-echo method). In this respect it can be seen as a global measuring technique which may be an advantage, but it also might complicate the process of interpretation. Testing normally involves a study of the compression wave only and frequencies usually are below the ultrasonic level. The response signal is analyzed in the frequency domain using a Fast Fourier Transform technique. Although in principle the impact-echo technique may be used for thicknesses up to several meters, it normally is used in concrete structures up to one meter in section. Applications of the method include determining the thickness and detecting flaws in plate-like structural members; detecting flaws in beams, columns, and hollow cylindrical structural members; assessing the quality of bond in overlays; and crack-depth measurements. Impact echo is most effectively used for testing large concrete areas and if the geometry of the structure is quite simple, the analysis procedure is also relatively simple. Since the signal input is by mechanical impact, the testing can be carried out quickly without the need for a coupling medium.

Spectral analysis of surface waves (SASW) has recently found use in testing concrete and in geophysical surveys. A mechanical impact on the surface of the concrete structure is used to generate surface waves that are picked up by two transducers placed at fixed distances from the impact source (Figure 4.4). The transducers are placed in line with the impact source and their spacing is determined by the depth to be measured. In the case of a massive concrete element this may require access to a large surface area. Surface wave velocity is affected by the material properties, and by analyzing the relationship between velocity and frequency; it is possible to obtain a profile of the velocity with depth (i.e., dispersion curve). The depth to which the surface waves are affected by the material is dependent on the wave frequency, with lower frequency waves affected by material stiffness at greater depths. The method is particularly well suited for testing layered systems and for determining the depths of foundations or the condition of underlying material.

Acoustic tomography is an advanced nondestructive evaluation method based on radiography that is used to examine concrete structures for cracks, voids, and other internal defects (Woodham and Schuller, 1999). Information from stress wave transmissions is used to reconstruct a map of velocities on a slice through the interior of a body. This is accomplished by conducting a large number of two-dimensional examinations of the structure and analyzing the results with sophisticated computer software that has been developed especially for this application. The advantage of this method over radiography is that it provides the possibility of internal inspections through development of three-dimensional displays from a series of reconstructed digitized detector measurements obtained from planes or slices through the thickness of the object inspected. The primary limitations of this method are that if a complete examination is not possible because of geometrical boundary conditions, additional calculations must be made for those areas, and the method is presently costly to perform.

4.1.1.3 Nuclear

Nuclear methods for nondestructive evaluation of concrete can be subdivided into three groups: radiometric, radiographic, and neutron source. All are based on the interaction between high-energy electromagnetic radiation and the material inspected. Radiometry is used to address the density of fresh or hardened concrete by measuring the intensity of electromagnetic radiation (gamma rays) that passes through the concrete. Of most interest for the present study is radiography which is well established and the method most often used to examine the quality of construction or materials in concrete (e.g., location of reinforcement and voids). The basic system consists of a radiation source (X-ray or gamma ray) emitting a beam through the test article and a photographic film placed on the opposite side of the test article from the source (Figure 4.5). Since a high-density medium absorbs a greater amount of emitted energy, the density of the material determines the energy being absorbed by the film. A two-dimensional projection of the area being inspected is displayed on the film. Other factors that can affect the intensity of radiation passing through the test article include its thickness and absorptive characteristics. Although γ -scintillation can be used in members greater than 1-m (3.28 ft) thick, most systems are capable of detecting small voids in members up to about 700-mm (27.6 in.) thick. The present sensitivity of the technique probably is not sufficient to detect voids in tendon ducts. Gamma radiometry systems consist of a source that emits gamma rays through the specimen and a radiation detector and counter. Direct transmission or backscattering modes can be used to make measurements. The count or count rate is used to measure the specimen dimensions or physical characteristics (e.g., density and composition). Neutron methods consist of an emission source and a gamma ray collection and counting system. The method can be used to measure the moisture content in a structure. In this method neutrons emitted by the decay of an X-ray source provide the ability to detect hydrogen present in water in the concrete. The concrete moisture content can be determined to a depth of approximately 90-mm (3.54 in.), and the accuracy of the measurement improves with increasing moisture content. Primary limitations of the most commonly used of these methods, radiography, are that radiation protection has to be observed while applying this

method, personnel must be licensed or certified, the concrete structure must be accessible from both sides, and concrete sections are generally limited to 1 m (3.28 ft) or less in thickness.

4.1.1.4 Magnetic

Magnetic methods provide information about the quantity and location of reinforcement which is useful in evaluations of the strength of reinforced concrete members. These methods monitor the interaction of the reinforcing bars with some other process such as a low-frequency, electromagnetic field. Commercial instruments (e.g., covermeters) are of two types: those based on the principle of magnetic reluctance, and those based on eddy currents. Magnetic reluctance covermeters are based on monitoring changes in the magnetic flux flowing through the magnetic circuit composed of the path through the yoke, concrete, and reinforcing bar. Eddy-current covermeters depend on the electrical conductivity of the bar, and they will detect magnetic as well as nonmagnetic metallic objects (signal from magnetic materials is stronger). The methods are useful in measuring the thickness of the concrete cover, and determining the size of embedded steel reinforcement and its spacing. The accuracy of rebar sizing is better than 90% when the equipment is properly calibrated. The method has a maximum range of about 90 mm (3.54 in.) of concrete depth and its accuracy for normal concrete cover thicknesses [e.g., ≤ 50 mm (1.97 in.)] is on the order of ~ 3 mm (.12 in.). Basic limitations of this method are that for best results the spacing between two adjacent reinforcement bars must be greater than the concrete cover, and since the method is based on the induction principle, the results are affected by anything that affects the magnetic field within the range of the instrument (e.g., electrical cables, metal tie wires, and iron content of cement).

4.1.1.5 Infrared Thermography

Infrared thermography is based on the theory of heat transfer (ASTM D 4788). It senses the emission of thermal radiation and produces a visual image from the thermal signal. Infrared thermography for testing concrete utilizes two heat transfer mechanisms: conduction and radiation. The basic equipment includes an infrared scanner/detector head, a data acquisition/analysis device, and a visual image recorder. The scanner head is an optical camera, with lenses that transmit only infrared radiation in the short- and medium-wavelength ranges. The detector consists of sensors composed of a two-dimensional array of materials sensitive to incident infrared radiation. The data acquisition and analysis system consists of an A/D converter, a computer with high-resolution monitor and data storage device, and data analysis software. Since subsurface anomalies in a material affect heat flow through the material, heat transfer sensed through surface radiance variations can be used to locate subsurface voids, delaminations, or other defects. The magnitude of the temperature difference between deteriorated and sound areas provides an indication of the depth of the defect. The advantage of this method is its capability to cover a large concrete surface area within a short period of time. The primary limitation of the method is that in order to execute this inspection method, it is necessary to produce a movement of heat in the structure, therefore, some in-situ parameters such as surface moisture, ambient temperature, and wind speed could influence the accuracy of the readings.

4.1.1.6 Radar

Ground-penetrating radar is the electromagnetic analogue of sonic and ultrasonic pulse-echo techniques and is well developed in the geophysical field. It has been adapted and can be used in its various forms to obtain information from concrete structures and their foundations and substrate. The use of radar for inspection of concrete structures is relatively common in some countries. One of the advantages of radar is that the antenna used for scanning does not require contact with the test surface and large areas can be scanned rapidly. Short pulses of electromagnetic energy are transmitted through the structure and the energy is reflected by boundaries between layers of different dielectric properties. The receiving antenna

and readout circuitry indicate the depth to these layers. A major use of radar inspection is detection of steel reinforcement, other embedments, and voids. The ability to detect the depth of reflectors such as reinforcing bars or tendon ducts is dependent on knowledge of the dielectric properties of the concrete, which in turn is dependent on the moisture level. In thick concrete structures the moisture variations can be considerable, even decades after construction. Closely spaced reinforcement near the concrete surface tends to disrupt radar signals and mask deeper lying objects of interest (e.g., voids). At present, objects such as tendon ducts can be detected in concrete to a depth of at least 300 mm (11.8 in.) provided the concrete is not too moist (i.e., high moisture levels hinder radar signals from penetrating concrete, particularly if the water contains salts that increase conductivity). The effects of moisture presence may be an advantage, however, in trying to detect leaks in water-retaining structures such as dam walls or waterproof membranes. The position of reinforcement can be resolved at depths to 500 mm (19.7 in.) (Robery, 1990). Cracks and delaminations are not easy to detect unless moisture is also present in the cracks or regions of the delamination. Currently the primary limitation of the method is the resolution capability, but there are on-going programs to develop signal processing tools to overcome this limitation. Many significant developments in system hardware, data analysis, and enhancement software have been reported. The development of antennas with frequencies in the 1-5 GHz range is on-going and will improve resolution and increase the capability of the technique to detect objects that lie behind near-surface reinforcement mats. Other developments include methods of measuring moisture profiles and determining the dielectric constant on site. At the moment this has to be estimated, although there is some equipment that can help in establishing this information.

4.1.1.7 Audio

By dragging a chain across a concrete surface or using a metallic object to strike the concrete surface, it is possible to locate areas of delamination and voids, through sound differentials that occur between good and defective concrete (ASTM D 4580). Solid areas of concrete will produce a characteristic “metallic ringing” sound when impacted, while defects in the form of debonds, cracks, or other delaminations, will produce a “hollow” sound when struck. Basic limitations of this method relative to application to NPP reinforced concrete structures are that it only can be applied to local and selected test areas because of accessibility constraints and the large size of these structures (i.e., thicknesses up to several meters). The technique is usually effective for defects not exceeding the concrete cover depth, and it may miss small delaminations.

4.1.1.8 Rebound Hammer

The rebound hammer is one of the most commonly used nondestructive evaluation methods (ASTM C 805). The method uses the rebound distance (measured on an arbitrary scale) of a spring-loaded weight impacted against the concrete to estimate quality or compressive strength of the in-situ concrete. The primary usefulness of the rebound hammer is in assessing concrete uniformity in-situ, delineating zones (or areas) of poor quality or deteriorated concrete in structures, and indicating changes with time of concrete characteristics. The effectiveness of the rebound hammer method is often enhanced through combination with other techniques such as ultrasonic pulse velocity measurements. Primary limitations of this method are that the test results only measure surface characteristics and test results may be influenced by parameters such as the test surface smoothness and moisture content, orientation of the hammer during impact, type of cement used, and type of aggregate; and application-specific calibration curves have to be developed to provide reasonably accurate (e.g., $\pm 15\%$) compressive strength results. Surface treatments may also exclude direct application of the technique.

4.1.1.9 Penetrability

Many of the degradation mechanisms in concrete involve the penetration of aggressive materials such as sulfates, carbon dioxide, and chloride ions. In most cases water must also be present to sustain the degradation mechanisms. As a result, the condition of the surface zone of concrete is a key factor in concrete durability. There are three ingress mechanisms by which external agents can penetrate concrete: absorption (ingress of liquids due to capillary forces), permeation (flow of fluid under action of pressure head), and diffusion (movement of molecular or ionic substances from regions of higher concentrations to regions of lower concentrations). Several methods have been developed to assess the ability of the surface zone of concrete to resist the passage of external agents that may lead either to deterioration of the concrete or depassivation of the steel reinforcement. The methods are based on either water absorption, water permeability, or air permeability. Absorption tests measure the rate at which water is absorbed into the concrete under a relatively low pressure head. In-place water permeability methods measure the flow of water into a concrete surface under a fixed pressure. The air permeability test is similar to the water permeability test, but is based on measurement of the flow of air, or other gases, through concrete. Both the water- and air-based tests involve drilling a hole into the concrete surface or application of a chamber to the surface. Limitations associated with these methods include sensitivity to moisture and temperature changes, changes in transport mechanism during the test, variance of air permeability with applied pressure, and influence of drilling on test values (ACI 228.2R, 1998).

4.1.2 Destructive Testing

Destructive testing can be utilized to determine concrete strength, density, and quality; locate voids or cracks in concrete; locate steel reinforcement and determine depth of concrete cover; and detect corrosion of steel reinforcing materials. Destructive testing techniques include (1) break-off, (2) core testing, (3) probe penetration, (4) pull-out, (5) chloride-ion content, (6) carbonation depth, and (7) petrography.

4.1.2.1 Break-Off

The break-off method is used in-situ to indicate concrete compressive strength. To perform this test, a specimen of 55-mm (2.17 in.) diameter and 70-mm (2.76 in.) deep is formed either by using a plastic cylinder placed into the fresh concrete, or drilling a core with the same outer dimensions in existing concrete. A load cell is placed into a circular groove at the top of the concrete surface and load is applied using a hydraulic pump until failure of the specimen occurs in flexure. The pressure reading of the load cell is correlated to the concrete strength by using calibration curves. Limitations of this method are that it cannot be used with concrete mixes having maximum aggregate sizes exceeding 19 mm (.748 in.) or concrete structures having sections less than 100 mm (3.94 in.) thick.

4.1.2.2 Core Testing

Removal and evaluation of concrete core samples from structures provides a direct method for examination of the concrete. Requirements for obtaining concrete samples to provide a sufficient number of specimens for statistical evaluations are generally described in national codes and standards for building and construction. When cores are removed from areas exhibiting distress, strength tests and petrographic studies (discussed later in this section) can be used to investigate the cause and extent of deterioration. Other applications of concrete cores include calibrations of nondestructive testing devices, and down-hole cameras can be used to examine the interior of the structure in locations where concrete cores were removed. Primary limitations of the method are with respect to the number of samples that must be removed to meet requirements related to ensuring that the probability of obtaining a strength less

than desired is below a certain level, the results can be influenced by several factors (e.g., aggregate size, core diameter and slenderness ratio), and areas where cores are removed may require repair.

4.1.2.3 Probe Penetration

Probe penetration tests estimate concrete compressive strength, uniformity, or general quality through measurements of the resistance of concrete to penetration of a steel probe that is driven by a given amount of energy (ASTM C 803). Compressive strength is determined by using calibration curves. Advantages of the method are that it is relatively simple to operate and the results correlate fairly well to concrete compressive strength. Primary limitations of this method are that the thickness of the specimen to be tested has to be at least three times the depth of the penetration, the method should not be applied within about 200 mm (7.87 in.) of specimen edges or other tests, and aggregate size and hardness influence results.

4.1.2.4 Pull-Out Test

Originally known as cast-in-place pull-out, this test is performed by using a hydraulic device to pull an embedded metallic insert with an enlarged head from concrete (ASTM C 900). The concrete compressive strength is related to the pull-out force through calibration curves. Recent developments have eliminated the requirement that the pullout inserts be cast into the specimen. Primary limitations of the test are that the results are affected by the size of coarse aggregate, and a correlation relationship between pull-out strength and compressive strength is generally required for each application. Also some repair may be required.

4.1.2.5 Chloride-Ion Content

Determination of the concrete chloride-ion content is an important aspect of the analysis of concrete structures relative to the potential for corrosion of embedded steel reinforcement. Two of the most commonly used methods for determination of chloride contents in concrete are the water-soluble and total-chloride tests (ASTM C 1218; ASTM C 1152). The water-soluble test involves obtaining concrete samples by coring or drilling, and grinding the sample to produce a powder. The powder is boiled in water for five minutes and soaked for twenty-four hours. The water is then tested for dissolved chlorides and is presented as a percentage of the cement or concrete. The total-chloride test is an acid-soluble test and involves digesting a ground sample of hardened concrete in nitric acid. The solution is then tested for chloride content and is presented as a percentage by weight of the material being analyzed. Other methods that require a powder sample include x-ray fluorescence, gas chromatograph, Quantab chloride titrator strips, specific ion electrode, spectrophotometer, and argentometric digital titrator. Primary limitations of these methods are that they require coring or drilling to obtain samples at locations in a structure where chloride ion contents are desired, and the chloride content reported includes chlorides that were present in the concrete mix constituents. A potential technique to determine the amount of chlorides that was present in the mix is to obtain (if possible) a baseline for the chloride ion content in an area of the structure where chlorides from external sources are known not to be present.

4.1.2.6 Carbonation Depth

Depth of carbonation can be easily determined either in-situ or in a laboratory by treating a freshly broken concrete surface with phenolphthalein. The carbonated portion will be uncolored. Periodic determinations can be used to establish the rate of penetration. This test often is performed in conjunction with chloride-ion content determinations. The primary limitation of this method is that it requires exposure of a fresh concrete surface for each test.

4.1.2.7 Petrography

Petrographic examinations of samples of hardened concrete removed from existing concrete structures can provide valuable information for use in an aging management program. Several purposes for which petrographic examinations of these structures may be conducted include detailed determination of the condition of the concrete in the structure; determination of causes of inferior quality, distress, or deterioration; determination of whether the concrete in the structure was or was not as specified; description of the cementitious materials matrix (e.g., kind of binder, degree of hydration, nature of hydration products, and presence of mineral admixtures); determination of the presence of alkali-aggregate reactions; determination if the concrete has been subjected to chemical attack or early freezing; determination of the nature of the air void system; and survey of the structure relative to its safety (ASTM C 856). The primary disadvantage of petrographic examinations is that they require removal of samples from the structure for test and evaluation.

4.2 Detection Methods for Reinforcing Steel

Assessments of mild steel reinforcing are primarily related to determining its characteristics (e.g., location and size) and evaluating corrosion occurrence. Only evaluation of the occurrence of corrosion will be addressed in this section as magnetic methods associated with determining characteristics of embedded steel reinforcing were addressed in the previous section. Methods available for corrosion monitoring and inspection of steel include visual inspection, mechanical and ultrasonic tests, core sampling with chemical and physical testing, electrical methods (half-cell potential, linear polarization, resistivity), rate of corrosion probes, and galvanostatic pulse. Of these methods, only the electrical, rate of corrosion probe, and galvanostatic methods will be discussed as the other methods already have been addressed. These methods are semi-destructive.

4.2.1 Half-Cell Potential

Electrical methods are used to evaluate corrosion activity of steel reinforcement (ASTM C 876). When a bar is corroding, electrons flow through the bar and the ions flow through the concrete. When the bar is not corroding, there is no flow of electrons and ions. The half-cell potential method is used to detect this negative charge and thereby provide an indication of corrosion activity. Potential measurements at a number of locations on the concrete surface using a reference half-cell (e.g., copper-copper sulfate) connected to the steel reinforcement are used to indicate the likelihood of corrosion occurrence (i.e., >90% probability of no corrosion, corrosion activity is uncertain, or >90% probability that corrosion is occurring) (Figure 4.6). The surface of the concrete being investigated is usually divided into a grid system to define measurement locations. Results generally are plotted in the form of an equipotential diagram so that areas exhibiting potential corrosion can be readily identified. In addition to using the value of the potential measurements as an indicator of the likelihood of corrosion, potential gradients also are indicative of active corrosion (e.g., > 100mV) (Ingvarsson, 1987). Modified types of instrumentation, consisting of a number of half-cells mounted in parallel or on a roller bar, have been developed to accelerate the examination process. Primary limitations of this method are that neither the magnitude nor rate of corrosion are provided, surface coatings or coated steel reinforcement present problems, measurements are affected by temperature and moisture, electrical continuity is required, and concrete constituents can affect results (e.g., type of cement and chloride ingress). The half-cell potential method, despite its sensitivity to moisture level, is a useful indicator for locating areas on concrete surfaces where risk of reinforcement corrosion is high. It is a useful complement to other techniques in selecting test points for further analysis, such as chloride measurements. It may be used to detect adverse external effects such as leakage currents that may be detrimental to the reinforcement, or to monitor the effect of

cathodic protection systems. Also, results in Sweden from potential mapping of bridge piers in a marine environment indicate that there may be a linear relationship between measured chloride content and the half-cell potential observed (Ingvarsson, 1987).

4.2.2 Linear Polarization

In the polarization resistance test the current to cause a small change in the value of the half-cell potential of the corroding bar is measured. For small perturbations about the open circuit potential, a linear relationship exists between the change in voltage and the change in current per unit area of bar surface. The ratio between the voltage and current change is the polarization resistance. A relationship exists between the corrosion rate of the bar and the polarization resistance. The corrosion rate is expressed usually as the corrosion current per unit area of bar. It is possible to convert the corrosion rate into the mass of steel that corrodes per unit of time (ACI 228.2R). If the bar size is known, the corrosion rate can be converted to loss in diameter of the bar.

Figure 4.7 presents the schematic of a three-electrode system. One electrode is composed of a reference half-cell, the second is the reinforcement (working electrode), and the third is the counter which supplies polarization current to the bar. Supplementary instrumentation measures the voltages and currents during different stages of the test. The corrosion rate at a particular point in a structure is expected to depend on several factors such as moisture content of concrete, oxygen availability, and the temperature; thus, due to seasonal variations multiple measurements may be required over time. No standard procedures currently exist for interpretation of corrosion-rate measurements obtained by different devices. Also, there are a number of limitations with respect to the concrete and steel [e.g., cover < 100 mm (3.94 in.); concrete surface smooth, free of visible moisture, and uncracked; and steel being monitored must be in contact with concrete and not be coated or galvanized].

4.2.3 Resistivity

Under field conditions there is a direct correlation between concrete resistivity and rate of corrosion of steel (Flis et al., 1993). Conditions such as high pore water content and the presence of electrolyte salts that lead to low resistivity usually favor corrosion. Concrete resistivity can be measured using a four-electrode technique (Figure 4.8). Four equally spaced probes are installed in a straight line on the concrete to be tested with the electrode spacing equal to the depth to which measurement of the average resistivity is desired. The average resistivity is a function of the voltage drop between the center pair of probes with current flowing between the outside probes. The resistivity is then determined (in ohm-cm). Depending on the value of resistivity measured, corrosion is unlikely, corrosion will probably occur, or corrosion is almost certain to occur. It has been reported that significant corrosion is not likely when the resistivity exceeds 8,500 to 12,000 ohm-cm (Hope and Ip, 1985). Results may also provide an indication of concrete quality as sensed by the amount of moisture present. Limitations of the method are that the resistivity measurements are obtained relatively close to the concrete surface, and when the electrode spacings are increased to allow evaluations at deeper concrete depths, the steel reinforcement may interfere with results obtained.

4.2.4 Rate of Corrosion Probes

Probes embedded into the concrete can be used to indicate the rate of corrosion. Two primary types are available: (1) two to three short sections of steel wire or reinforcement in conjunction with polarization techniques, and (2) steel wire or hollow cylinder to provide cumulative rate of corrosion data from periodic measurements. The primary limitation of this technique is that it requires some excavation of the

concrete to insert the probe(s). As a consequence, rate of corrosion probes have found primary application in evaluation of the effect of rehabilitation procedures.

4.2.5 Galvanostatic Pulse Technique

The galvanostatic pulse technique is a polarization method that has recently been developed for in-situ application and can be used for detecting corrosion in wet and anaerobic environments (Elsener, 1994; Newton and Sykes, 1988; Klinghoffer, 1995). The method set up is similar to the half-cell potential method and involves use of a counter electrode and reference electrode that are placed on the concrete surface above the reinforcement (Figure 4.9). A short-time anodic current pulse is impressed galvanostatically from the counter electrode which in turn shifts the reinforcement potential with the shift recorded by a data logger. The reinforcement is polarized in the anodic direction relative to its free corrosion potential. The extent of polarization depends on the corrosion state. The reinforcement is easy to polarize in the passive state, as illustrated by the large difference between free corrosion and polarized potential. The difference is much smaller when corrosion is occurring. The method is superior to the half-cell potential method, in particular when testing wet concrete where there is a risk of misinterpretation of results. Together with more reliable qualitative information concerning classification of passive and corroding areas, the galvanostatic pulse technique allows quantitative information to be obtained through calculation of the corrosion current. If the area of the polarized reinforcement is known, then the corrosion current can be converted to a corrosion rate. It is possible in this way to estimate corrosion rates in the case of general corrosion, but not in the case of local pitting corrosion. The galvanostatic pulse technique measurements take considerably longer to execute than the half-cell potential measurements and require an experienced person to perform the technique.

4.3 Condition Assessment

The importance of reinforced concrete structures to the overall safety of nuclear power plants (NPPs) is well established. In contrast to mechanical and electrical components, civil structures are intended to have service lives on the order of 50 to 100 years or more, and traditional codes of practice (ACI 318, 1995; ACI 349, 1985; ACI 359, 1989) in the past have not explicitly addressed aging. Structural systems in NPPs were designed primarily for safety, with serviceability and durability issues dealt with only indirectly. The inherently conservative nature of design was intended to ensure the structure's performance in service. Structural deterioration was not considered explicitly, and there was no presumption in the codes that periodic inspection, maintenance, and repair would be carried out.

Properly designed and maintained structures normally perform well over extended periods of time. However, as noted in Section 2, these structures are subject to a phenomenon known as aging, which refers to time-dependent changes that occur that may impact the ability of these structures to withstand various demands from operation, the environment, and accident conditions. The time-dependent behavior of these changes should be considered in the overall condition assessment of a structural system. Failures can occur when excessive degradation takes place, frequently due to design or construction errors or an unanticipated aggressive service environment. Such failures often are related to serviceability rather than safety. Structural systems and components in NPPs are considered to be passive (i.e., no change of state) in mitigating design-basis conditions. Probabilistic risk assessments of NPPs confirm that structural systems are important to the overall safe operation of a NPP (Meyers et al., 1990). Structural components are more likely to be involved in common-cause failures, since structural failures may affect plant safety systems. Thus aging in structural components may also be significant in common-cause failures. Moreover, in comparison with mechanical and electrical equipment, structural components are less readily inspectable. Furthermore, it may be very difficult to access and repair structural components and systems without major impact on the operation of a NPP. In fact, replacement of some structural components (e.g., containment and basemat) may not be feasible.

Knowledge gained from a condition assessment can serve as a baseline for evaluating the safety significance of any damage that may be present in a structure and defining in-service inspection programs and maintenance strategies. Condition assessment and management of aging in NPP concrete structures requires a more systematic approach than simple reliance on existing code margins of safety (Christensen, 1990). What is required is the integration of structural component function, potential degradation mechanisms, and appropriate control programs into a comprehensive, and ideally quantitative, evaluation procedure. A methodology for use in demonstrating the continued reliable and safe performance of these structures should include (1) identification of structures important to public health and safety; (2) identification of environmental stressors, aging mechanisms and their significance, and likely sites for occurrence; and (3) a monitoring or in-service inspection based methodology that includes criteria for resolution of existing conditions.

A classification system for grouping safety-related structures in nuclear plants has been developed (Ashar and Bagchi, 1999). In this system the structures are assigned to one of five groups: (1) structures that resist and/or retain differential pressures (containment structures); (2) structures that support and protect other safety-related structures, systems, and components (majority of structures); (3) structures that serve as radiation fields (biological shield); (4) structures that retain fluids (fuel-related pools and free-standing tanks); and (5) miscellaneous structures not included in above (intake, cooling tower, etc.). Techniques for identification and ranking of structures of primary importance also have been developed (Hookham, 1991; Ellingwood and Song, 1996). Furthermore, primary degradation factors as well as their likely sites for occurrence have been identified (Naus, Oland, and Ellingwood, 1996). Tables 4.3 and 4.4 provide guidance that has been developed to assist in classification of environmental exposures (i.e., relate several prominent deterioration mechanisms for concrete and steel reinforcement to different environments) (Litzner and Becker, 1999). The balance of this section will address development of an in-service inspection program and guidelines to help interpret results of inspections.

4.3.1 Considerations for Development of In-Service Inspection Programs

The stability and durability of a concrete structure can only be guaranteed when it has an appropriate safety margin against expected loads and environmental influences during its intended lifetime. To assess deterioration in a concrete structure an inspection is needed. In some cases a visual inspection may be sufficient, while in others (e.g., indications of deterioration) the visual inspection requires supplemental techniques such as nondestructive and destructive testing, analytical evaluation, or a combination of these. Reinforced concrete structures are inspected for several reasons: (1) to control the functional requirements and provide assurance that the structure is safe and fit for its designated use; (2) to identify actual and potential sources of trouble and misuse at the earliest possible stage, and to prevent serious deterioration and failure, consequently increasing service life; (3) to monitor the influence of the environment since there is a relationship between aggressiveness of the environment and the durability of concrete structures; (4) to provide feedback of information for designers, constructors and owners on the factors governing maintenance problems to which necessary attention is best paid during the design and construction stages; and (5) to provide information on which decisions concerning preventative measures and work can be made (e.g., optimum inspection/maintenance strategies) (FIP, 1986).

In-service inspection programs for safety-related NPP reinforced concrete structures have the primary goal of ensuring that these structures have sufficient structural margins to continue to perform in a reliable and safe manner. A secondary goal of these programs is to provide a means to identify any environmental stressor or aging factor effects before they reach sufficient intensity to potentially degrade structural margins.

4.3.1.1 Condition Assessment Methods

Damage to a reinforced concrete structure refers to any deficiency and/or deterioration caused by external loading or environmental conditions, as well as human errors in design and construction, that causes or can lead to a decrease in performance. Reasons for deterioration of reinforced concrete structures are either physical or chemical processes that cause visible (or sometimes invisible) signs of damage. The most common types of damage in reinforced concrete structures are surface damage, cracks and spalling, and reinforcement corrosion. Each damage type may occur by itself or in combination with other types. As a result, the effect of more than one type of damage must be considered when classifying overall damage.

Determining the existing performance characteristics and extent and causes of any observed distress is accomplished through a condition assessment. Common in the condition assessment approaches that have been developed is the conduct of a field survey, involving visual examination and application of nondestructive and destructive testing techniques, followed by laboratory and office studies. Guidelines for structural condition assessments of existing buildings are available (ANSI/ASCE, 1990; ACI 364, 1993).

4.3.1.1.1 Field Survey

General direction on conduct of surveys of concrete structures is available (Perenchio, 1989) and has been used to assist in the preparation of information presented in the balance of this section. It is vital that the results of all inspections be accurately and completely recorded, even if no indications of deterioration are found, so that a history of the structure inspected is readily available.

Visual Survey

The condition survey usually begins with a review of the “as-built” drawings and other information pertaining to the original design and construction so that information, such as accessibility and the position and orientation of embedded steel reinforcing and plates in the concrete, is known prior to the site visit. Next is a detailed visual examination of the structure. Material deterioration is often indicated by surface cracking and spalling of concrete, and examination of the crack patterns may provide a preliminary indication of the cause. Figure 4.10 presents schematics of some typical crack patterns that represent the common causes of concrete degradation. Reinforcement corrosion (advanced) is often indicated by splitting (cracking) and spalling along the lines of reinforcement, possibly with rust staining, whereas sulfate attack may produce a random pattern accompanied by a white deposit leached on the surface. Alkali-aggregate reaction is sometimes (but not always) characterized by a star-shaped crack pattern, and freezing and thawing attack may give patchy surface spalling and scabbing. However, because of similarities resulting from different causes of degradation, it will not always be possible to determine causes by visual inspection alone. Visual inspection can provide the basis for selection of additional tests.

The initial visual examination is used to document easily obtained information on instances that can result from or lead to structural distress such as cracking, spalling, leakage, and construction defects such as honeycombing and cold joints in the concrete. The instances of cracking, spalling, leakage, delamination, efflorescence, chemical attack, or structural distress are observed and documented. The color and texture of corrosion products, the surface appearance of exposed rebar, the pattern of cracking and the location of corrosion products are all important features of the corrosion process. Where spalling is noted, the appearance of surface staining (or its absence) should be noted. The color, hardness, and texture of

incrustations can be an indication of associated corrosion and the rate at which incrustation formed (Paull, 1987). Also, important environmental factors such as the presence of water should be noted. The presence of moisture is instrumental in almost all forms of concrete degradation. Table 4.5 provides an indication of the influence of moisture state on several durability processes (CEB, 1992). Typical forms of distress and deterioration noted in a visual condition assessment, as well as typical causes, are summarized in Table 4.6 (Poston, Whitlock, and Kesner, 1995). A comprehensive listing of defects and photographs is available to assist in the visual survey (ACI 201.1R, 1968). Table 4.7 presents one approach to a listing of the minimum information that should be obtained from a field survey of a concrete structure (Stuzman, 1991).

Cracking Survey

Cracks are common in concrete and do not always jeopardize the safety or loading capacity of a structure. The possible effects of cracks must be considered in the context of cause, location, environment, and utilization of the structure. A crack survey is usually done by drawing the locations, orientations, and widths of cracks on copies of project plans for the purpose of locating, marking, identifying cracks, and their relationship with other destructive phenomena. In the way of guidance, cracks less than 0.05 to 0.1 mm (.002 to .0039 in.) are noticeable only when drying out or in strong light, cracks 0.1 to 0.5 mm (.0039 to .02 in.) are noticeable with unaided eye, and cracks greater than 0.5 mm (.02 in.) have both edges visible as distinct interruption in concrete surface (Pullar-Strecker, 1987). Direction on measurement of crack widths is available (Haavik, 1990; ACI 224, 1984). Types of cracks that may be present include: longitudinal formed after concrete hardened (corrosion), transverse cracks formed after the concrete hardened (shrinkage, thermal contraction, or structural loading), shear cracks formed after the concrete hardened (structural loading or movement), plastic shrinkage cracks (rapid moisture loss at surface during hydration), plastic settlement cracks (excessive settlement and bleeding), map cracks formed over an extended period of time (alkali-aggregate reactions), and surface crazing formed over an extended period of time (shrinkage at surface during hydration). Longitudinal cracks along reinforcing, whether or not caused by corrosion, are of most concern. Transverse cracks may or may not be of concern depending on their width, location, and exposure. Cracking patterns may appear that suggest weaknesses in the original design, construction deficiencies, unanticipated thermal movements, chemical reactivity, detrimental environmental exposure, restrained drying shrinkage, or overloading. Figure 4.11 provides a summary of crack-inducing phenomena associated with the design, construction, and service phases of a reinforced concrete structure (Richardson, 1987). Distress associated with cracks such as efflorescence, rust stains, or spalling are noted. Photographs or video recordings are made to provide a permanent record of this information, and notes are made on the survey sheets to indicate the area photographed. After the visual survey has been completed, the need for additional surveys may be indicated.

Delamination Plane Survey

One such form of additional survey is for internal delaminations that are not visible. These internally cracked regions are usually caused by corrosion of embedded metals or internal vapor pressure. The most commonly used method for determining the existence and extent of delaminations is sounding. Depending on the orientation and accessibility of the concrete surface, sounding can be performed using a steel hammer, rod, or chain. Good quality concrete with no delaminations produces a sharp, ringing sound; delaminated areas emit a dull, hollow sound. If a more detailed study is warranted, the results of the visual and delamination surveys are used to select portions of the structure that will be studied in greater detail. The detailed study on the suspect areas can include nondestructive tests, destructive tests, or a combination of the two tests.

Pachometer Survey

A pachometer (or covermeter) survey may be performed as part of the detailed study to confirm the location of steel reinforcement. The pachometer consists of a search coil that emits a magnetic field and is connected to electronic circuitry that senses any disruption in this field. A display dial is graduated to indicate the depth of the steel reinforcing bars, if the size of the bar is known. The equipment can be calibrated for depth using a reinforcing bar and various thicknesses of an inert material, or on the job by drilling or coring to the depth of the steel. Where there is evidence of severe corrosion, the steel bar should be uncovered to allow visual inspection and measurement of cross-sectional area loss.

Corrosion Survey

Concrete normally provides a high degree of corrosion protection to embedded metals because the high pH environment forms a thin protective film of iron oxide on the steel surface. Disruption of the protective film due to carbonation or presence of chlorides causes corrosion to occur. To locate areas of corrosion activity within reinforced concrete, copper-copper sulfate half-cell studies can be performed. By taking readings at multiple locations on the concrete surface, an evaluation of the probability of corrosion activity of embedded reinforcing steel (or other metals) can be made. If sufficient readings are taken on a grid pattern, a diagram can be prepared that resembles a contour map. On such a diagram, points of equal electrical potential are connected by isopotential lines, permitting areas of high potentials or high corrosion probability to be readily identified.

Concrete powder samples or cores can be removed from several depths, extending to and beyond the embedded outer layer of reinforcing steel, from the structure where significant chloride penetration is suspected. If the concrete contains more acid soluble chloride than about 0.026 to 0.033% [approximately 0.6 to 0.8 kg/m³ (.037 to .05 pcf)] total chloride ion content by mass of concrete, it is considered to contain sufficient chloride to support electrochemical corrosion of embedded steel when in a moist environment that has oxygen availability. Particularly susceptible to damage by chloride ions are dissimilar metals. Where aluminum or galvanized electrical conduit has been embedded in concrete and is in contact with the reinforcing steel, the conduit can corrode rapidly, acting as an anode to the steel.

If elements are exposed to a marine environment, most of the concrete elements will eventually contain significant amounts of chloride ions. Water intake and discharge structures present unique and severe environmental conditions where water with dissolved chlorides, sulfates, and other minerals and salts are routinely in contact with the concrete. Some regions are always wet while other regions may experience wet and dry periods. Experience has shown that regions experiencing wet and dry cycles exhibit the greatest distress. Concrete columns and walls contain capillary channels that can cause saltwater to wick upward for several feet. The columns and walls in such structures can exhibit delaminations and spalls caused by corrosion due to the upward moisture movement. Chloride contents should even be determined in indoor structures if cracking patterns suggest reinforcing steel corrosion.

4.3.1.1.2 Laboratory Tests, Office Studies, and Design Verification

Laboratory Tests

During the site survey, samples of concrete and steel from areas exhibiting degradation are collected for testing within the laboratory. The samples may be investigated using different techniques, such as:

- Petrographic methods: thickness, distribution of cement, aggregate studies, estimation of water-cementitious materials ratios, air-void distribution, types of distress, recognition of

unstable aggregates, deterioration mechanisms, and age at which cracking occurred (ASTM C 856).

- **Chemical techniques:** chemical constituents of the cementitious materials, characteristics of the paste and aggregates, presence and quantity of chemical admixtures, quantification of chemical compounds within the cement paste, efflorescence, and carbonation effects.
- **Concrete strength testing:** compressive strength, modulus elasticity, tensile strength, flexural strength, and bond strength of patches or overlays.
- **Steel materials:** yield and ultimate strengths of reinforcing bars.

Office Studies

A crack survey map is prepared and studied for meaningful patterns. Half-cell data are studied and isopotential lines are drawn to assist in identifying sites where corrosion may be active. Chloride ion results are plotted versus depth to determine the profile and the chloride content at the level of the steel. Any elements that appear to be structurally marginal, due either to unconservative design or to the effects of deterioration, are identified and appropriate calculation checks made. If the calculations are inconclusive, suitable load testing may be indicated.

Design Verification

Based on physical test results, chemical analysis of elements and present condition of the structure, a redesign of various questionable elements should be accomplished to verify compliance with present codes and design requirements. Based upon the initial survey results, additional destructive or nondestructive testing may be appropriate. From design documentation and measurements made in the field, structural analyses may then be accomplished. Compressive and tensile strengths and elastic properties of materials may be determined from laboratory measurements and used in the structural analyses. These analyses may identify distress in the structure that has been caused by structural overload and indicate safety factors.

4.3.1.1.3 Report

After all of the field and laboratory results have been collated and studied, and all calculations have been completed, the report is prepared. It should start with an introduction stating how and by whom the work was instigated, who did the investigation, why the investigation was performed, and when. A brief description of the structure should be included. Photographs of the entire structure as well as of significant features and exploratory excavations are helpful, along with maps showing crack, delamination, and spall locations, and where core and powder samples were removed.

The testing techniques used and the results determined in the laboratory are described, and results interpreted. Any structural analyses performed should be presented and discussed. A general discussion that summarizes all of the findings and characterizes the condition of the structure should follow. Any unsafe conditions should be identified, and temporary corrective actions suggested.

The final section of the report should discuss possible repair techniques, and which appear to be appropriate in view of the results of the investigation and the environment of the structure. Appendices may be added if a complete compilation of the data is desired. A condition survey done in this manner will provide information in which a sound, economical repair specification can be based.

4.3.1.2 Inspection Approaches

Inspection and testing approaches generally fall into three categories: (1) visual inspection, (2) nondestructive and destructive testing, and (3) analytical assessments.

4.3.1.2.1 Visual Inspection

Although relatively simple in principle, visual inspections are one of the most valuable of the condition survey methods because many of the manifestations of concrete deterioration appear as visible indications or discontinuities on exposed concrete surfaces. Visual inspections encompass a variety of techniques (e.g., direct and indirect inspection of exposed surfaces, crack and discontinuity mapping, physical dimensioning, environmental surveying, and protective coatings review). To be most effective, the visual inspection should include all exposed surfaces of the structure; joints and joint materials; interfacing structures and materials (e.g., abutting soil); embedments; and attached components (e.g., base plates and anchor bolts). Degraded areas of significance are noted and measured. The condition of the surrounding structures should also be examined to detect occurrence of differential settlement or note aggressiveness of the local operating environment. Results obtained should be documented and photographs or video images taken of any discontinuities and pertinent findings.

4.3.1.2.2 Nondestructive and Destructive Testing

Nondestructive testing techniques employ specialized equipment to obtain specific data about the structure in question, and in certain instances (e.g., inaccessible surfaces) its surrounding environment (i.e., structure-specific or environment-specific). The structure-specific methods are used to inspect internal portions of the structure for discontinuities (e.g., presence of voids, cracks, and steel reinforcement) or to provide an indication of constituent material characteristics (e.g., compressive strength, modulus of elasticity, and size and location of steel reinforcement). Generally, the most comprehensive means of assessing structural condition and increasing the probability of defect detection is to use two or more of these techniques in tandem (e.g., ultrasonic pulse velocity and rebound hammer). Environment-specific methods are used where surfaces of structures are not accessible for direct inspection due to the presence of soils, protective coatings, or portions of adjacent structures. These methods are used to provide an indirect assessment of the physical condition of the structure (i.e., potential for degradation) by qualifying the aggressiveness of the environment adjacent to the structure (e.g., air, soil, and groundwater). Methods employed are primarily based on chemical evaluations that provide results such as chloride or sulfate contents of groundwater adjacent to the structure. If results of these tests indicate that the environment adjacent to the structure is not aggressive, there is some justification that the structure is not deteriorating. However, when conditions indicate that the environment is potentially conducive to degradation, additional assessments are required that may include exposure of the structure for visual or limited destructive testing.

Destructive testing involves the removal of samples of material from the structure for the purpose of determining physical, chemical, or mechanical characteristics. Since destructive testing involves a direct examination of the material sample removed, it provides information of significant value for use in aging management programs. Both the presence and impact of deterioration can be determined quantitatively. Also, supplemental testing can be done using these samples to indicate future performance (e.g., durability evaluations through accelerated testing techniques, and to determine the potential for alkali-aggregate reactions). Information on selected nondestructive testing methods for condition assessment of concrete structures is presented in Table 4.8 (Poston, Whitlock, and Kesner, 1995).

4.3.1.2.3 Analytical Assessments

Analytical methods involve the use of supplemental calculations or analytical procedures to reevaluate the behavior and resistance of the structure (e.g., structural margins determinations). This reevaluation may be required due to either a change in performance requirements (e.g., plant modification) or the identification of deterioration. Finite-element and ultimate strength design methods provide two techniques for reanalysis.

4.3.1.3 Acceptance Criteria

The influence of degradation on the performance of reinforced concrete structures is difficult to assess. Material discontinuities, such as steel impurities or local regions of improper concrete consolidation, unless excessive, are generally of minor structural significance. However, errors during construction and the initiation and propagation of various degradation mechanisms may result in loss of function and load-carrying ability. Degradation mechanisms often occur at time-varying rates (e.g., chemical attack or migration of chloride ions). In-service inspections of structures at risk are conducted to identify and mitigate the potential degradation factor effects before a repair is required or structural margins have eroded to unacceptable levels.

As noted, concrete cracking is a very common damage by-product from a large number of degradation mechanisms. Active concrete cracking is difficult to assess in terms of impact on structural behavior and is difficult to repair. Thus, inspection methods that support the early identification, sizing, and cause of cracking in concrete structures are of primary interest for future inspections. Also, the primary concern for all metallic constituents of concrete structures is corrosion and corrosion-related damage. Inspections that identify early signs of corrosion cell initiation and indicate the rate of propagation are similarly valuable.

Two approaches have been developed for assistance in the classification and treatment of conditions or findings that might emanate from in-service inspections of NPP reinforced concrete structures. These approaches primarily are based on the results of visual inspections since these inspections provide the cornerstone of any condition assessment program for concrete structures. Also, with the exception of some guidance on half-cell potential (ASTM C 876) and ultrasonic pulse velocity measurements (U.S. Army Corps of Engineers, 1986), few standards have been published presenting acceptance criteria for results obtained from nondestructive evaluation tests. The information below is provided only as a basis for development of acceptance criteria as each structure is unique due to its application, geometry, materials of construction, and environmental exposure. Interpretation of results should be done by a suitably qualified and experienced engineer.

4.3.1.3.1 Visual-Based Approach

The visual-based approach uses a “three-tiered” hierarchy (ACI 349, 1996; Hookham, 1995). Through use of different levels of acceptance, minor discontinuities can be accepted and more significant degradation in the form of defects can be evaluated in more detail. The three acceptance levels include acceptance without further evaluation, acceptance after review, and additional evaluation required.

Acceptance Without Further Evaluation

Conditions presented below are considered to be acceptable and require no further evaluation at present. Definitions and pictorial representations of typical forms of concrete degradation are available (ACI 201, 1968). In the event that the conditions provided below are exceeded, or observed conditions are

determined to deserve further evaluation, a more detailed review is required. Structures that are partially or totally inaccessible for visual inspections may require supplemental evaluations as environments may be present that are conducive to degradation.

1. **Unlined Concrete Surfaces – Concrete surfaces that are exposed for inspection and meet the following surface condition attributes are generally acceptable without further evaluation if the following criteria are met:**

- a. Absence of leaching and chemical attack;
- b. Absence of abrasion, erosion, and cavitation;
- c. Absence of drummy areas (poorly consolidated with paste deficiencies);
- d. Popouts and voids less than 20 mm (.79 in.) in diameter or equivalent surface area;
- e. Scaling less than 5 mm (.2 in.) in depth;
- f. Spalling less than 10 mm (.39 in.) in depth and 100 mm (3.94 in.) in any dimension;
- g. Absence of any signs of corrosion in reinforcing steel system or anchorage components (including concrete staining or spalling);
- h. Passive cracks less than 0.4 mm (.016 in.) in maximum width (“passive cracks” are defined as those having an absence of recent growth and absence of other degradation mechanisms such as leaching at the crack);
- i. Absence of excessive deflections, differential settlements, or other physical movements that may affect structural performance; and
- j. Absence of cement-aggregate reactions, chemical attack, fire damage, or other active degradation mechanism.

2. **Concrete Surfaces Lined by Metal or Plastic – Concrete structures with inner surfaces protectively lined with either a metallic or plastic (non-metallic) system are judged to be acceptable without further evaluation if the following criteria are met:**

- a. **Without Active Leak Detection System**
 1. Absence of bulges or depressions in liner plate (those that appear age-related as opposed to being created during construction);
 2. Absence of corrosion or other liner damage; and
 3. Absence of cracking in liner weld or base metal.
- b. **With Active Leak Detection System**
 1. No detectable leakage observed in leak detection system;
 2. Absence of any liner damage, such as noted in 2(a) above; and
 3. Absence of fluid penetration indications by leak chases or other detection system components.

3. **Areas Around Embedments in Concrete – The condition of the concrete around embedments is acceptable without further evaluation if the following criteria are met:**

- a. Concrete surface condition attributes of Criteria 1 above are met;
- b. Absence of corrosion on the exposed surfaces of embedded metal members and corrosion staining around the embedded metal;
- c. Absence of detached embedments or loose anchorages; and
- d. Absence of degradation due to vibratory loads from piping and other attached equipment.

4. **Joints, Coatings, and Non-Structural Components – The condition of joints, protective coatings, waterproofing membranes, and other non-structural elements is acceptable without further**

evaluation if the following criteria are met.*

- a. No signs of separation, environmental degradation, or water in-leakage are present in coatings, joints, or joint sealant material;
- b. Loss or degraded areas of coatings for structures that do not serve as a barrier to aggressive chemical flows are limited in surface area to 4,000 square millimeters (6.2 in.²) or less at one area, and 0.01 square meters (15.5 in.²) over the gross surfaces of the structure;
- c. Absence of degradation in any waterproofing membrane protecting below-grade concrete surfaces (within the inspected area); and
- d. Non-structural components such as dewatering systems are serving their intended function.

5. Post-Tensioning Systems – Components of post-tensioning systems are acceptable if requirements provided elsewhere are met (ASME, 1995).

Acceptance After Review

Findings listed below require review and interpretation in order to evaluate acceptability. Such a review involves determining the likely source of degradation, its activity level, and its net effect on the component. Based on results of the review and evaluation, possible approaches include acceptance as-is, further evaluation using enhanced visual inspection (e.g., magnification), scheduling follow-up inspections at a later date, or use of nondestructive or destructive testing techniques. An analytical assessment of the necessity for repair may also be required. The analytical assessment should examine the impact of existing degradation on the performance characteristics of the structure. Accessibility of the components in question will also enter into the decision process relative to the action to be taken.

1. Unlined Concrete Surfaces – The following surface conditions shall be reviewed to determine if they are either acceptable, require further evaluation, or require repair. Discontinuities exceeding the quantitative limits below require additional evaluation.
 - a. Appearance of leaching or chemical attack;
 - b. Areas of abrasion, erosion, and cavitation degradation;
 - c. Drummy areas that may exceed the cover concrete thickness in depth;
 - d. Popouts and voids greater than 20 mm (.79 in.) but less than 50 mm (1.97 in.) in diameter or equivalent surface area;
 - e. Scaling greater than 5 mm (.2 in.) but less than 20 mm (.79 in.) in depth;
 - f. Spalling greater than 10 mm (.39 in.) but less than 20 mm (.79 in.) in depth, and less than 200 mm (7.87 in.) in any planar dimension;
 - g. Corrosion staining on concrete surfaces;
 - h. Passive cracks greater than 0.4 mm (.016 in.) but less than 1 mm (.039 in.) in maximum width; and
 - i. Passive settlements or deflections exceeding the original design limits or expected value.
2. Concrete Surfaces Lined by Metal or Plastic
 - a. Without Active Leak Detection System – Presence of any condition listed in Criteria 2(a) of previous section shall be further evaluated to determine acceptability; and

* Additional information on protective coatings for NPP applications is provided elsewhere (ASTM, 1990; 1990a; EPRI, 1998).

- b. With Active Leak Detection System – Presence of leakage in excess of amounts and flow rates committed to in the original design or Plant Technical Specification will necessitate a root cause investigation and assessment of the need for follow-up action. Leakage within the prescribed limits may be acceptable if the source is known and found to be inconsequential.
3. Areas Around Embedments in Concrete – Presence of any condition listed in Criteria 1 above for concrete surfaces or presence of any of the attributes presented in Criteria 3(b) through 3(d) of previous section shall be further evaluated to determine acceptability.
4. Joints, Coatings, and Non-Structural Components – Presence of any condition exceeding the descriptions and limits of Criteria 4 in previous section shall be further evaluated to determine acceptability. Any observation of widespread adhesion/cohesion problems, environmental attack, or poor performance indicators is considered unacceptable.

Additional Evaluation Required

Conditions outside the criteria provided in the previous two sections must be evaluated to determine the appropriate course of action. This will generally involve extensive application of both nondestructive and destructive testing methods. Detailed analytical evaluations frequently will be required to better characterize the current condition of the structure and provide the basis for formulation of a repair strategy (if needed). Even if the analysis results indicate that the component is acceptable at present, additional assessments should be conducted to demonstrate that the component will continue to meet its functional and structural requirements during the desired service life (i.e., take into account the current structural condition and use service life models to estimate the future impact of pertinent degradation factors on performance). If the structure's desired service life is short, and its loss of function due to degradation is occurring at a rate such that sufficient margins will be maintained during this period, no action may be required. However, when the opposite is true and loss of function due to degradation is occurring at a rate such that margins will not be adequately maintained during the desired service life period, the analytical and test results should be utilized to develop an in-service inspection/repair strategy that will maintain the margins during the desired service life.

4.3.1.3.2 Degradation-Based Approach

This approach is based on the concept that the degradation of a component in service is manifested in physical evidence or signs (e.g., measurable values), and that these signs can be categorized or classified into distinct stages or conditions in accordance with their potential impact on performance (e.g., structural margins). The effects of degradation mechanisms on the performance of a structure can range from cosmetic to structurally degrading. Provided below is information intended to be of assistance in quantifying the significance of degradation that is detected through visual inspections, nondestructive testing, or a combination of these methods. General criteria are developed in terms of parameters that can be measured associated with cracking and surface defects, corrosion of steel embedded in concrete, and alkali-silica reactions.

Concrete Cracking and Surface Defects

Cracking in concrete can result from a number of factors as noted previously. Designs of reinforced concrete structures generally consider that the concrete is incapable of supporting tensile forces. Steel reinforcement is included in the structural members to both carry the tensile loads and to provide control

of cracking (i.e., limit width and spacing of concrete cracks). Both the width of concrete cracks and the environmental exposure are important.

Limited information on concrete cracking, surface defects, and their classification with respect to damage is available. Table 4.9 presents one approach to classifications and ratings that were developed for concrete cracks and surface defects (RILEM, 1994). Damage is rated on a scale from one to five, with five being most significant. From an aging management perspective, the presence of concrete cracks (emphasis of this study) is of importance because they provide possible avenues of access for environmental stressors (e.g., chloride ions and sulfate solutions). There have been a number of studies over the years that related maximum permissible concrete crack widths to environmental factors, and these results are summarized in Table 4.10 (Krauss, 1994). Limits in this table were provided to reduce the potential for enhanced degradation through ingress of contaminants, primarily leading to corrosion of steel reinforcement. Some of the research studies have found correlations between crack width and deterioration of concrete, while others have not. An analysis of the relationship between crack width and corrosion has led to the conclusion that there is no clear relationship between crack width and the amount of corrosion, but the presence of cracks can accelerate corrosion occurrence. Larger crack widths increase the probability of corrosion (Beeby, 1979a). Values of crack width are not always a reliable indication of the corrosion and deterioration to be expected (ACI 224, 1990). Other factors need to be taken into consideration besides the crack width in assessing the corrosion potential (i.e., crack arrangement, crack depth, shape orientation with respect to reinforcement, intensity of crack, type of structure, and service environment) (Campbell-Allen and Lau, 1978).

Limited research results are available classifying the impact of alkali-aggregate reactions on structural integrity (i.e., alkali-silica, alkali-carbonate, and alkali-silicate). As a result of these reactions, expansion and cracking occurs that can lead to loss of strength, reduced stiffness, or decreased durability of concrete. A quantitative ranking methodology has been developed for beam and plate elements that potentially can be used as guidance for NPP reinforced concrete structures should the presence of alkali-aggregate reactions be confirmed (Danish Ministry of Transport, 1990). Criteria have been developed on the basis of visual inspections and petrographic analyses of core specimens removed from a large number of structures exhibiting various intensities of alkali-aggregate reactions. For structures having sustained Category 1 (crack width 0 - 0.2 mm (0 - 0.0079 in.), some gel exuded) or Category 2 (crack width 0.2 - 1.0 mm (0.0079 - 0.039 in.), gel in air voids and small external cracks) damage, the reactions have likely not caused significant structural damage. Structures observed as having damage in Category 1 should be considered for more frequent inspection and possibly for rehabilitative measures similar to that for Category 2 damage. For structures in Category 2, maintenance measures aimed at preventing exposure to moisture, such as adding a protective coating or sealer, should be considered. Additional core samples may be needed to assess the degree of reaction. More frequent inspection is also warranted. Structures in Category 3 (crack width 1.0 - 2.0 mm (0.039 - 0.079 in.), gel in many air voids and cracks) and Category 4 (crack width > 2.0 mm (0.079 in.), reactive aggregate with signs of reactivity) require evaluation for structural repair. Because a single aggregate source was generally used in the construction of a NPP, the balance of plant structures should be inspected if Category 3 or 4 conditions are observed in any one structure.

Corrosion

As noted in Section 2, there are two primary factors that can depassivate the steel reinforcement: carbonation and presence of chloride ions. Presented below is some general guidance to assist in assessment of the significance of corrosion-damaged reinforced concrete structures.

If the carbonation front reaches the reinforcing steel and there is adequate moisture present around the steel surface then corrosion is likely to be initiated. In general, progress of the carbonation front in high

quality concrete structures such as those contained in NPPs is slow. The presence of cracks, however, can accelerate the process and this was addressed previously. A limited amount of guidance has been developed to aid in the classification of carbonation-induced damage (Parrott, 1990). Table 4.11 presents one proposed classification system. The system is based on methods of assessment that are also contained in the table.

A sample damage-state chart has been prepared based on information provided above to assist in the resolution of results obtained from in-service inspections or testing. It should be noted that these charts are only provided as examples, they have not incorporated all factors required for a detailed assessment,* and application of the methodology should utilize the judgment of suitably qualified and experienced responsible engineers. Figure 4.12 provides a relationship between environmental exposure in terms of extent of carbonation or chloride ion content of the environment, the width of cracks present, and the necessity for additional evaluation or repair. As noted in the figure, the extent of action required increases as the severity of environmental exposure increases or the width of cracks present increases. Figure 4.13 provides a relationship between environmental exposure, half-cell potential readings, and necessity for further evaluation or repair. Superimposed on the half-cell potential axis are visual inspection results that might be anticipated for different degrees of severity of corrosion of steel reinforcement. Crack width information based on the quantitative ranking methodology (Danish Ministry of Transport, 1990) and limited industry-published acceptance criteria (ASTM C 876; Pullar-Strecker, 1987) were used to develop the relationships presented in these figures. Further evaluation would consider the use of other inspection, testing, or analytical tools to obtain additional information on the current condition of the structure and the potential for further degradation of its functional and performance requirements with time.

4.3.1.4 Implications of Corrosion and Performance

Many consider the service life of a corroding structure to be finished when depassivation of the reinforcement occurs (Browne, Geoghegan, and Baker, 1983). Others prefer to identify the end of service life when cover cracking occurs (Braun, 1987), however, as noted previously, at this point the structural integrity has not been diminished significantly. Two limit states have been associated with reinforced concrete structures undergoing corrosion (Andrade, Alonso, González, and Rodríguez, 1989). The first refers to a serviceability limit state that corresponds to a limiting condition resulting from damage such as excessive deflections due to formation of cracks. A reduction of 10 to 25% in reinforcement cross section has been suggested to cause serviceability failure (CEB, 1983). The second refers to an ultimate limit state at which loss of load bearing capacity results due to loss of steel reinforcement cross section, or bond between the concrete and steel reinforcement.

Establishing the limiting state at which steel corrosion decreases structural margins to an unacceptable level is a formidable task, especially if visual indicators are to form the basis of the assessment. Definitions of deterioration based on visual evidence, such as rust stains and longitudinal cracking, have been attempted, but flexural testing has shown limited correlation with these parameters (Mangat and Elgarf, 1999). In establishing a limit state for steel corrosion, several factors are of importance: (1) initiation of corrosion, (2) formation of cracks due to corrosion, (3) limitation of loss of steel cross section, and (4) spalling of the cover concrete and loss of bond. The time required for initiation of corrosion of steel reinforcement depends on a number of factors (e.g., concrete quality, concrete cover, and concentration of aggressive ions). Visible indications or indicators prior to initiation of corrosion in all likelihood will be absent. During the early stages of active corrosion indications of corrosion also will

* In assessing the potential for corrosion, the current density is a more useful parameter than the absolute value of potential. Potential values are of most use when viewed as contour plots so that the rate of potential change can be examined.

be absent unless monitoring of the structure is in effect (e.g., half-cell potential or corrosion current readings). Formation of cracks, especially those that form along the steel reinforcement, probably provides the best visible indicator for use in corrosion assessments and trying to develop a relationship between corrosion and performance (i.e., reduction in structural margins).

Figure 4.14 presents one approach or concept to the evolution of structural safety with time as dictated by steel corrosion (RILEM, 1988a). In the figure, T_0 indicates the initiation of degradation factor effects, T_1 is the time to initiation of depassivation of the steel, T_2 is the time to concrete cracking, T_3 is the time to loss of a critical percentage of steel reinforcement cross section (predefined limit state prior to failure), T_4 is the time to concrete spalling, and T_5 is the time to structural collapse due to a critical loss of steel cross section. Collapse is considered to occur relatively soon after concrete spalling. Figure 4.15 presents a representation of the progressive change with time of the deterioration levels (loss of durability) and loss of structural performance of a reinforced concrete member subjected to chloride attack (JCI, 1996). Although dependent on several factors, loss of structural performance initiates after the appearance of longitudinal cracks (Region III) and accelerates with time due to decreased cross section of the reinforcement and loss of bond (Region IV).

In addressing the service life of concrete structures subject to corrosion, many researchers make a conservative estimate of the service life by only considering the initiation period which is evaluated using Fick's second law of diffusion (Tuutti, 1982). Corrosion is initiated when the concentration of chlorides at the depth of the steel equals the threshold concentration needed to initiate steel corrosion. The time to initiation of steel corrosion is usually much longer than the time for propagation or for sufficient corrosion to occur to induce concrete cracking [e.g., up to five times has been observed in one bridge deck (Tuutti, 1982)]. Computational approaches using numerical simulation (e.g., finite-element modeling) have been developed to predict onset of concrete cracking due to chloride-induced corrosion, but they have not been validated (Shimomura, 1999; Yamamoto et al., 1995). The relation between pressure buildup and cracking of cover concrete has been investigated experimentally (Morinaga, 1988). Results presented previously (Table 3.5) indicate that for 16-mm (.63 in.) diameter rebar having concrete cover of either 2 or 3 mm (.079 or .118 in.), the time to occurrence of visible cracks [~ 0.1 mm (.0039 in.)] in the concrete cover using representative corrosion rates is on the order of 0.2 to 2 years. For cover crack widths from 0.1 to 0.2 mm (.0039 to .0079 in.), the time required ranges from 1 to 15 years. After cracking of the cover concrete, the rate of corrosion increases significantly (Morinaga, 1999). At this time, however, it has been shown that the structural properties are not damaged significantly (Morinaga, 1999). As the rate of corrosion increases rapidly after concrete cracking, spalling of the concrete follows shortly thereafter. It has been estimated that the spalling will generally occur about two to three years after appearance of the first concrete crack induced by corrosion (Naus, 1999). Estimations of the time to failure of reinforced concrete structures (based on reduction of yield point of reinforcement to a specified value), after concrete cover cracking due to corrosion, have been made based on corrosion rates obtained from a number of Japanese cities (Morinaga, 1999). It was found that the times were on the order of 10 years or less.

As noted, there are a wide number of factors that can affect the relationship between concrete cracking or spalling and corrosion significance with respect to structural performance. Results presented in Section 3 relative to the performance of degraded concrete structures indicate that for corrosion losses on the order of up to 1 to 1.5% (or more depending on test conditions) of the rebar cross-section area, there may be an improvement in performance. Results seem to indicate that up to (and probably beyond) the point of initial concrete spalling due to corrosion, the capacity of structural members is not significantly impacted. Although it is difficult to define a relationship between surface crack width and level of corrosion, as the crack width increases, the probability of corrosion will increase as well as corrosion occurrence. Results in this report indicate that crack widths ≥ 0.15 mm (.00591 in.) are capable of accelerating the onset of corrosion. Relating concrete cover crack width to loss of reinforcement section, however, is very complex

because of the number of factors that can influence the results (e.g., concrete cover and rebar diameter). In the performance of structural evaluations using visible indicators for guidance, the critical parameter is the occurrence of cracks along the steel reinforcement due to corrosion. At this point in all likelihood there will have been no degradation in structural capacity and sufficient time will remain to implement a repair strategy. Although sufficient structural capacity can still remain at the onset of concrete spalling due to corrosion, the time period from onset of spalling to loss of structural margins may be relatively short.

4.3.2 Inspection Scheduling

Inspection intervals are a matter of engineering judgement and must be determined for each specific application. They depend on factors such as type and importance of structure, loading conditions and severity of loading, consequences of failure, and presence of an aggressive environment. International guidelines on good practice for inspection and maintenance of reinforced concrete structures have addressed inspection intervals in terms of the class of a structure and the environmental (and loading) conditions (FIP, 1986). The inspections are categorized into three classes: routine, extended, and special. Routine inspections are carried out methodically at regular intervals using a checklist that had been prepared beforehand. An extended inspection is carried out in place of every second routine inspection and involves a more intensive examination of the structure. A special inspection is conducted when unusual circumstances are present (e.g., after seismic event or specific degraded conditions of concern have been found in similar structures) and may involve supplementary testing, structural analysis, and possibly research. Table 4.12 provides an example of inspection intervals for routine and extended inspections that addresses environmental conditions and class of the structure (FIP, 1986). Three classes of structure are identified in the table. Class 1 involves structures where possible failure would have catastrophic consequences or serviceability is of utmost importance. Class 2 refers to structures where failure might cost lives and serviceability is of considerable importance. Class 3 involves those structures where it is unlikely that failure would lead to fatal consequences and the structure being out of service for a period could be tolerated.

Information has been developed for light-water reactor plants in the United States on recommended frequencies for conduct of routine visual inspections of safety-related concrete structures other than containments (ACI 349, 1996; Hookham, 1995). These recommendations, summarized in Table 4.13, provide frequency of visual inspections in terms of exposure conditions. The recommended inspection frequency schedules take into account the relative aggressiveness of environmental conditions and physical exposures of these structures, and help to assure that any age-related degradation is detected at an early stage of development so appropriate mitigative actions can be taken. As access to many of the plant structures is restricted during normal plant operation, the frequency of inspections has been designated to coincide with planned plant outages (e.g., refueling) to provide improved plant access. The plant owner does have the option of electing to perform certain inspections (e.g., tendon surveillances) at other times as long as the code-mandated frequencies and schedules are met.** The above frequencies

**Other countries utilize different inspection intervals. For example, in the United Kingdom the gas-cooled reactors re-inspection interval is based on the structure's environment, its safety significance, and the condition observed at the last inspection. Depending on the station, there is a legal requirement to shut the reactors down for inspection at regular intervals (i.e., every two to three years). Periodic Safety Reviews are conducted at each station every ten years to demonstrate a station's fitness for continued operation. In France, after the first refueling the containments are tested and inspected for cracks at 10-year intervals. Since grouted tendon systems have been utilized in the French containments, extensive monitoring devices have been installed to verify the level of prestressing (e.g., strain gages, thermocouples, dynamometers). Every two years an evaluation of the monitoring results is performed and a (Footnote continued on the next page)

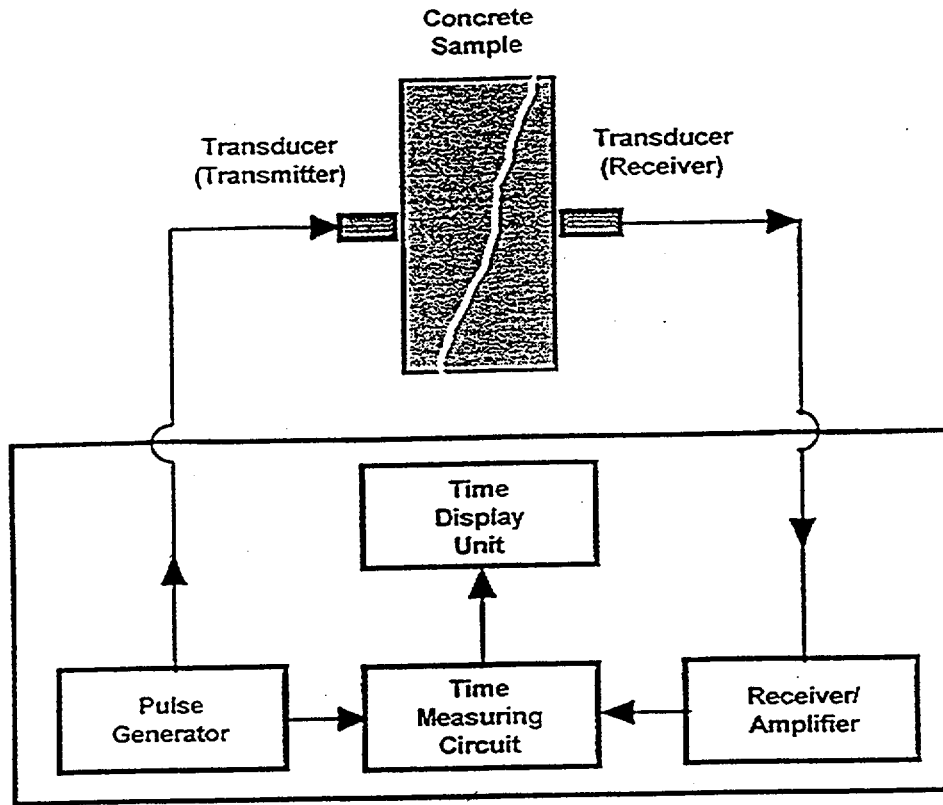
may be modified to smaller intervals if plant environments are particularly severe or degradation has been observed to occur. When the observed degradation exceeds criteria provided previously, increased visual inspections should be supplemented by nondestructive, and possibly destructive testing (e.g., extended or special inspections).

Reliability-based methods also can be used to schedule inspections of safety-related concrete structures. These methods assess the reliability of the NPP reinforced concrete structures in terms of damage state and rate of degradation, inspection methods, detectability functions, remedial actions, and frequency of inspections. Optimized strategies for inspection and maintenance can be developed that minimize future costs associated with inspection, repair, and loss of service, while maintaining the component probability of failure at or below a target value over the service life of the structures (Mori and Ellingwood, 1993; Ellingwood and Mori, 1994a; 1994b).

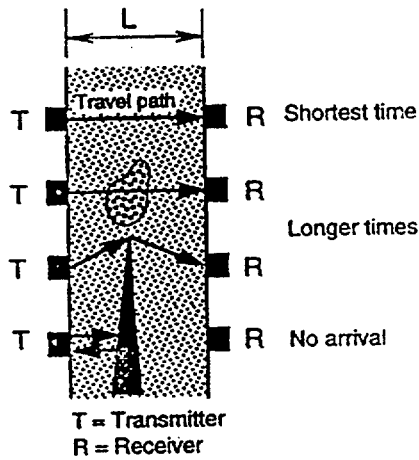
4.3.3 Qualification of Inspection Personnel

The complexity of structures and the damage that can occur makes appraisal of structures and damage assessment an activity for experienced engineers. The quality and usefulness of results obtained from inspections of existing NPP reinforced concrete structures are dependent to a great deal on the qualifications and capabilities of the personnel involved. To ensure that these inspections are properly performed, minimum qualifications and skills should be defined. As a minimum, the complete inspection team should include both civil/structural engineers and concrete inspectors and technicians familiar with the structural and functional requirements of the facilities inspected, concrete aging and degradation mechanisms, and long-term performance issues. The program should be under the direction of a suitably qualified and experienced "Responsible Engineer." Additional guidance on qualification of inspection personnel is provided elsewhere (ASME, 1995).

diagnosis of the plant provided. In general, in countries where containments contain extensive instrumentation systems for monitoring performance the periodic condition assessment intervals tend to be longer.



(a) Schematic Diagram of Pulse Velocity Test Circuit.



(b) Effects of Defects on Travel Time of ultrasonic pulse (ACI 228.2R, 1999).

Permission to use this copyrighted material is granted by the American Concrete Institute.

Figure 4.1 Ultrasonic Pulse Velocity Test.

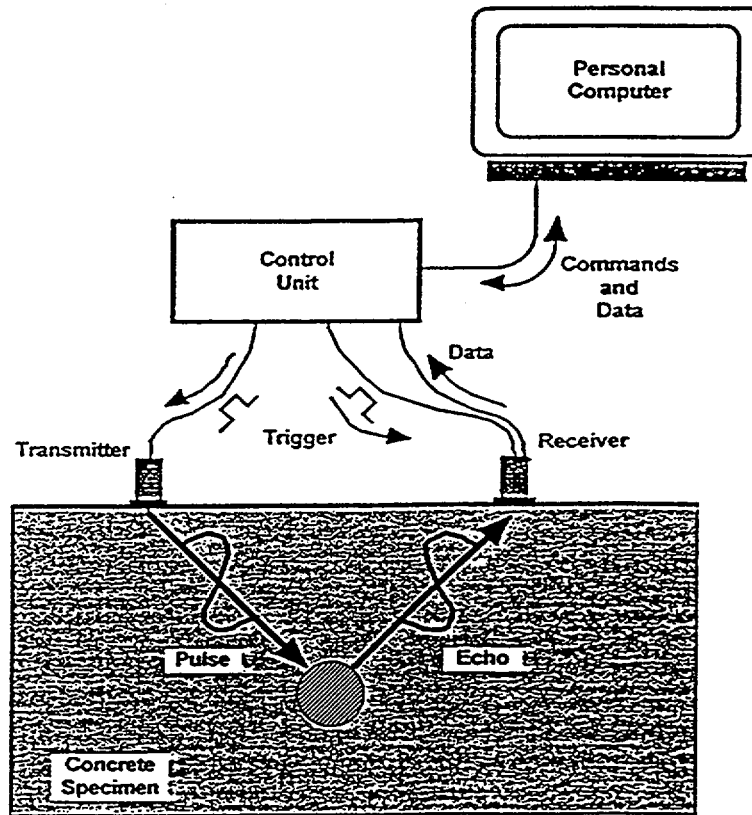


Figure 4.2 Schematic of Ultrasonic Pulse-Echo Test Setup. (IAEA, 1998)
 Permission to use this copyrighted material is granted by IAEA.

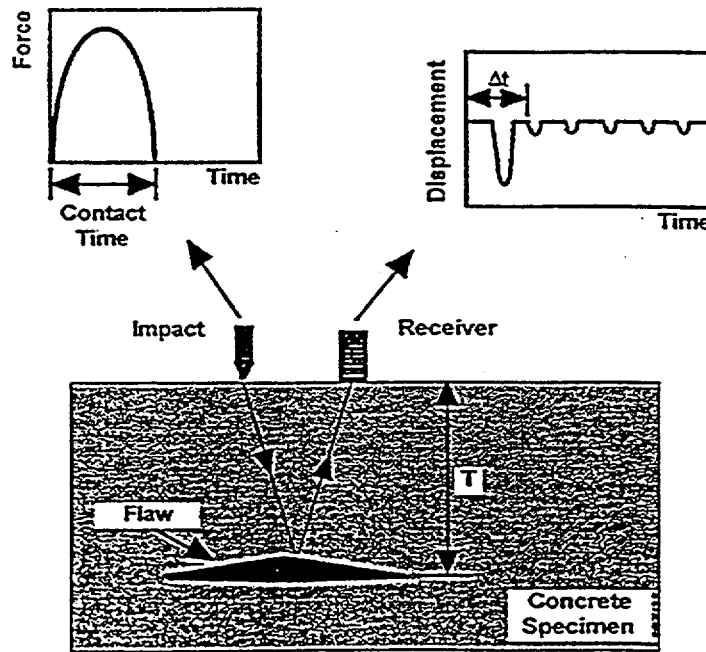


Figure 4.3 Principle of Impact-Echo System. (IAEA, 1998).
 Permission to use this copyrighted material is granted by IAEA.

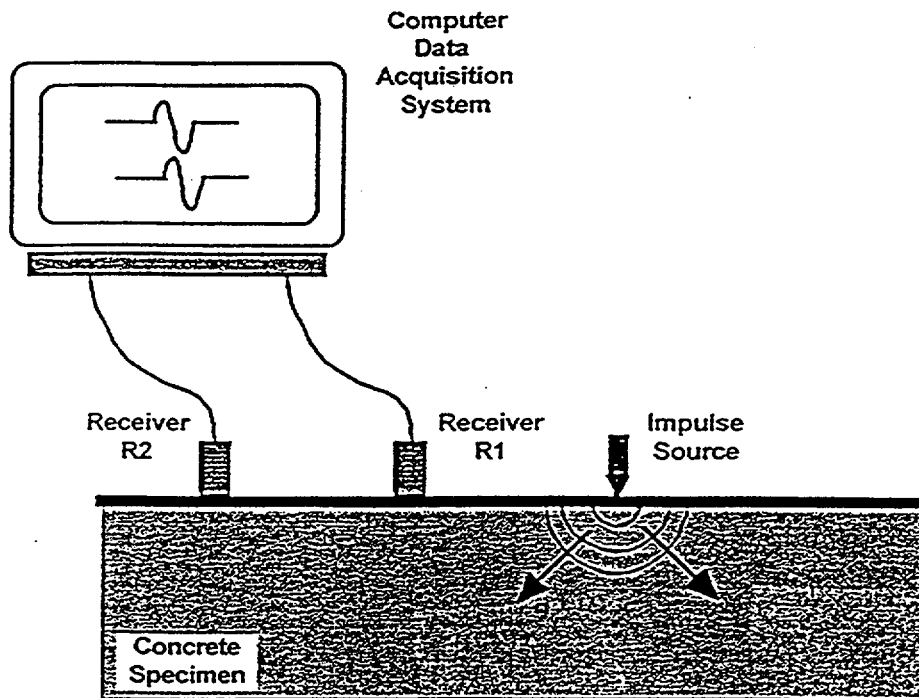


Figure 4.4 Spectral Analysis of Surface Waves (SASW) Test Setup (IAEA, 1998).
 Permission to use this copyrighted material is granted by IAEA.

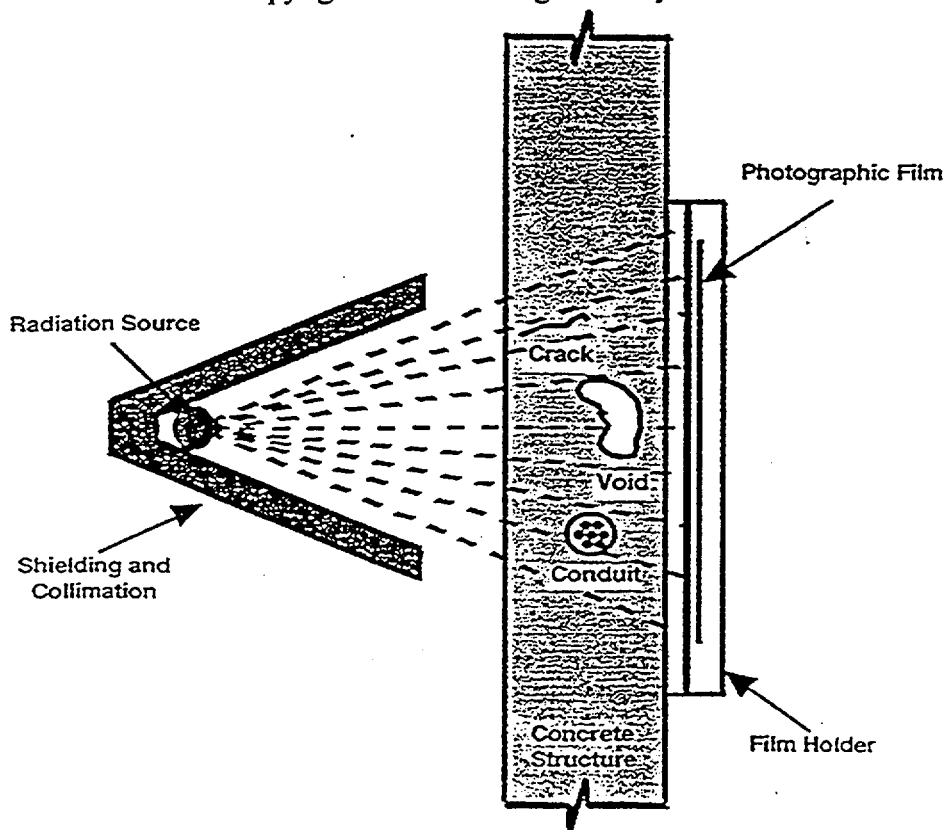


Figure 4.5 Schematic of Radiography Method (IAEA, 1998).
 Permission to use this copyrighted material is granted by IAEA.

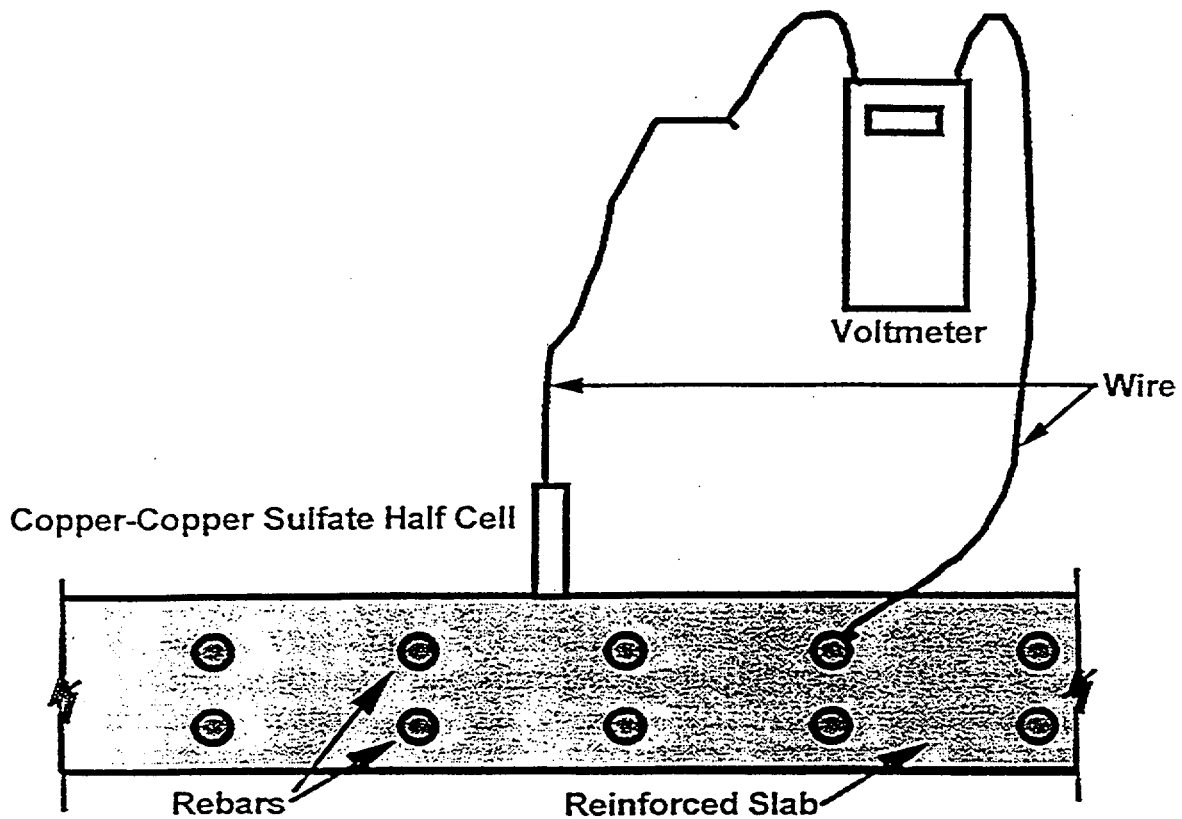


Figure 4.6 Schematic of Copper-Copper Sulfate Half-Cell Potential System (IAEA, 1998). Permission to use this copyrighted material is granted by IAEA.

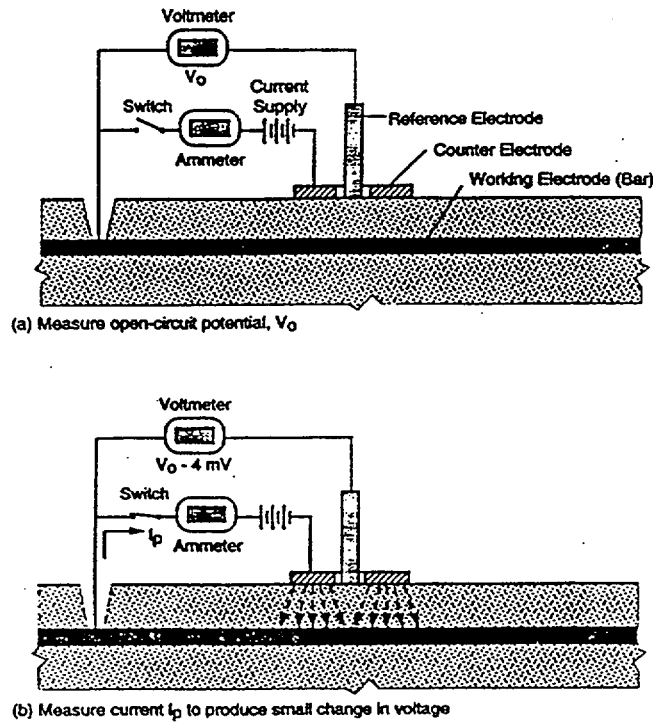


Figure 4.7 Three-Electrode Linear-Polarization Method to Measure Corrosion Current (ACI 228.2R, 1999). Permission to use this copyrighted material is granted by the American Concrete Institute.

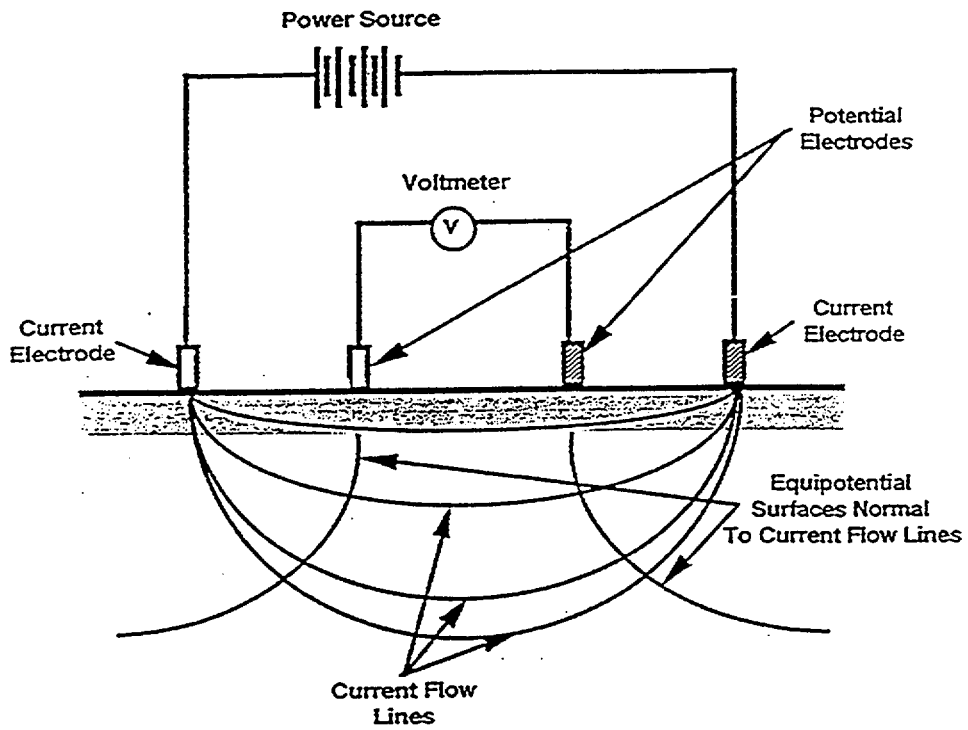


Figure 4.8 Schematic of Four-Electrode Method for Measurement of Concrete Resistance (IAEA, 1998). Permission to use this copyrighted material is granted by IAEA.

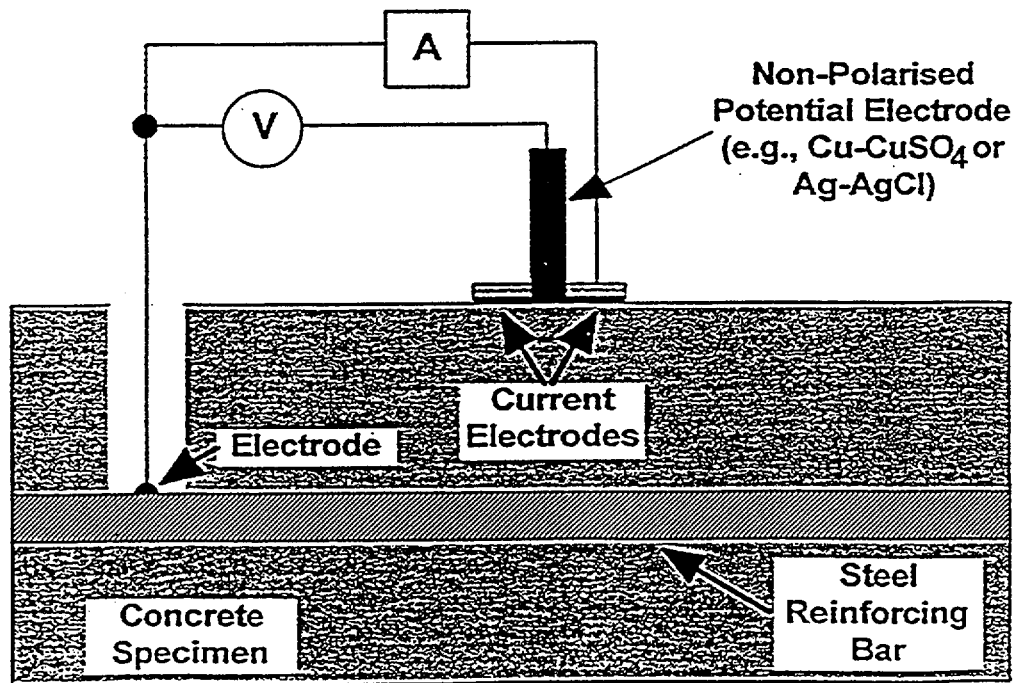


Figure 4.9 Schematic of Setup for Galvanostatic Pulse Measurement (IAEA, 1998). Permission to use this copyrighted material is granted by IAEA.

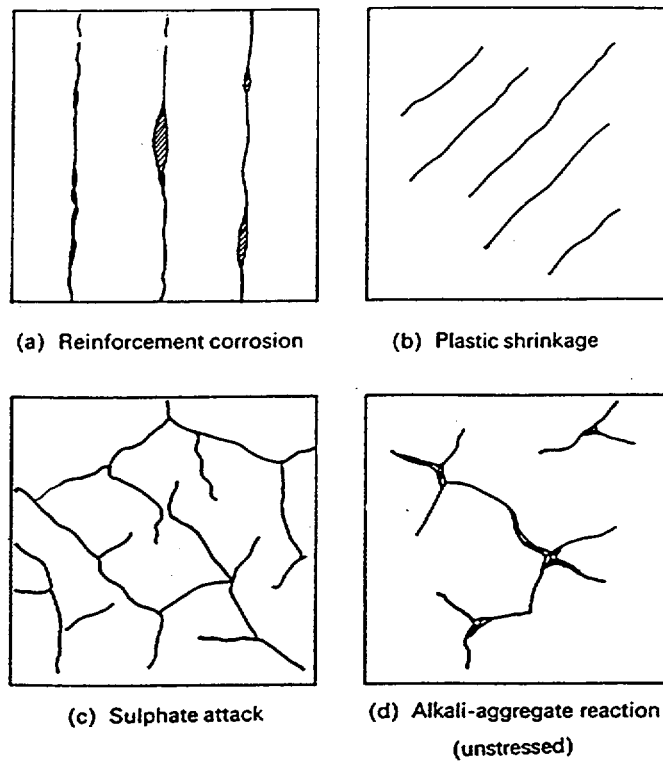


Figure 4.10 Schematics of some typical crack patterns that represent the common causes of concrete degradation (Bungey, 1996).

Permission to use this copyrighted material is granted by the above author(s).

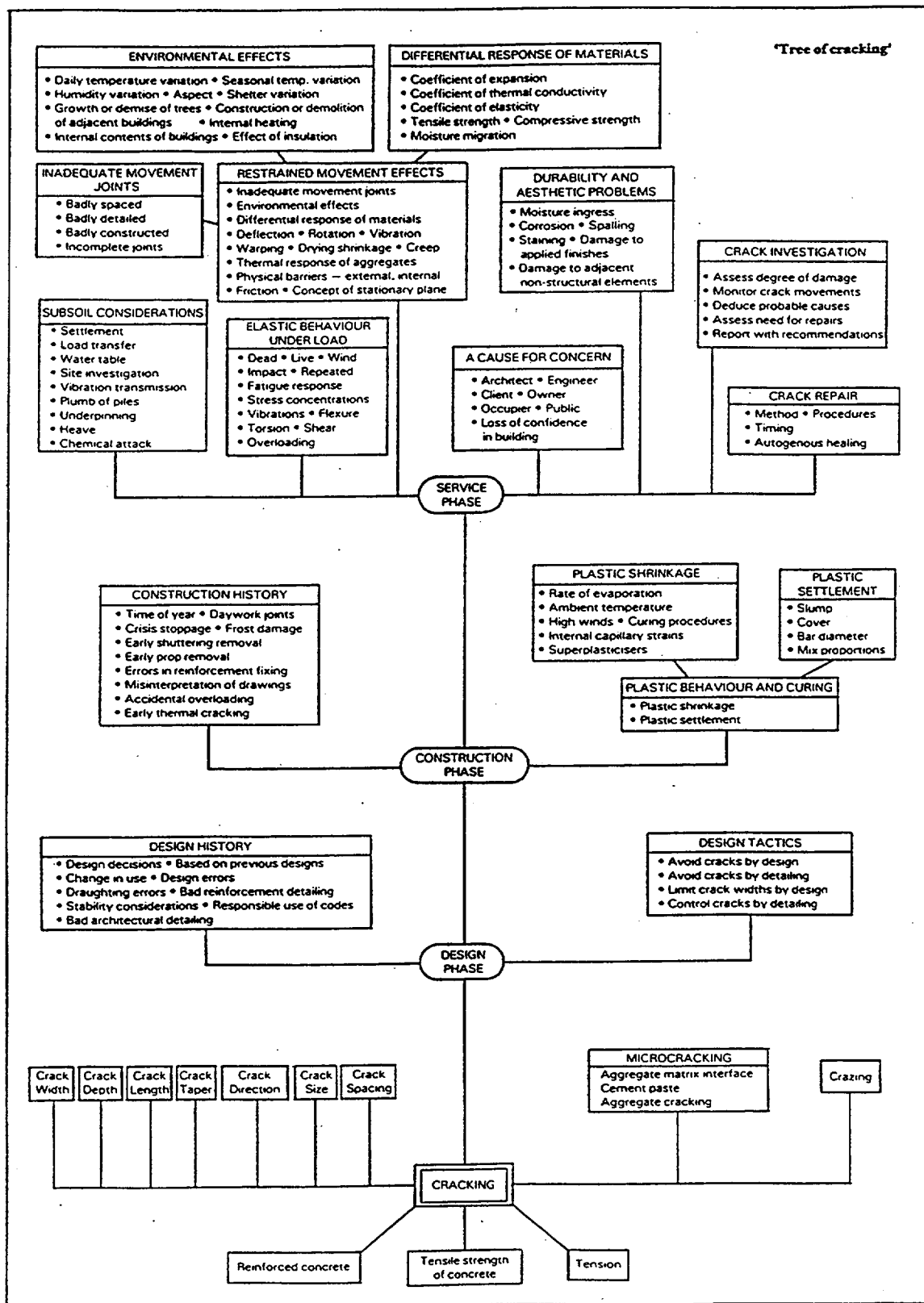


Figure 4.11 Summary of crack-induced phenomena associated with the design, construction, and service phases of a reinforced concrete structure (Richardson, 1987). Permission to use this copyrighted material is granted by the American Concrete Institute.

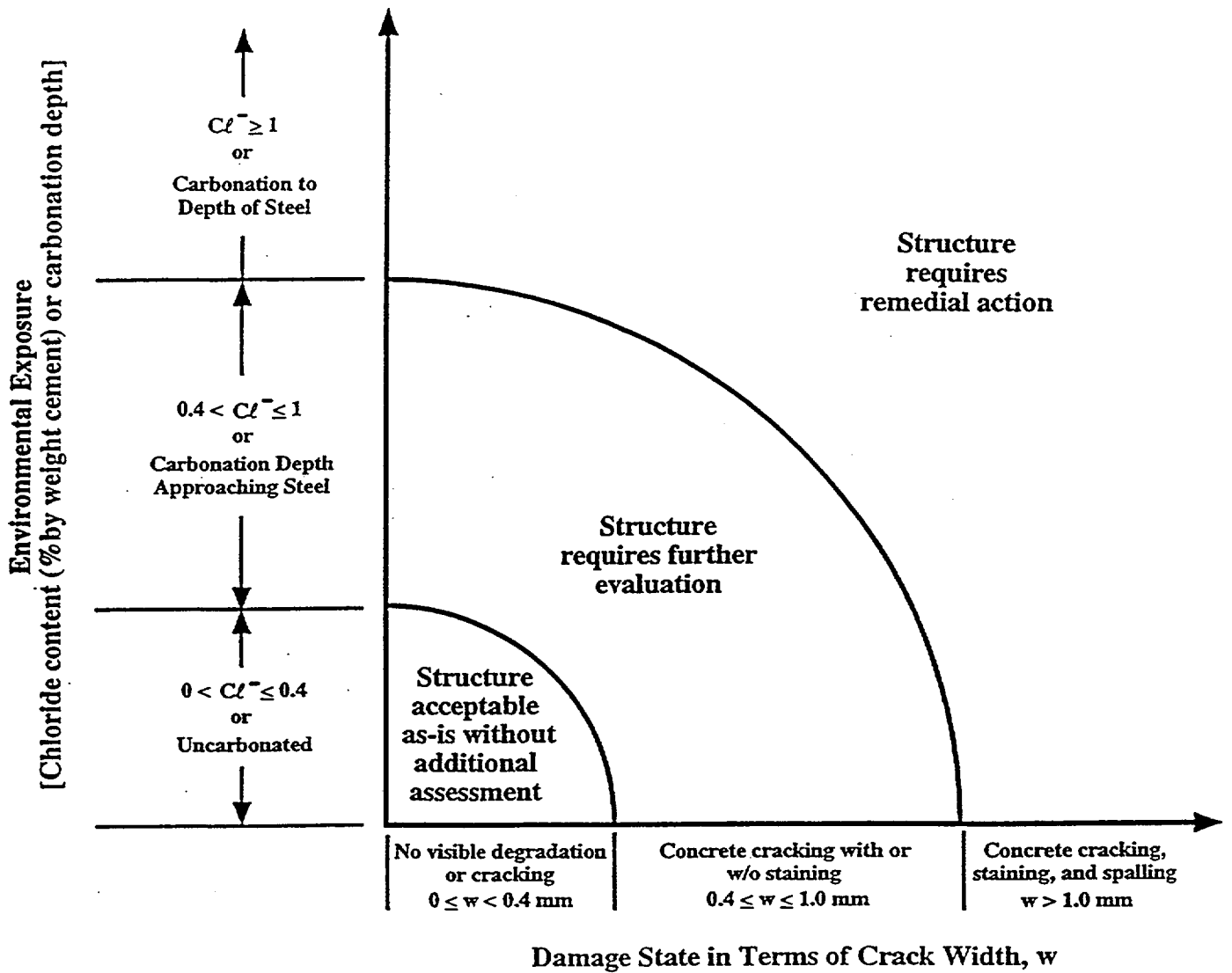


Figure 4.12 Damage State Chart Relating Environmental Exposure, Crack Width, And Necessity for Additional Evaluation or Repair (Naus et al., 1996).

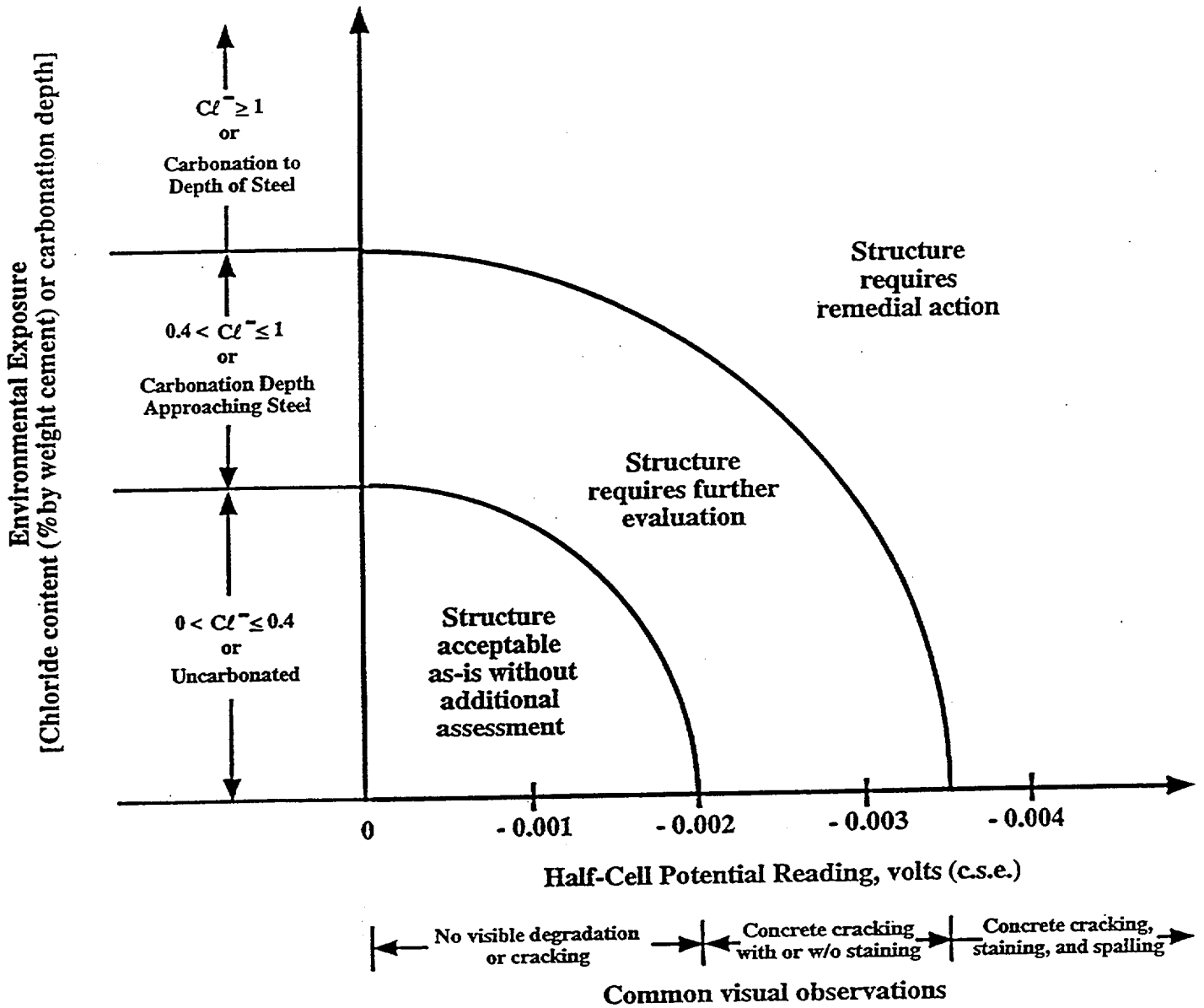


Figure 4.13 Damage State Chart Relating Environmental Exposure, Half-Cell Potential Reading, And Necessity for Additional Evaluation or Repair (Naus et al., 1996).

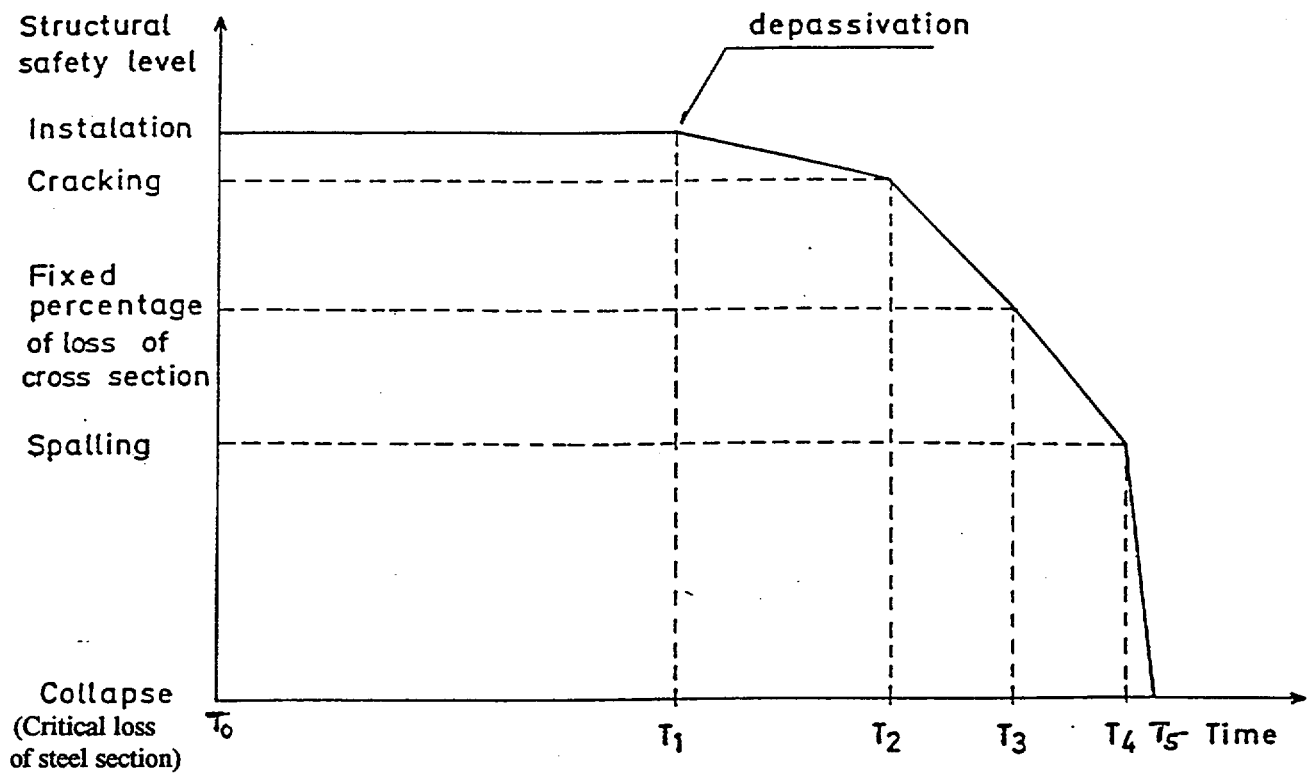


Figure 4.14 One Approach to the Evolution of Structural Safety with Time as Dictated by Steel Corrosion (RILEM, 1988a). Permission to use this copyrighted material is granted by RILEM.

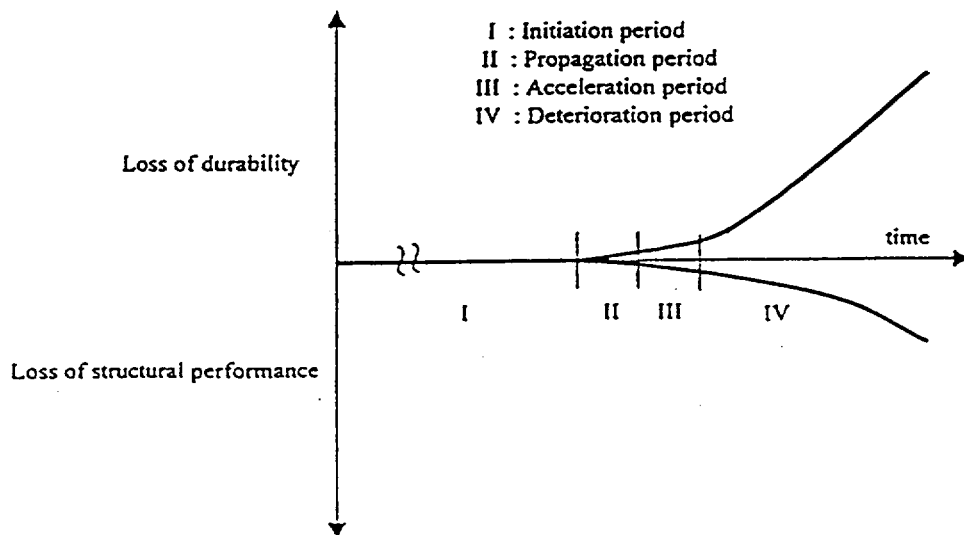


Figure 4.15 Representation of the Progressive Change with Time of the Deterioration Levels and Loss of Structural Performance of a Reinforced Concrete Member Subject to Chloride Attack (JCI, 1998). Permission to use this copyrighted material is granted by the Japan Concrete Institute.

Table 4.1 Nondestructive Test Methods for Determining Material Properties of Hardened Concrete in Existing Construction (ACI 228.2R, 1999). Permission to use this copyrighted material is granted by the American Concrete Institute.

Property	Possible Methods		Comment
	Primary	Secondary	
Compressive strength	Cores for compression testing (ASTM C 42 and C 39)	Penetration resistance (ASTM C 803; pullout testing (drilled-in))	Strength of in-place concrete; comparison of strength in different locations. Drilled-in pullout test not standardized
Relative compressive strength	Rebound number (ASTM C 805); Ultrasonic pulse velocity (ASTM C 597)		Rebound number influenced by near surface properties; Ultrasonic pulse velocity gives average result through thickness
Tensile strength	Splitting-tensile strength of core (ASTM C 496)	In-place pulloff test (ACI 503R; BS 1881; Part 207)	Assess tensile strength of concrete
Density	Specific gravity of samples (ASTM C 642)	Nuclear gage	
Moisture content	Moisture meters	Nuclear gage	
Static modulus of elasticity	Compression test of cores (ASTM C 469)		
Dynamic modulus of elasticity	Resonant frequency testing of sawed specimens (ASTM C 215)	Ultrasonic pulse velocity (ASTM C 597); impact-echo; spectral analysis of surface waves (SASW)	Requires knowledge of density and Poisson's ratio (except ASTM C 215); dynamic elastic modulus is typically greater than the static elastic modulus
Shrinkage/expansion	Length change of drilled or sawed specimens (ASTM C 341)		Measure of incremental potential length change
Resistance to chloride penetration	90-day ponding test (AASHTO-T-259)	Electrical indication of concrete's ability to resist chloride ion penetration (ASTM C 1202)	Establishes relative susceptibility of concrete to chloride ion intrusion; assess effectiveness of chemical sealers, membranes, and overlays
Air content; cement content; and aggregate properties (scaling, alkali-aggregate reactivity, freeze/thaw susceptibility)	Petrographic examination of concrete samples removed from structure (ASTM C 856, ASTM C 457); Cement content (ASTM C 1084)	Petrographic examination of aggregates (ASTM C 294, ASTM C 295)	Assist in determination of cause(s) of distress; degree of damage; quality of concrete when originally cast and current
Alkali-silica reactivity	Cornell/SHRP rapid test (SHRP-C-315)		Establish in field if observed deterioration is due to alkali-silica reactivity
Carbonation, pH	Phenolphthalein (qualitative indication); pH meter	Other pH indicators (e.g., litmus paper)	Assess corrosion protection value of concrete with depth and susceptibility of steel reinforcement to corrosion; depth of carbonation
Fire Damage	Petrography; rebound number (ASTM C 805)	SASW; Ultrasonic pulse velocity; impact-echo; impulse-response	Rebound number permits demarcation of damaged concrete
Freezing and thawing damage	Petrography	SASW; Impulse response	
Chloride ion content	Acid-soluble (ASTM C 1152) and water-soluble (ASTM C 1218)	Specific ion probe (SHRP-S-328)	Chloride ingress increases susceptibility of steel reinforcement to corrosion
Air permeability	SHRP surface airflow method (SHRP-S-329)		Measures in-place permeability index of the near-surface concrete (15 mm)
Electrical resistance of concrete	AC resistance using four-probe resistance meter	SHRP surface resistance test (SHRP-S-327)	AC resistance useful for evaluating effectiveness of admixtures and cementitious additions; SHRP method useful for evaluating effectiveness of sealers

Table 4.2 Nondestructive Test Methods to Determine Structural Properties and Assess Conditions of Concrete (ACI 228.2R, 1999). Permission to use this copyrighted material is granted by the American Concrete Institute.

Property	Methods		Comment
	Primary	Secondary	
Reinforcement location	Covermeter; Ground penetrating radar (GPR) (ASTM D 4748)	X-ray and γ -ray radiography	Steel location and distribution; concrete cover
Concrete component thickness	Impact-echo (I-E); GPR (ASTM D 4748)	Intrusive probing	Verify thickness of concrete; provide more certainty in structural capacity calculations; I-E requires knowledge of wave speed, and GPR of dielectric constant
Steel area reduction	Ultrasonic thickness gage (requires direct contact with steel)	Intrusive probing; radiography	Observe and measure rust and area reduction in steel; observe corrosion of embedded post-tensioning components; verify location and extent of deterioration; provide more certainty in structural capacity calculations
Local or global strength and behavior	Load test, deflection or strain measurements	Acceleration, strain, and displacement measurements	Ascertain acceptability without repair or strengthening; determine accurate load rating
Corrosion potentials	Half-cell potential (ASTM C 876)		Identification of location of active reinforcement corrosion
Corrosion rate	Linear polarization (SHRP-S-324 and S-330)		Corrosion rate of embedded steel; rate influenced by environmental conditions
Location of delaminations, voids, and other hidden defects	Impact-echo; Infrared thermography (ASTM D 4788); Impulse-response; Radiography; GPR	Sounding (ASTM D 4580); pulse-echo; SASW; intrusive drilling and borescope	Assessment of reduced structural properties; extent and location of internal damage and defects; sounding limited to shallow delaminations

Table 4.3 Exposure Classes for Concrete Structures (Litzner and Becker, 1999).
Permission to use this copyrighted material is granted by RILEM.

Deterioration mechanism	Class designation	Description of the environment	Informative examples where exposure classes may occur
1. No risk of corrosion or attack	X0	Very dry	Concrete inside buildings with very low humidity (RH < 45%)
2. Steel corrosion induced by carbonation	XC1	Dry	Concrete inside buildings with low humidity (RH < 65%)
	XC2	Wet, rarely dry	Parts of water-retaining structures, many foundations
	XC3	Moderate humidity (RH < 80%)	Concrete inside buildings with moderate or high air RH; external concrete sheltered from rain
	XC4	Cyclic wet and dry	Surfaces subjected to water contact, not within class XC2
3. Steel corrosion induced by chlorides	XD1	Moderate humidity	Concrete surfaces exposed to direct spray containing chlorides
	XD2	Wet, rarely dry	Swimming pools; concrete exposed to industrial water containing chlorides
	XD3	Cyclic wet and dry	Parts of bridges; pavements; car park slabs
4. Steel corrosion induced by chlorides from sea water	XS1	Exposed to airborne salt, not in direct contact with sea water	Structures near to or on the coast
	XS2	Submerged	Parts of marine structures
	XS3	Tidal, splash and spray zones	Parts of marine structures
5. Freeze/thaw attack on concrete	XF1	Moderate water saturation, no de-icing agents	Vertical concrete surfaces exposed to rain and freezing
	XF2	Moderate water saturation, with de-icing agents	Vertical concrete surfaces of road structures exposed to freezing and airborne de-icing agents
	XF3	High water saturation, no de-icing agents	Horizontal concrete surfaces exposed to rain and freezing
	XF4	High water saturation, with de-icing agents	Road and bridge decks exposed to de-icing agents and vertical concrete surfaces exposed to direct spray containing de-icing agents and freezing
6. Chemical attack on concrete	XA1, XA2, XA3	Aggressive chemical environment	See Table 4.4

Table 4.4 Limiting Values for Exposure Class XA in Table 4.3 (Litzner and Becker, 1999).
Permission to use this copyrighted material is granted by RILEM.

Chemical characteristic	XA1	XA2	XA3	Test method
SO ₄ ²⁻ mg/l in water	≥ 200 and ≤ 600	> 600 and ≤ 3000	> 3000 and ≤ 6000	EN 196-2[7]
SO ₄ ²⁻ mg/kg in soil ¹⁾ total amount	≥ 2000 and ≤ 3000 ²⁾	> 3000 ²⁾ and ≤ 12000	> 12000 and ≤ 24000	EN 196-2 ³⁾
pH of water	≤ 6.5 and ≥ 5.5	< 5.5 and ≥ 4.5	< 4.5 and ≥ 4.0	DIN 4030-2 [8]
Acidity of soil	> 200 Baumann Gully			DIN 4030-2
CO ₂ mg/l aggressive in water	≥ 15 and ≤ 40	> 40 and ≤ 100	> 100	DIN 4030-2
NH ₄ ⁺ mg/l in water	≥ 15 and ≤ 30	> 30 and ≤ 60	> 60 and ≤ 100	ISO 7150-1[9] ISO 7150-2[10]
Mg ²⁺ mg/l in water	≥ 300 and ≤ 1000	> 1000 and ≤ 3000	< 3000	ISO 7980 [11]

Footnotes:

1. Clay soils with a permeability below 10⁻³ m/s may be moved into a lower class.
2. The 3000 mg/kg limit is reduced to 2000 mg/kg, in the event of a risk of accumulation of sulphates in the concrete due to drying and wetting cycles or capillary suction.
3. The test method prescribes the extraction of SO₄²⁻ by hydrochloric acid; alternatively, water extraction may be used, if experience is available, in the place of concrete.

Table 4.5 Influence of Moisture State on Durability Processes (CEB-FIB, 1992).
 Reprinted with permission of *fib*, Federation Internationale du Beton (CEB-FIB).

Effective relative humidity	Process*				
	Carbonation	Corrosion of steel		Frost attack	Chemical attack
		In carbonated concrete	In chloride contaminated concrete		
Very low (< 45%)	1	0	0	0	0
Low (45–65%)	3	1	1	0	0
Medium (65–85%)	2	3	3	0	0
High (85–98%)	1	2	3	2	1
Saturated (> 98%)	0	1	1	3	3

* 0 = insignificant risk; 1 = slight risk; 2 = medium risk; 3 = high risk.

Table 4.6 Forms of Distress and Deterioration to be Noted in a Visual Condition Assessment (Poston et al, 1995). Permission to use this copyrighted material is granted by the American Concrete Institute

Description	Typical Causes
Cracking	Plastic shrinkage Drying shrinkage Restraint Subgrade support deficiencies Vapor barrier Expansion Corrosion of reinforcing steel/prestressing steel or other embedded metal components Thermal loading Vehicular impact Overloading Aggregate reaction
Scaling	Inadequate air content Finishing problems Freeze-thaw cycling Chemical deicers
Spalling	Aggregate reaction Corrosion Freeze-thaw cycling Construction Poor preparation of construction joints Early age loading
Disintegration	Frozen concrete Freeze-thaw cycling Low strength Chemical attack Sulfate attack
Honeycombing and surface voids	Poor placement Poor consolidation Congested reinforcement
Discoloration and staining	Different cement production Different water-cement ratios Corrosion Aggregates Use of calcium chloride Curing Finishing Nonuniform absorption of forms
Efflorescence	Calcium carbonate and other mineral deposits

Table 4.7 Outline of Recommended Information for a Survey
and Sampling of Field Concrete (Stuzman, 1991).

STRUCTURE IDENTIFICATION:

STRUCTURE LOCATION:

STRUCTURE DESCRIPTION:

CONSTRUCTION:

INSPECTION DATE:

AGE:

CONCRETE TYPE: mass, reinforced, prestressed

LOCATION ENVIRONMENT: region, topography

LOCATION EXPOSURE CONDITIONS:

mean annual temperature, temperature ranges, annual rainfall, humidity, pressure, freeze/thaw cycles, water immersion, tide exposure, sea water, ground water, soft water, de-icing salt, type of contact, concentration of aggressive substances, frequency and duration of exposure, wear, overloading, and special environmental influences (e.g. stray electrical currents)

OVERALL CONCRETE QUALITY:

Hammer Test: Ring/Dull

Concrete Friability: powdery, well cemented

Cement/Aggregate Bond: Good/Bad

Unusually Wet/Dry Areas: Yes/No

SURFACE FEATURES/DEFECTS:

Honeycomb Air Surface Voids Form-Streaking
Aggregate Transparency Subsidence Cracking
Color Variation Sand Streaking Layer Lines
Form Offsets Cold Joints

CRACKING SURVEY:

Crack type, width, direction, abundance, location
Features associated with cracking (i.e. efflorescence, exudations, carbonation, spalling, offsets)

EMBEDDED ITEMS:

Description:

Location:

Condition: clean, corroded, decayed, associated voids, cracks, mineralization

CONCLUSIONS:

SAMPLING LOCATION RECOMMENDATIONS:

Reprinted from "Characterization of Field Concrete," P.E. Stuzman, NISTIR:4516, National Institute of Standards and Technology, Gaithersburg, Maryland, January 1991. Not copyrightable in the United States.

**Table 4.8 Selected NDT Methods for Condition Assessment of Concrete Structures
(Poston et al., 1995). Permission to use this copyrighted material is granted by the
American Concrete Institute**

Mechanical/Physical/ Chemical Property	Test Types	Reason for Test
Compressive strength	Swiss Hammer (ASTM 805) Windsor Probe (ASTM C 803) Core for Compression Testing (ASTM C 42) Ultrasonic Pulse Velocity (ASTM 597)	Strength of in-place concrete; comparison of concrete strength in different locations (UPV and Swiss Hammer provide relative differences in strength only)
Reinforcement location	Pachometer X-ray Radar (ASTM D 4748)	Steel location and distribution; concrete cover
Corrosion potentials	Half-cell potential (ASTM C-876) Linear polarization (SHRP S-330)	Identification of location of active reinforcement corrosion Corrosion rate
Chloride ion content	Acid-Soluble and Water-Soluble Titration (AASHTO T-260) Specific Ion Probe (SHRP-S/FR-92-108)	Susceptibility of steel reinforcement to chloride-induced corrosion
pH	Phenolphthalein; direct measurement with pH meter	Assess corrosion protection value of concrete with depth and susceptibility of steel reinforcement to corrosion; depth of carbonation
Air content; cement & aggregate properties; scaling, alkali-silica reactivity & freeze/thaw susceptibility	Petrographic examination of core removed from structure (ASTM C-856) (ASTM C-457)	Assist in determination of causes of distress; degree of damage; quality of concrete when originally cast
Permeability	Electrical Indication of Concrete's Ability to Resist Chloride Ion Penetration (ASTM C 1202 and AASHTO T277) Resistance of Concrete to Chloride Ion Penetration (90-day ponding test) (AASHTO-T259) Absorption test (ASTM C-642)	Establish relative susceptibility of concrete to chloride ion intrusion; assess effectiveness of chemical sealers, membranes and overlays in repair
Alkali-silica reactivity (ASR)	SHRP Rapid Test (SHRP-C/FR-91-101)	Establish in field if observed deterioration is due to ASR
Location of delaminations, voids, and other hidden defects	Limited information from sounding (ASTM D 4580) Impact-Echo Infrared Thermography (ASTM D 4788) Pulse Echo-Radar (ASTM D 4748)	Assessment of reduced structural properties; extent and location of unobserved damage and defects
Steel area reduction; defect identification	Invasive probing	Observe and measure rust and area reduction in steel; observe corrosion of embedded post-tensioning components; verify location and extent of deterioration; provide more certainty in capacity calculations
Concrete component thickness	Impact-Echo Radar (ASTM D 4748) Invasive probing	Verify thickness of concrete; provide more certainty in capacity calculations
Local or global strength and behavior	Load test Strain measurements Acceleration Deformation Displacement measurements	Uncertainty in integrity and behavior; ascertain acceptability without repair or strengthening; determine accurate load rating
Tensile strength	Pull-off tests (ACI 503R) Splitting tests (ASTM C 446) Tension tests Bend test	Assess tensile strength of concrete and steel; relative quality of material
Material property determination	Density (ASTM C 642) Moisture content (ASTM C 642) Shrinkage (ASTM C 596, C 426) Dynamic Modulus (ASTM C 215) Modulus of Elasticity (ASTM C 464)	Determine mechanical properties of materials and volumetric properties

Table 4.9 Classification and Rating of Cracks and Surface Damage
 Developed by RILEM 104-DDC (RILEM, 1994).
 Permission to use this copyrighted material is granted by RILEM.

a. Cracks		
Type	Rating	Appearance
<i>Diagonal</i>	1 (very slight)	< 1 mm in width
<i>Longitudinal</i>	2 (slight)	1–10 mm in width
<i>Transverse</i>	3 (moderate)	10–20 mm in width
	4 (severe)	20–25 mm in width
	5 (very severe)	> 25 mm in width, spalling and/or faulting
<i>Craze</i>	1 (very slight)	barely noticeable
<i>Pattern</i>	2 (slight)	clearly visible-no raveling
<i>Checking</i>	3 (moderate)	clearly visible-some raveling
<i>Plastic</i>	4 (severe)	cracks raveled over substantial area
<i>Plastic</i>	5 (very severe)	cracks severely raveled or spalled
<i>Corner crack</i>	1 (very slight)	< 1 mm in width
	2 (slight)	1–10 mm in width
	3 (moderate)	10–20 mm in width
	4 (severe)	20–25 mm in width
	5 (very severe)	> 25 mm in width, spalling and/or faulting
<i>D cracking</i>	1 (very slight)	crack width < 1 mm, effective width < 150 mm from joint or crack
	2 (slight)	effective width < 250 mm from joint or crack, no spalling
	3 (moderate)	as above but with moderate spalling
	4 (severe)	as above but with severe spalling
	5 (very severe)	as above but with very severe spalling

Note: 1 mm = .0394 in.

Table 4.9 (cont.) Classification and Rating of Cracks and Surface Damage
 Developed by RILEM 104-DDC (RILEM, 1994).
 Permission to use this copyrighted material is granted by RILEM.

b. Surface Damage		
Type	Rating	Appearance
<i>Chalking</i>		Formation of a loose powder resulting from the disintegration of a surface of concrete or of applied coating
<i>Delamination</i>		Separation along a plane parallel to a surface
<i>Dusting</i>		Development of a powdered material at the surface of hardened concrete
<i>Exudation</i>		Liquid or viscous gel-like material discharged through concrete surface defect
<i>Blistering</i>	1 (very slight)	noticeable
<i>Cavitation</i>	3 (moderate)	thickness of damage < 10 mm
<i>Peeling</i>	5 (very severe)	thickness of damage > 10 mm
<i>Exfoliation</i>		
<i>Popouts</i>	1 (very slight)	barely noticeable
	2 (slight)	noticeable
	3 (moderate)	holes up to 10 mm in diameter
	4 (severe)	holes between 10 and 50 mm in diameter
	5 (very severe)	holes > 50 mm in diameter
<i>Scaling</i>	1 (very slight)	noticeable
	2 (slight)	loss of surface mortar without exposure of coarse aggregate
	3 (moderate)	loss of surface mortar 5 to 10 mm in depth with exposure of coarse aggregate
	4 (severe)	loss of surface mortar 10 to 20 mm in depth surrounding coarse aggregate
	5 (very severe)	loss of coarse aggregate and mortar to a depth in excess of 20 mm
<i>Spalls</i>	1 (very slight)	barely noticeable
	2 (slight)	clearly noticeable
	3 (moderate)	holes larger than popout of coarse aggregate
	4 (severe)	holes 150 mm in diameter and at least 150 mm deep
	5 (very severe)	holes larger than 150 mm
<i>Loss of coarse aggregate</i>	1 (very slight)	barely noticeable
	2 (slight)	noticeable
	3 (moderate)	pock- marked appearance
	4 (severe)	closely spaced pock-marks
	5 (very severe)	surface has raveled appearance

Table 4.10 Crack Widths to Prevent Corrosion of Steel Reinforcement (Krauss, 1994).

Author	Environment factors	Permissible width, mm
Rengers	Dangerous crack width	1.0 to 2.0
	Crack width allowing corrosion within 1/2 year saline environment	0.3
Abeled	Structures not exposed to chemical influences	0.3 to 0.4
Boscard	Structures exposed to a marine environment	0.4
Engel and Leeuwen	Unprotected structures (external)	0.2
	Protected structures (internal)	0.3
Voellmy	Safe crack width	up to 0.2
	Crack allowing slight corrosion	0.2 to 0.5
	Dangerous crack width	over 0.5
Bertero	Indoor structures	0.25 to 0.35
	Normal outdoor exposure	0.15 to 0.25
	Exposure to seawater	0.025 to 0.15
Haas	Protected structures (interior)	0.3
	Exposed structures (exterior)	0.2
Brice	Fairly harmless crack width	0.1
	Harmful crack width	0.2
	Very harmful crack width	0.3
Salinger	For all structures under normal conditions	0.2
	Structures exposed to humidity or to harmful chemical influences	0.1
Wastlund	Structures subjected to dead load plus half the live load for which they are designed	0.4
	Structures subject to dead load only	0.3
Efsen	Exterior (outdoor) structures exposed to attack by seawater and fumes	0.05 to 0.25
	Exterior (outdoor) structures under normal conditions	0.15 to 0.25
	Interior (indoor) structures	0.25 to 0.35
Rüsch	Ordinary structures	0.3
	Structures subjected to the action of fumes and sea environment	0.2

Note: 1 mm = .0394 in.

Table 4.11 Classification of Carbonation-Induced Damage (Parrott, 1990).
Permission to use this copyrighted material is granted by RILEM.

Damage severity	Concrete condition	Reinforcement condition	Carbonation: cover ratio	Test methods (see Table 1)	Further action
Safe	Not cracked	Not corroded	<0.5	2.1, 2.2, 3.1, 4.1	None
Mild	Not cracked	Not corroded	>0.5	2.1-2.4, 3.1-3.7, 4.1	Estimate time to carbonate cover, monitor or apply coating
Significant	Minor cracks	Minor corrosion	~1.0	2.1-2.4, 3.1-3.7, 4.1, 4.2	Initiate repair, apply coating or monitor
Serious	Cracked, minor spalling	Significant corrosion	>1.0	2.1-2.5, 3.1-3.7, 4.1-4.3	Full survey and repair soon
Critical	Cracked, major spalling	Loss of area	>>1.0	2.1-2.5, 3.1-3.7, 4.1-4.3	Assess residual strength and immediate repair

Table 1 Check-list for field assessment of concrete damaged by carbonation-induced corrosion

1	Description of inspection site Date inspected and age of structure Type of structure and structural element Surface condition of concrete and presence of any coating Location of structure and structural element Exposure conditions (moisture, temperature, carbon dioxide)
2	Visual assessment
2.1	Cracking parallel to reinforcement and crack widths
2.2	Rust staining and spalling of concrete
2.3	Water seepage and dampness
2.4	Voids due to poor consolidation
2.5	Visible loss of reinforcement area
3	Measurement of concrete quality and condition
3.1	Depth of carbonation
3.2	Surface indentation or penetration resistance
3.3	Ultrasonic pulse velocity
3.4	Surface strength
3.5	Surface permeability
3.6	Moisture content or internal relative humidity
3.7	Electrical resistivity
4	Reinforcement
4.1	Thickness of concrete cover (covermeter)
4.2	Electrode potential
4.3	Removal of concrete for direct observation

**Table 4.12 Inspection Intervals for Routine and Extended Inspections
Based on Environmental Conditions (CEB-FIP, 1986).
Reprinted with permission of *fib*, Federation Internationale du Beton (CEB-FIB).**

Indication of inspection intervals (in years)

Environmental and loading conditions	Classes of structure					
	1		2		3	
	Routine inspection	Extended inspection	Routine inspection	Extended inspection	Routine inspection	Extended inspection
Very severe	2*	2	6*	6	10*	10
Severe	6*	6	10*	10	10	—
Normal	10*	10	10	—	Only superficial inspections	

*Midway between extended inspections.

Table 4.13 Recommended Inspection Intervals for NPP Concrete Structures (Hookham, 1995).

Structure Exposure Category	Frequency of Visual Inspection
• Below-Grade	10 Years (each ISI Interval)
• Natural Environment (Direct/Indirect)	5 Years (two per ISI interval)
• Inside Primary Containment	5 Years (two per ISI interval)
• Continuous Fluid (without liner)	5 Years (two per ISI interval)
• Fluid/Pressure Retaining (with liner)	5 Years (two per ISI interval)
• Controlled Interior (i.e., secondary containment, auxiliary building, etc.)	10 Years (each ISI interval)